DATA REVIEW AND EVALUATION OF GROUNDWATER MONITORING

WHITE MESA URANIUM MILL
BLANDING UTAH

AUGUST 2015
PROJECT NO. 2015.A025

PREPARED FOR:

Ute Mountain Ute Tribe
P.O. Box 448
Towaoc, CO 81334

PREPARED BY:

Geo-Logic Associates
1760 E. River Road, Suite 115
Tucson, AZ 85718

Geo-Logic ASSOCIATES

TABLE OF CONTENTS

TABLES

FIGURES

1.0 INTRODUCTION

Geo-Logic Associates was contracted by the Ute Mountain Ute Tribe to conduct a review and evaluation of available data and reports related to groundwater monitoring at the White Mesa Uranium Mill near Blanding, Utah. The objective of this review was to provide an independent assessment of current groundwater conditions and evaluate potential groundwater impacts from the facility.

There have been a considerable number of studies conducted at the mill site, with the scope and extent of such studies significantly increasing following the discovery of nitrate and regulated organic constituents in the groundwater during a complete groundwater sampling round in May 1999. Corrective actions consisting of groundwater pumping have been implemented at the site following this discovery.

2.0 FACILITY DESCRIPTION AND HISTORY

Information on facility operations comes from previous reports and DRC documents (Titan, 1994; Intera, 2009; MWH, 2010; USGS, 2011; and DRC, 2004). The White Mesa mill began operations in 1980. The facility was licensed and regulated by the Nuclear Regulatory Commission (NRC) until August 2004 when the Utah Department of Radiation Control (DRC) assumed regulatory authority for the mill. The White Mesa Uranium Mill processes natural uranium ores and alternate feeds. The mill uses sulfuric acid leaching and a solvent extraction recovery process to extract and recover uranium and vanadium from the ore material. As of 2011, the mill was licensed to process an average of 2,000 tons of ore per day. The produced tailings and process water are disposed in lined tailing cells at the facility.

Information on the tailings cells along with other ponds associated with the processing facilities is summarized in Table 1 and their locations (as well as neighboring stock watering ponds) are shown in Figure 1. All of the tailings cells were excavated into the Dakota Sandstone and the edges are bermed with compacted material. Perched groundwater is found at approximately 40 to 90 feet below the base of the tailings cells. Tailings Cells 1, 2, and 3 are single liner (30 mil PVC) facilities constructed in the early 1980s with a leak detection system (LDS) composed of a collection pipe placed along the down gradient (south) side of the cell, with the bottom of the cell sloped towards the south. This type of LDS can only detect larger leaks from the cells as they require saturation of the bedding material surrounding the collection pipe in order to observe water flow into the LDS. Tailings Cells 4A and 4B have a dual liner (60 mil HDPE) constructed in 1989 and 1990 (Tailings Cell 4B was relined in 2007-2008) and thus are able to detect and collect significantly smaller leakage through the primary liner.

Although a comprehensive review of recorded leakage from the liners is beyond the scope of this study, it is noted that leaks have been observed in most of the cells and liners listed in Table 1. Tailings Cell 1 had a reported leak in June of 2010, which prompted significant repairs of the liner between September 2009 and June 2012. Tailings Cell 3 has had indicated leakage (water collected from leak detection system) in 1991, 2009, and 2010. Tailings Cell 4A has

indicated leakage through the primary liner (water collected from leak detection system) every year from 2009 to 2014. The cell was relined in 2007-2008 due to damage to the liner from sun exposure. Similar indicated leakage has been observed for Tailings Cell 4B in 2011, 2012, and 2014. While it is noted that leakage from Tailings Cells 4A and 4B is collected by the secondary liner and is within regulated limits, the presence of leakage from the primary liner of these newer facilities indicates that leakage is almost certainly occurring from the older tailings cells (1, 2, and 3).

TABLE 1 - DETAILS OF TAILINGS CELLS AND OTHER FACILITY PONDS

CELL OR POND	CONTENTS	LINER	POND AREA (ACRES)	PERIOD OF OPERATION
Tailings Cell 1	Process solution (evaporation pond)	15 cm clean sand slimes drain, protective blanket, 30 mil PVC liner, 15 cm compacted bedding, currently active	50.8	Jun-81
Tailings Cell 2	Barren tailings sands (originally received all tailings)	15 cm clean sand slimes drain, protective blanket, 30 mil PVC liner, 15 cm compacted bedding, disposal ceased prior to 2004, currently covered with clean soil awaiting final closure	65.7	May-80
Tailings Cell 3	Barren tailings sands and solutions	15 cm clean sand slimes drain, protective blanket, 30 mil PVC liner, 15 cm compacted bedding, limited disposal as nearing capacity, 17 acres covered with clean soil	66.6	Sep-82
Tailings Cell 4A	Barren tailings sands and solutions	Slimes drain, 60 mil HDPE geomembrane liner, geonet drainage layer, 60 mil HDPE geomembrane liner, geosynthetic lay liner, prepared subgrade, currently active	41.6	Nov-89 relined in 2007-2008
Tailings Cell 4B	Barren tailings sands and solutions (until Sept 2008 used only for process solution storage)	Slimes drain, 60 mil HDPE geomembrane liner, geonet drainage layer, 60 mil HDPE geomembrane liner, geosynthetic lay liner, prepared subgrade, currently active	37.3	1990
Roberts Pond	Emergency catchment basin for process flow spills or tank failures	Hypalon liner removed in 2002 and replaced with 60 mil HDPE liner, currently being abandoned or retrofitted	0.67	1980
Fly ash pond	Disposal of some fly ash from mill boiler, received runoff from mill site	Unlined pond originally intended for construction water, excavated and backfilled in 1989	0.56	1980 to 1989
Lawzy Lake	Temporary storage of municipal sewage reclaim water	Unlined pond used for temporary storage and transfer of reclaimed sewage water from Frog Pond	0.08	mid-1980s to 1991
Wildlife ponds	Fresh water ponds for use of wildlife	Total of 4 ponds: 2 near northeast corner of mill site; 2 to east of Cell 4A south of mill site	7.0 combined	1980s (see text) to 2012

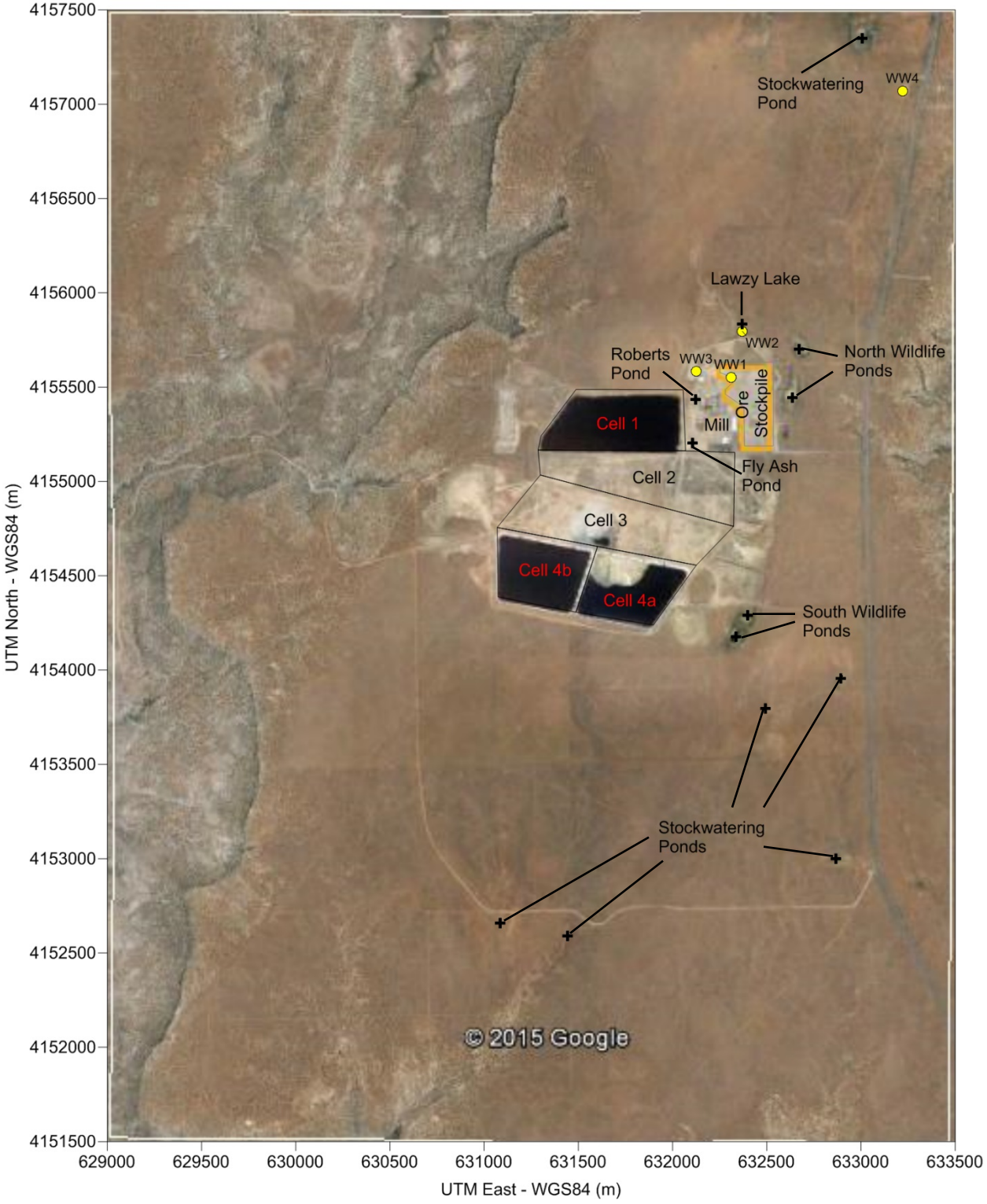

FIGURE 1 - WHITE MESA MILL FACILITY LAYOUT

The changes in operating status of the tailings cells and ponds based on observations from aerial and satellite photos are summarized in Table 2. It is noted that these are only snapshots in time and may not represent the actual pond status during periods between when the photos were taken. The wetted area refers to the total area of exposed fluids in each facility. Although Tailings Cells 2 and 3 currently show little or no exposed fluids, recent measurements (MWH, 2015) indicate that residual tailings solution is still present within the cells with a phreatic surface at depths of 3.9 to 11.5 ft below the tailings surface in Cell 2 and depths of 3.5 to 8.7 ft below the tailings surface in Cell 3.

TABLE 2 - VISUAL OBSERVATIONS ON POND STATUS (% OF WETTED AREA/TOTAL AREA)

PHOTO DATE	PHOTO SOURCE	PHOTO RESOLUTION	TAILINGS CELL 1	TAILINGS CELL 2	TAILINGS CELL 3	TAILINGS CELL 4A	TAILINGS CELL 4B	ROBERTS POND	FLY ASH POND	SOUTH LOWER WILDLIFE POND	SOUTH UPPER WILDLIFE POND	NORTH LOWER WILDLIFE POND	NORTH UPPER WILDLIFE POND
Average			97%	0%	15%	43%	100%	56%	Closed	35%	25%	37%	53%
07/02/97	USGS	Low	100%	0%	30%	16%	N.B.	100%		57%	35%	63%	51%
04/17/04	Digital Globe	High	100%	0%	13%	0%	N.B.	71%		57%	38%	79%	95%
09/14/04	USDA	Low	71%	0%	34%	0%	N.B.	N.C.		39%	67%	74%	81%
09/24/06	USDA	Mod	100%	0%	30%	0%	N.B.	41%		45%	26%	65%	91%
08/27/09	USDA	Mod	100%	0%	9%	83%	N.B.	45%		38%	24%	52%	68%
08/08/10	Digital Globe	High	100%	0%	12%	81%	U.C.	C.C.		26%	0%	0%	66%
10/02/11	USDA	Mod	100%	0%	1%	72%	100%	67%		45%	16%	0%	21%
06/25/13	Google Earth	Highest	100%	0%	1%	68%	100%	14%		6%	21%	0%	0%
04/05/15	Google Earth	Highest	100%	0%	2%	63%	100%	U.R.		0%	0%	0%	0%

Notes: N.B. = Not built, U.C. = under construction, N.C. = not clear due to photo resolution, C.C. = cloud cover obscures pond

Roberts Pond (a.k.a. Mill Area Retention Basin) is a lined basin which has received process fluids, periodic mill floor drainage, and other wastewaters and runoff from the mill. Although earlier documents suggest that the pond only received occasional or emergency flows, subsequent documents suggest that it was operated as a waste water pond with weekly monitoring of pond levels in much the same manner as performed for the tailings cells (Energy Fuel Resources, 2014a). All available aerial photos for the period 1997 to 2015 show the pond to be at least partially filled (average 56% wetted/total area). In 2002 the original liner was removed and replaced (Roberts, 2004). Both the liner and some underlying soil which exhibited elevated uranium (no other indicators of contamination were used) were excavated and

disposed into one of the tailings cells indicating leakage from the pond prior to 2002. The liner was reported to be damaged during removal of sediments in July 2012 and repaired and returned to service in August 2012 (Energy Fuels Resources, 2015). Liner damage was again noted in March 2014 and believed to be related to the prior maintenance operations in 2012. Attempts to repair the damage after drainage of the pond resulted in further damage to the liner resulting in the need to remove the liner and excavate and dispose of residual sediments and soils below the liner into one of the tailings cells. Uranium and radium-226 were used as indicators of contaminated soil during the 2014 excavation.

The fly ash pond was originally an unlined pond which collected surface runoff and was used during site construction (Intera, 2009). The pond was subsequently used for disposal of fly ash during "upset situations" (fly ash normally disposed of in Tailings Cell 2) from a coal fired steam boiler which operated from 1980 to 1989. It may also have occasionally received process spills and surface runoff until it was filled and re-contoured in 2007. The pond was emptied in 1989 and the residual ash was disposed in Tailings Cell 2. The cell was backfilled with random fill. Sampling data from 1991 (Titan 1994) indicated the presence of heavy metals as well as nitrate in water held in this pond.

There is considerable discrepancy in the operational history of the wildlife ponds. Energy Fuels Resources (2014b) reported that in the early 1980s the two north wildlife ponds were constructed. Older reports indicate that these were only small (70 ft diameter) stock watering ponds initially (International Uranium Corp, 2000; Denison Mines, 2007) and were normally dry. Intera (2007) indicates that the upper north wildlife pond was an old stock watering pond but that the lower north wildlife pond was constructed in 1979. The south wildlife ponds were constructed in 1995 (Energy Fuels Resources, 2014b) or 1994 (International Uranium Corp, 2000, Intera, 2007). Another recent report (Hurst and Solomon, 2008) indicates that the wildlife ponds were constructed in the mid-1990s. The wildlife ponds are reported to have received fresh water from Recapture Reservoir although this water was not available until 1992. In addition, reclaimed water from a nearby municipal sewage treatment pond was reportedly used as make-up water in the mill processing from the mid-1980s until 1991. Some of this water was pumped to the upper north wildlife pond for storage prior to being pumped to the mill's pre-leach tanks. Discharge to the north wildlife ponds ceased in March 2012 (HGC, 2014). Discharge to the south wildlife ponds apparently ceased shortly thereafter based on aerial photo observations and a sudden observed decline in water level in the neighboring piezometers (Piezos 4 and 5) at the start of 2013.

Lawzy Lake, which is dry in all aerial photos since 1997, was also reported to be used as a temporary storage location for the reclaimed make-up water (Intera, 2009). Water from Lawzy Lake was pumped to the Lawzy Sump and then to the mill's pre-leach tank which was used for water storage.

Several small stock watering ponds exist at the site as noted in Figure 1. These ponds capture surface water runoff and based on examination of aerial photos since 1997 are either dry or

contain very small amounts of collected water. This normally dry condition has also been reported by others (International Uranium Corp, 2000).

There is no available water balance information for the facility although indicated average water use for the facility was about 650 gpm (Intera, 2009). The facility is permitted as a zero discharge facility so that excess water in the tailings is disposed by evaporation. A limited amount of solution is recycled for secondary extraction, although the water is not recycled through the main mill processing circuit due to the low pH (USGS, 2011). A quick calculation of expected water loss solely from tailings deposition (based on continuous ore processing of 2,000 tons/d and a tailings porosity of 48%) via evaporation in the tailings cells and retained tailings pore water yields approximately 380 gpm of water consumption since 2011. The difference of 270 gpm could be attributable to other consumptive uses at the facility, discharge to the wildlife ponds, and seepage from other mill facilities.

A total of five deep wells (completed in the Navajo Sandstone) were installed at the site at the time of facility construction as listed in Table 3 (Titan, 1994). Locations of four of the five deep wells are shown in Figure 1 (WW5 is located to the east of WW4 outside of the figure boundaries). Tested yield of the wells (at the time of installation) averaged about 200 gpm per well. These wells were used for water supply for the mill until about 1992 (Intera, 2009) when water from Recapture Reservoir was made available via a pipeline. Prior to 1992, additional makeup water (25 to 200 gpm) was obtained from effluent from the municipal sewage treatment facility (i.e. Frog Pond) which reportedly contained higher concentrations of nitrates and chloride. The Frog Pond water was stored in the upper northeastern wildlife ponds, as well as a smaller pond (Lawzy Pond) north of the mill site, as discussed previously.

TABLE 3 - DEEP WATER SUPPLY WELLS INSTALLED AT MILL SITE (DATA FROM TITAN, 1994)

WELL ID	UTM COORDINATES (WGS84)		DEPTH (ft)	TESTED YIELD (gpm)
	East (m)	West (m)		
WW1	632309	4155552	1870	223
WW2	632370	4155796	1885	Not tested
WW3	632127	4155583	1850	245
WW4	633222	4157070	1820	238
WW5	633651	4156997	1800	120

3.0 DATA ANALYSIS

3.1 Hydrogeologic Conditions

The following section describes and evaluates hydrogeologic conditions at the site in order to understand groundwater occurrence, lateral and vertical movement, and recharge and discharge at the site.

3.1.1 Climate

The site climate is arid with an average annual precipitation of 13.3 in/yr and annual pan evaporation of 68 in/yr. Based on reported conditions for nearby Blanding, Utah, maximum/minimum monthly temperatures range from a high of 89/58 ˚F in July to a low of 39/17 ˚F in January. Average monthly precipitation ranges from a low of 0.45 inches in June to a maximum of 1.45 inches in October. Monthly precipitation generally declines from January to June and then increases through October, remaining higher through the winter months. Precipitation increases with elevation so that most recharge to the regional aquifers in the area occurs in neighboring mountains areas or ridges. Based on the site climate, under natural (pre-mill) conditions groundwater recharge from infiltration is expected to be low with most recharge occurring during short periods of heavier rainfall or snowmelt. MWH (2010) indicated predicted infiltration rates of 1.3 in/yr based on simple rock covers over the tailings (versus monolithic evapotranspiration covers), although natural site conditions were not modeled. Nonetheless, groundwater recharge from infiltration is expected to be significant in the White Mesa (USGS, 2011).

3.1.2 Topography

The mill site is located on White Mesa and ranges in elevation from about 5,500 to 5,650 ft amsl, with elevation generally decreasing gradually to the south. The mesa is bounded by Westwater Canyon to the west and Corral Canyon to the east with an east-west extension of the top of the mesa of approximately 8,000 ft upstream of the mill, 9,000 ft in the vicinity of the mill, and 14,000 ft downgradient of the mill. The flat topography minimizes runoff and enhances potential infiltration of precipitation. The topography also determines the east and west limits of the perched aquifer as described below. The total surface area of White Mesa as measured from north (location of MW-1) to south (location of MW-22) is approximately 5 square miles.

3.1.3 Local Stratigraphy

The stratigraphy at the site has been described in several previous reports (UMETCO, 1993; Titan Environmental, 1994; HGC, 2009; USGS, 2011; HGC, 2014) and the following lithological descriptions represent a combination of those descriptions. The major stratigraphic units present at the site are (from youngest to oldest):

Quaternary Deposits: These consist primarily of unconsolidated pale reddish brown aeolian sands and silts that cover the mesa surface to a depth of between a few feet to a few tens of feet. The grains consist of angular to well-rounded quartz grains that range from 0.02 to 0.20 mm in diameter. These eolian sands are expected to have relatively high hydraulic conductivity which would enhance infiltration of precipitation (USGS, 2011).

Mancos Shale: The Mancos Shale consists primarily of uniform, dark-gray mudstone, shale, and siltstone which were deposited in a shallow shelf marine environment. It is present as only

minor erosional remnants of its original thickness in the study area. The Mancos Shale is commonly highly fractured within the near-surface weathered zone. These fractures are commonly filled with easily dissolvable gypsum filling (White et al, 2008). Recent studies (HGC, 2014) have mapped the thickness of the Mancos Shale over the mill site area from borehole logs, indicating it ranges from zero to over 30 feet. The greatest thicknesses were mapped directly below the mill site as well to the east of the tailings cells. The Mancos Shale remnants extend below the eastern portions of Tailings Cells 2, 3 and 4a, with thicknesses of up to 30 feet reported at the eastern edge of Cell 3. However, it is reported that all of the tailings cells were excavated into the underlying Dakota Sandstone (Titan, 1994), which is likely given that the Mancos Shale is a weak deposit that contains expansive clays which would provide a very poor foundation material. The Mancos Shale is also present north of the site in the western portion of White Mesa. A ridge of Mancos Shale measuring up to over 10 feet in thickness is also present along the western boundary of Cell 4B, extending due southward, corresponding to a high in the bedrock surface below the site.

Dakota Sandstone (late Cretaceous): The Dakota Sandstone consists of a pale grayish-orange to yellowish brown, massive, intricately cross-bedded, friable sandstone. Scattered irregularly through the Dakota Sandstone are discontinuous lenses of conglomerate and dark-gray claystone and siltstone seams, and lenticular carbonaceous seams. The sandstone consists chiefly of poorly sorted quartz grains that are moderately (upper part of formation) to well cemented by silica, calcite, and kaolinite clays. The grains are of two sizes; most common are angular grains about 0.06 mm in diameter that surround large numbers of well-rounded quartz grains about 0.40 mm in diameter. This lithological unit is continuous across the White Mesa site with an average reported thickness of about 60 ft.

Burro Canyon Formation (early Cretaceous): The Burro Canyon Formation is similar to the Dakota Sandstone. It consists of alternating beds of light to dark greenish-gray, gray, and light brown sandstone and conglomeratic sandstone formed from alluvial and floodplain deposits. It contains widely traceable conglomerate layers interpreted as braided channel deposits, and discontinuous lenses of light greenish-gray shale and siltstone layers. The shape of the sand grains range from angular to well rounded, and they have diameters ranging from 0.02 to 0.5 mm, with most being about 0.1 mm in diameter. This lithological unit is continuous across the White Mesa site with an average reported thickness of about 75 ft.

Morrison Formation - Brushy Basin Member (late Jurrasic): The contact between the Burro Canyon and the underlying Brushy Basin is considered to be disconformable as evidenced by local erosional relief of several feet and logs of site borings. The Brushy Basin Member of the Morrison Formation is composed of thinly laminated to medium bedded variegated claystone and siltstone that were deposited in a combination of lacustrine and marginal lacustrine environments, interbedded with thick lenses of gray sandstone. These beds are described as a moderate greenish yellow, streaked irregularly by pale red, light red, and light brownish gray. In general, the claystone matrix consists of minute (0.01 mm and smaller) angular grains of quartz cemented by calcite and silica. Angular to subrounded quartz grains that range from 0.05 to

about 0.21 mm in diameter, with most being about 0.1 mm, are scattered irregularly through the matrix. Much bentonitic clay of volcanic origin is also present. This lithological unit is continuous across the White Mesa site with a total thickness of approximately 300 feet.

Additional sedimentary formations below the above sequence include the Westwater Canyon, Recapture, and Salt Water members of the Morrison Formation, the Summerville Formation, the Entrada Sandstone, and the Navajo Sandstone.

3.1.4 Groundwater Occurrence

Perched groundwater is found below the mill site above the contact with the Brushy Basin Member within the Burro Canyon (and locally the Dakota Sandstone) at saturated thicknesses ranging up to 85 ft and averaging about 34 ft. Recharge to groundwater occurs from up gradient flow from the north of the site as well as infiltration from precipitation, water in unlined ponds, and releases from the mill facility. Although groundwater also exists within confined aquifers at deeper depths below the site, these are hydraulically isolated from the perched groundwater aquifers by the Brushy Basin Member which acts as an aquitard and are not considered in this study. However, perched groundwater at the site does seep vertically downward through the underlying aquitard. The perched groundwater also discharges to several springs located along the contact between the Burro Canyon and the Brushy Basin including Entrance Spring east of the mill site, Westwater (a.k.a. Mill) Spring west of the mill site, and Ruin and Corral Springs south of the mill site.

Figure 2 shows the phreatic surface of the perched aquifer based on groundwater elevations in March 2014. The groundwater springs located at the base of the perched aquifer were also used as indicated groundwater elevations with the exception of Cottonwood Spring which issues from the Brushy Basin formation. This figure indicates that groundwater generally flows from north to south below White Mesa. However, infiltration from the Wildlife Ponds (as well as one other location as discussed later) has created groundwater mounding below these areas which locally distorts the natural (pre-mill) direction of groundwater flow. Groundwater discharge to Westwater and Entrance springs is also indicated by the phreatic surface.

Using the measured groundwater levels shown in Figure 2 and the reported depth of the base of the perched aquifer (top of Brushy Basin) from boring logs, the current saturated thickness of the perched aquifer was determined as shown in Figure 3. The saturated thickness ranges from 0 to 85 ft. The greatest saturated thickness is generally found in the northern portion of the site due to higher groundwater levels and groundwater mounding in this area. However, significant saturated thicknesses are found in the southeastern portion of the site, although only a few wells are located in this area. Saturated thickness is less in the chloroform plume area (east of Tailings Cells 2 and 3) probably due to groundwater pumping in this area. The southwestern portion of the site has a very limited saturated thickness with an area extending to the southwest of Tailings Cell 4B that has only 0 to 5 ft of saturated thickness. Saturated thickness is expected to influence the transmissivity of the aquifer and contaminant migration due to the

presence of higher conductivity layers within the sandstones. As saturated thickness increases, there is a higher probability of these layers being saturated.

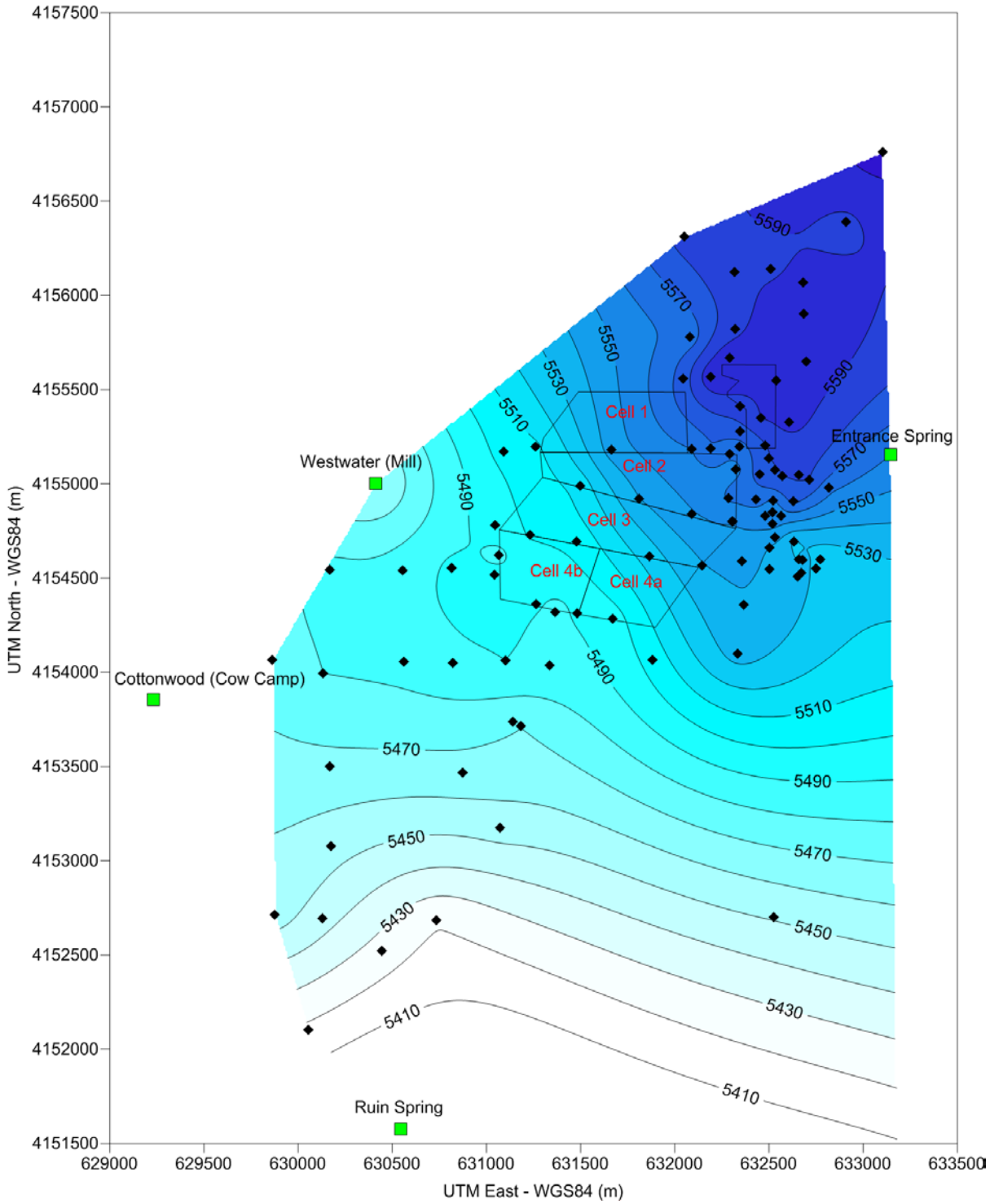

FIGURE2 - PHREATIC SURFACE OF THE PERCHED AQUIFER IN MARCH 2014

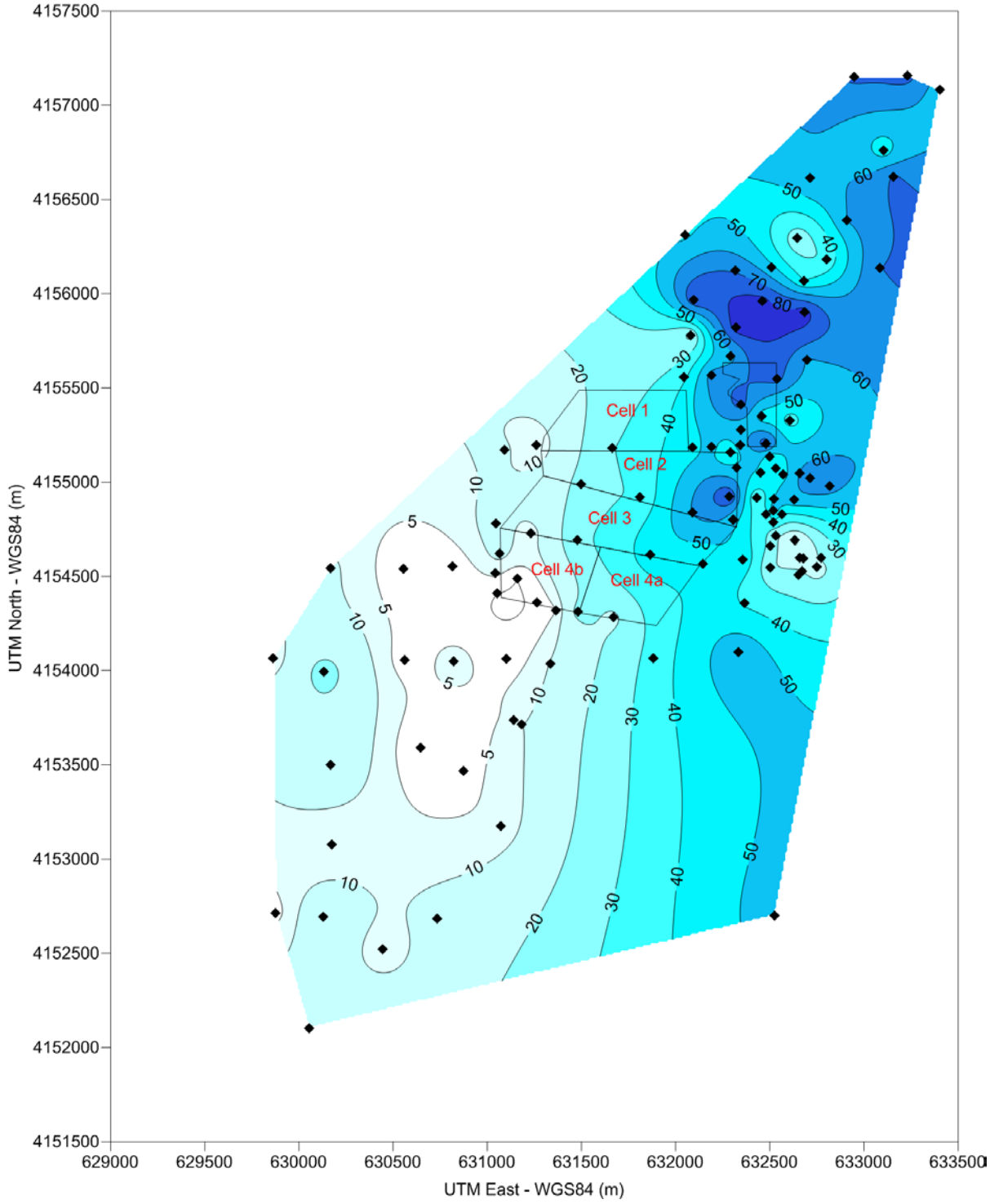

FIGURE 3 - SATURATED THICKNESS OF THE PERCHED AQUIFER IN MARCH 2014

3.1.5 Water Level Changes

Water levels changes were examined to evaluate the impacts of seepage from the wildlife ponds and other sources at the mill site as well as groundwater pumping in the chloroform plume area. Figures 4 through 8 show hydrographs (water level elevations versus time) as measured in the MW-series monitoring wells at the site.

The upgradient wells (Figure 4) indicate the impact of seepage from the wildlife ponds. MW-19, the closest monitoring well (located about 1,300 ft northwest from the lower north wildlife pond center), shows a water level increase of about 35 ft from 1993 to 2007. MW-18 (located about 2,350 ft northwest) shows a water level increase of about 22 ft from 1993 to 2010, while MW-1 (located about 3,330 ft to the northwest) shows a water level increase of about 12 ft from 1997 to 2013. Water levels are currently declining in these wells as discharge to the ponds ceased in 2012. Although MW-27 (located about 2,200 ft to the west) was not installed before the pond seepage began, the water level begins to decline in 2012. Given that the water level increases have occurred over a period of 14 to 17 years, it can be expected that they will require a similar amount of time to fully dissipate.

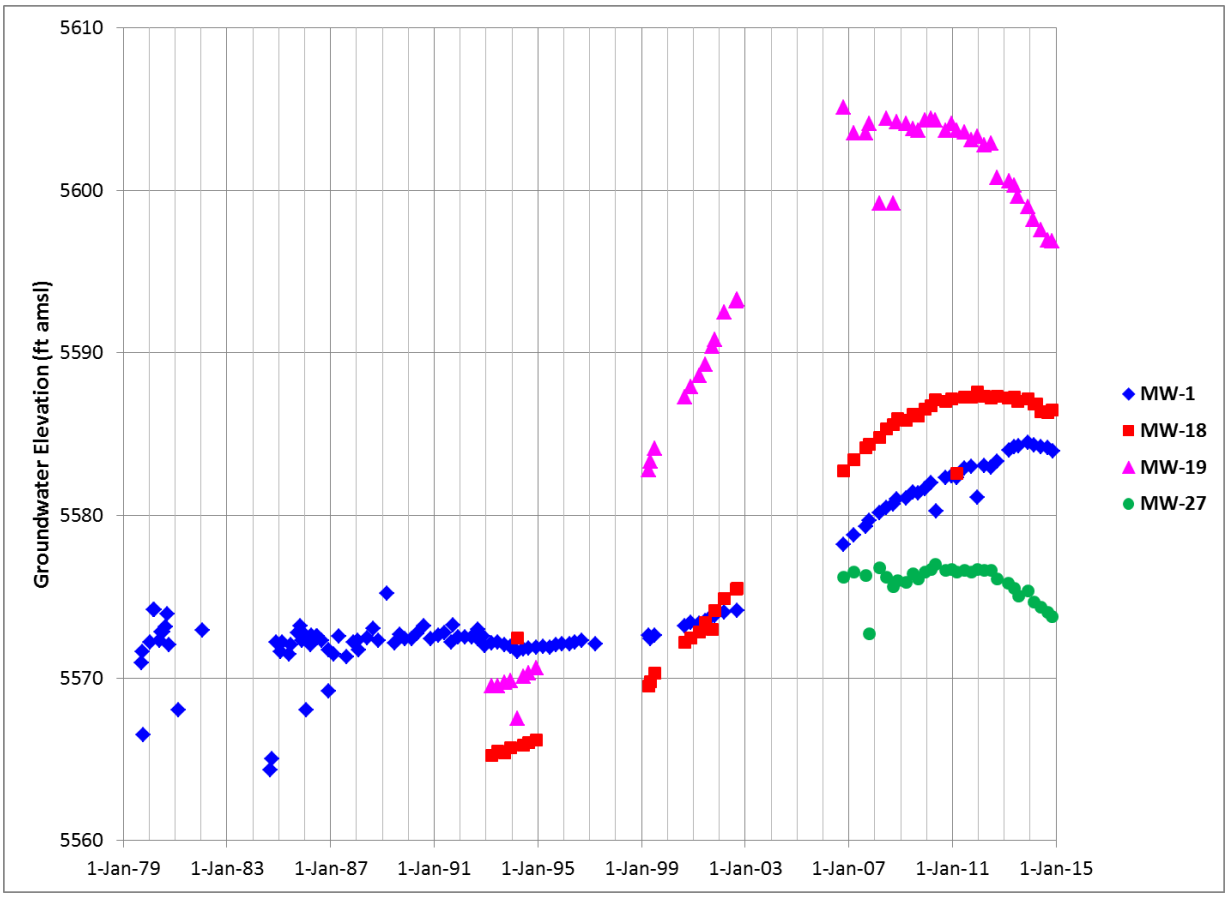

FIGURE 4 - HYDROGRAPHS OF UPGRADIENT MONITORING WELLS

The large increases in water level observed in the upgradient wells would suggest that the water chemistry of the background wells is significantly influenced by the chemistry of the water discharged to the ponds. As the northern ponds went into operation in the early 1980s, the presence of groundwater mounding would indicate that a significant release from other site facilities can reach the groundwater surface in 10 years or less. Water levels in MW-1 were stable prior to 1997, with observed fluctuations during this period likely the result of measurement error or performance of measurements after well development (prior to full water level recovery).

Apart from MW-2, the wells down gradient and lateral of Tailings Cells 1 and 2 (Figure 5) also show an apparent response to seepage from the wildlife ponds. MW-4 (located about 2,020 ft southwest of the lower north pond center) shows a water level increase of about 31 ft from 1993 to 2003. In 2003 MW-4 was put into service as a pumping well. Although the water level in MW-4 has fluctuated as a result of pumping, the water level has not dropped below its pre-1980 water level. Pumping of MW-4 has also not had any apparent impact on the water levels in any of the other wells. MW-26 was also operated as a pumping well within a year of its installation and exhibits similar water level fluctuations to that of MW-4. The pumping of both wells has not had any apparent impact on the water levels of the other Tailings Cells 1 and 2 monitoring wells, except for a much muted response in MW-32. MW-32 is located about 700 ft from MW-4 and about 900 ft from MW-26. The lack of response indicates that drawdown associated with pumping of wells MW-26 and MW-4 is localized. Except MW-2, all of the non-pumped monitoring wells have a shown a gradual increase in water level over time. The observed rate of increase in water level generally increases from west to east (i.e. with closer proximity to the wildlife ponds).

MW-4 has exhibited a gradual but continuous increase in water level since at least 1984. This increase indicates seepage from one of the neighboring site facilities (sewage drains at the mill, fly ash pond, Roberts Pond, or tailing cells).

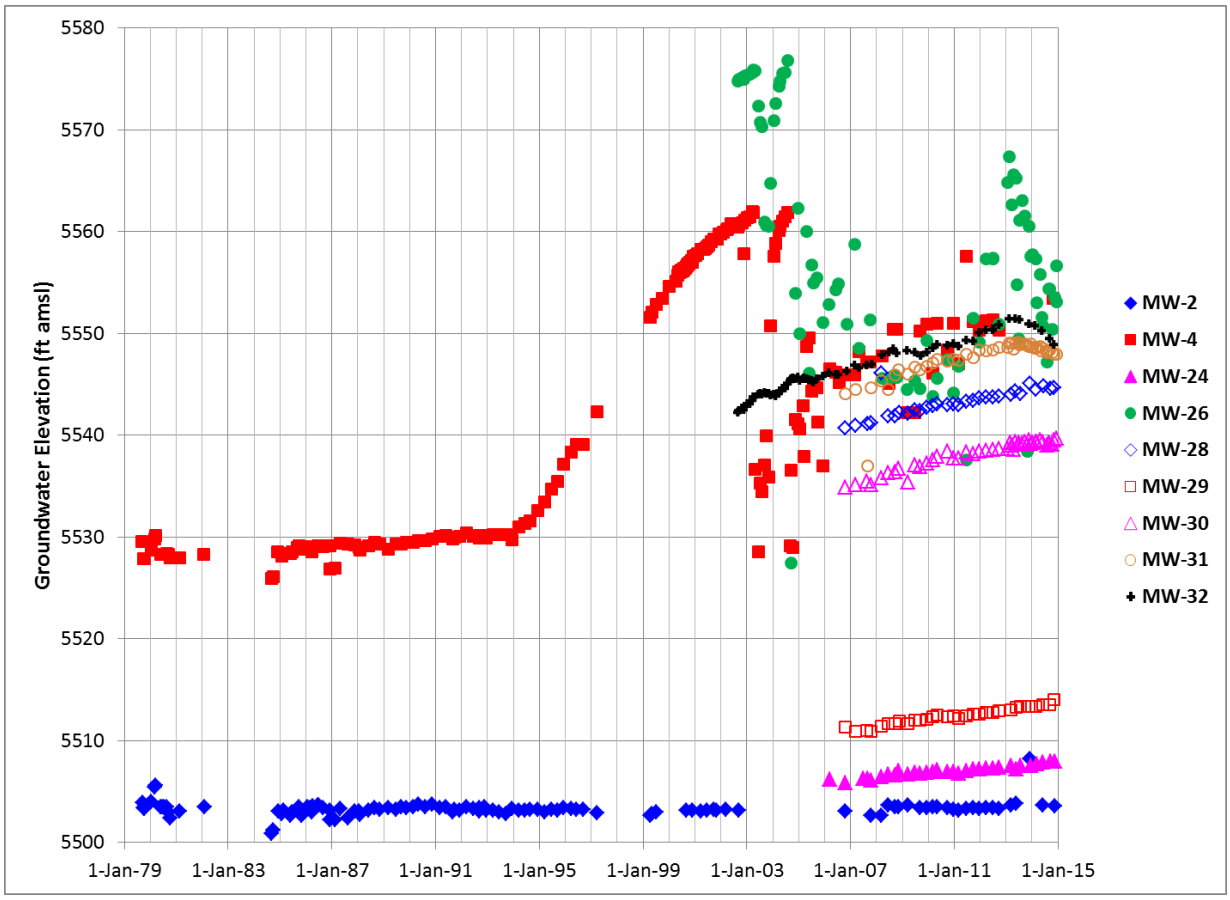

FIGURE 5 - HYDROGRAPHS OF MONITORING WELLS FOR TAILINGS CELLS 1 AND 2

With the exception of MW-23, monitoring wells downgradient of Tailings Cell 3 (Figure 6) exhibit increasing water levels over time. As seen for MW-4, MW-11 has also exhibited a slightly increasing water level since its installation in 1982 with the water level rising a couple of feet by 1993. This again indicates seepage from a neighboring facility. The water levels in MW-11 and MW-12 fluctuate prior to 1993. This fluctuation is attibuted to the use of different reference elevations for the water levels calculated from depth to water in different data sources.

The water level in MW-11 begins to increase at a more rapid rate starting in 1993, presumably as a result of seepage from the wildlife ponds as observed in the previous hydrographs (Figures 4 and 5). Since 1993 the water level in MW-11 has increased about 16 ft and continues to increase. The water level rise in the other monitoring wells is similar to that observed for the Tailings Cells 1 and 2 monitoring wells, with the magnitude and rate of rise increasing towards the east, indicating influence from the wildlife pond seepage. Only MW-23, on the western side exhibits a stable water level, although the water level fluctuates. This fluctuation is probably attributable to the low hydraulic conductivity of this well and perhaps the inclusion of some water level measurements performed after well development and sampling. Well MW-25, the eastern most monitoring well, shows the highest water level and a rapid decline in water level since 2013, indicating that it is also influenced by seepage from the wildlife ponds.

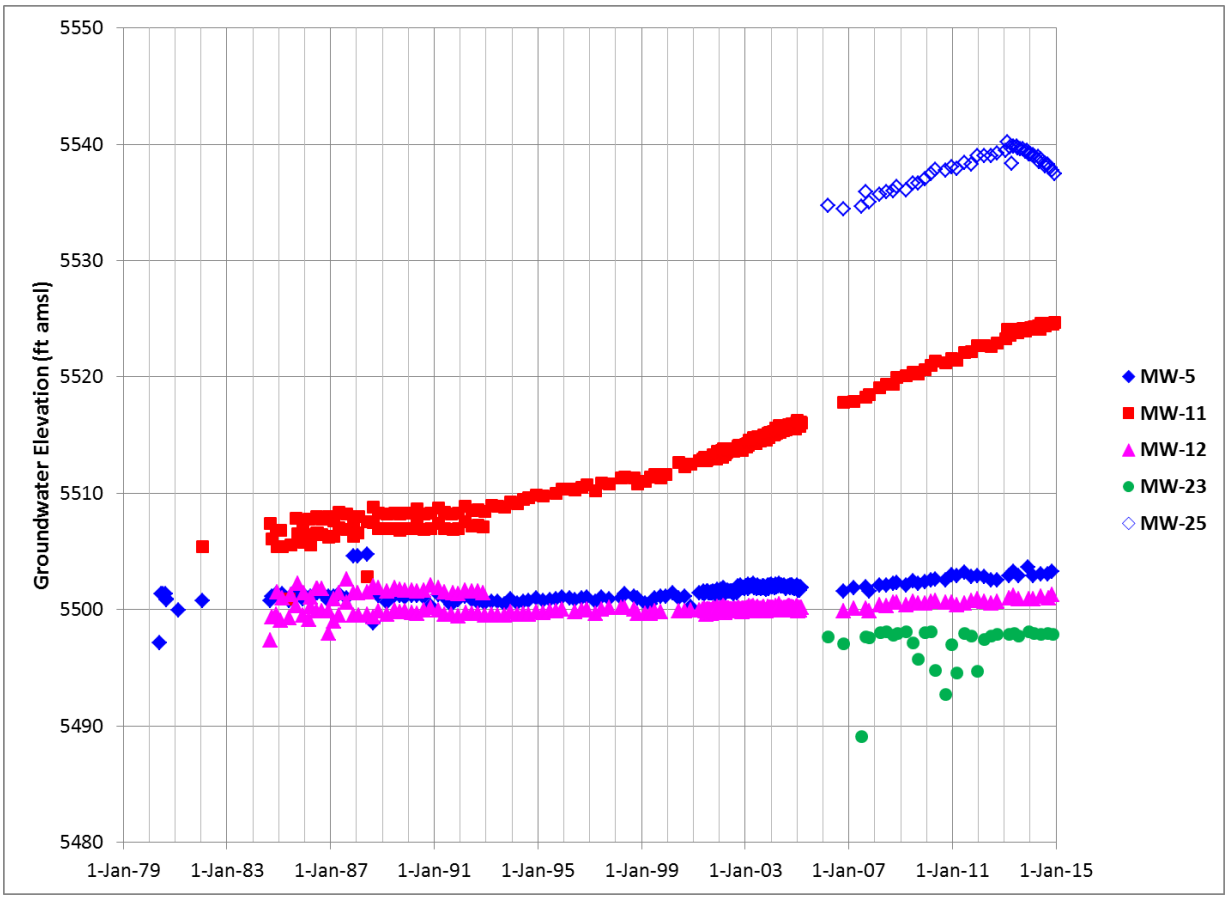

FIGURE 6 - HYDROGRAPHS OF MONITORING WELLS FOR TAILINGS CELL 3

Water levels in MW-14 and MW-15 (Figure 7) have exhibited a gradual and steady increase with time since their installation in 1989, with a total increase of a few feet. This increase corresponds with that observed in the older upgradient wells MW-11 and MW-4 and again shows leakage from a neighboring facility. More importantly MW-14 and MW-15 are not influenced by the wildlife pond seepage and thus show that whatever the other seepage source is, it continues to exist. The water level in MW-14 fluctuates prior to 1993 in the same manner as observed for wells MW-11 and MW-12. This fluctuation is attibuted to the use of different reference elevations for the water levels calculated from depth to water in different data sources.

Well MW-17 located to the southeast of Cell 4A shows a sharp rate of water level increase starting in 2000 with a total increase of about 16 ft by the end of 2014. This again indicates a response to seepage from the wildlife ponds. Given that the response was delayed by about 7 years from the upstream wells, it is anticipated that this rise will continue through 2019 or 2020.

The wells on the western and southern sides of tailing cell 4B (MW-35, 36, and 37) indicate a stable water elevation similar to that observed in upgradient wells MW-23 and MW-2. MW-37

exhibited lower water levels in 2011 and 2012 but has been stable since then. This is likely attributable to the inclusion of water level measurements after well purging and sampling.

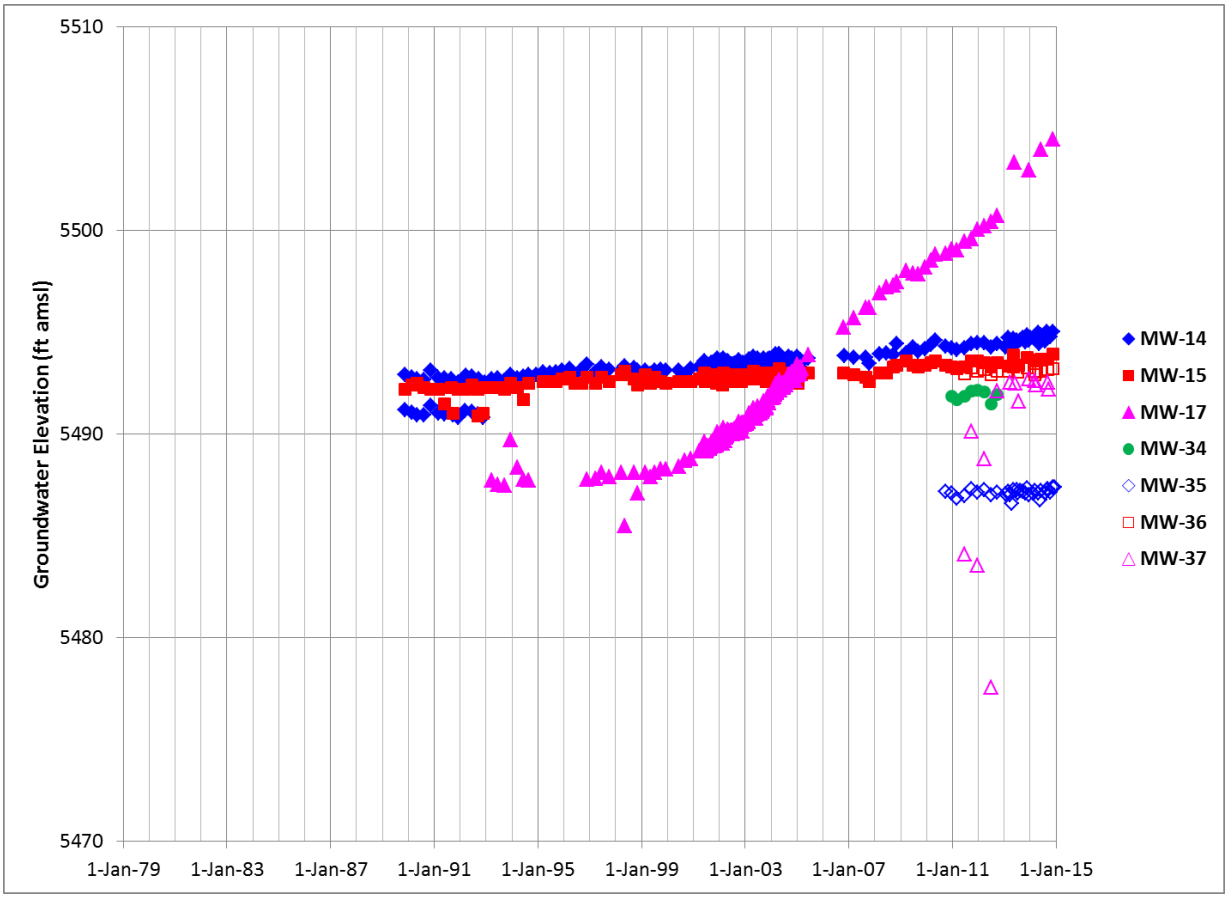

FIGURE 7 - HYDROGRAPHS OF MONITORING WELLS FOR TAILINGS CELLS 4A AND 4B

Water levels in downgradient well MW-3 and MW-3A (Figure 8) have remained relatively stable over time, but have begun to gradually increase since 2012. This increase appears to be associated with the seepage from the wildlife ponds although the response is about 15 years later than observed in the most upgradient wells. However, water levels in MW-22 have increased about 6 ft since the well was installed in 1994 before stabilizing in 2012. This timing coincides with the observance of seepage from the wildlife ponds and indicates that there is a high hydraulic conductivity connection between MW-22 and the upstream areas that exhibit a similar rapid response. MW-22 responded more quickly than the nearest upgradient well MW-17 suggesting a higher hydraulic conductivity conduit between this well and the upgradient areas. MW-20 exhibited a stable water level from 2000 to 2008, but since then has exhibited a declining and often erratic water level. The base of the Burro Canyon is at an elevation of 5448 ft amsl in this well.

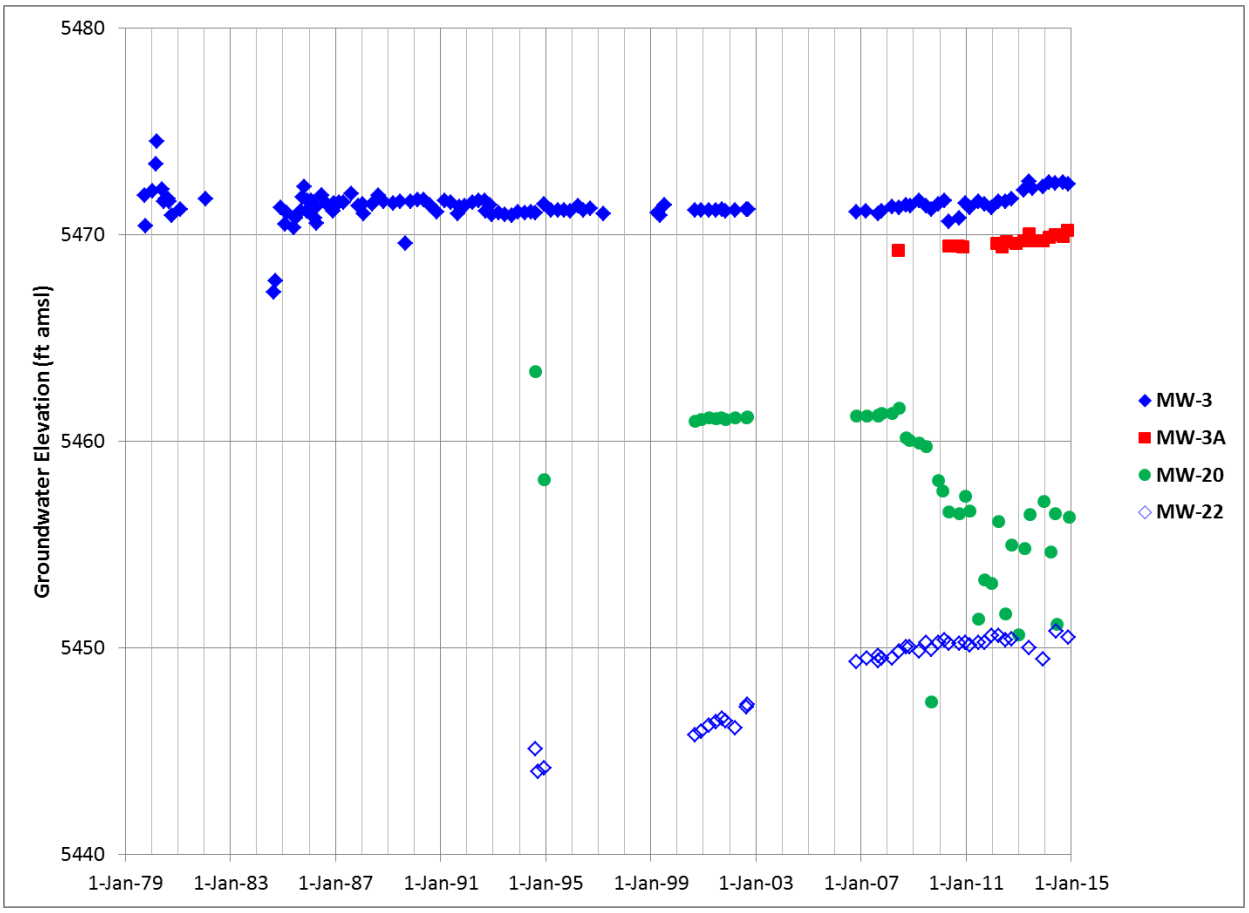

FIGURE 8 - HYDROGRAPHS OF DOWNGRADIENT MONITORING WELLS

Figure 9 presents the estimated change in water level from August 1994 to March 2014. This point in time was selected as it is generally before or just at the start of the appearance of the effects of seepage from the wildlife ponds. It also includes four recently installed wells (MW-18, 19, 20, and 22). As only 14 monitoring wells were available for water level measurements in August 1994, some additional water levels in downgradient areas with no expected water level change, as well as the most upgradient point, were included to produce Figure 9.

Figure 9 shows the extent of groundwater mounding that has been created by discharge to the wildlife ponds and other sources. Two of the points of highest groundwater level change are observed in the area of the lower north wildlife pond and the south wildlife ponds. However, there is also indication of another center of mounding near the northwest corner of the mill (vicinity of Roberts Pond and Lawzy Sump) that is also associated with a source of high nitrate and chloride. This has been previously attributed to a stock watering pond that existed in this area from the 1920s until the mill construction around 1980, and has been considered the source of the nitrate and chloride plume (HGC, 2104). However, the groundwater mounding in this area has occurred since August 1994, or long after the old stock watering pond was removed. Therefore the current mounding cannot be associated with this old pond.

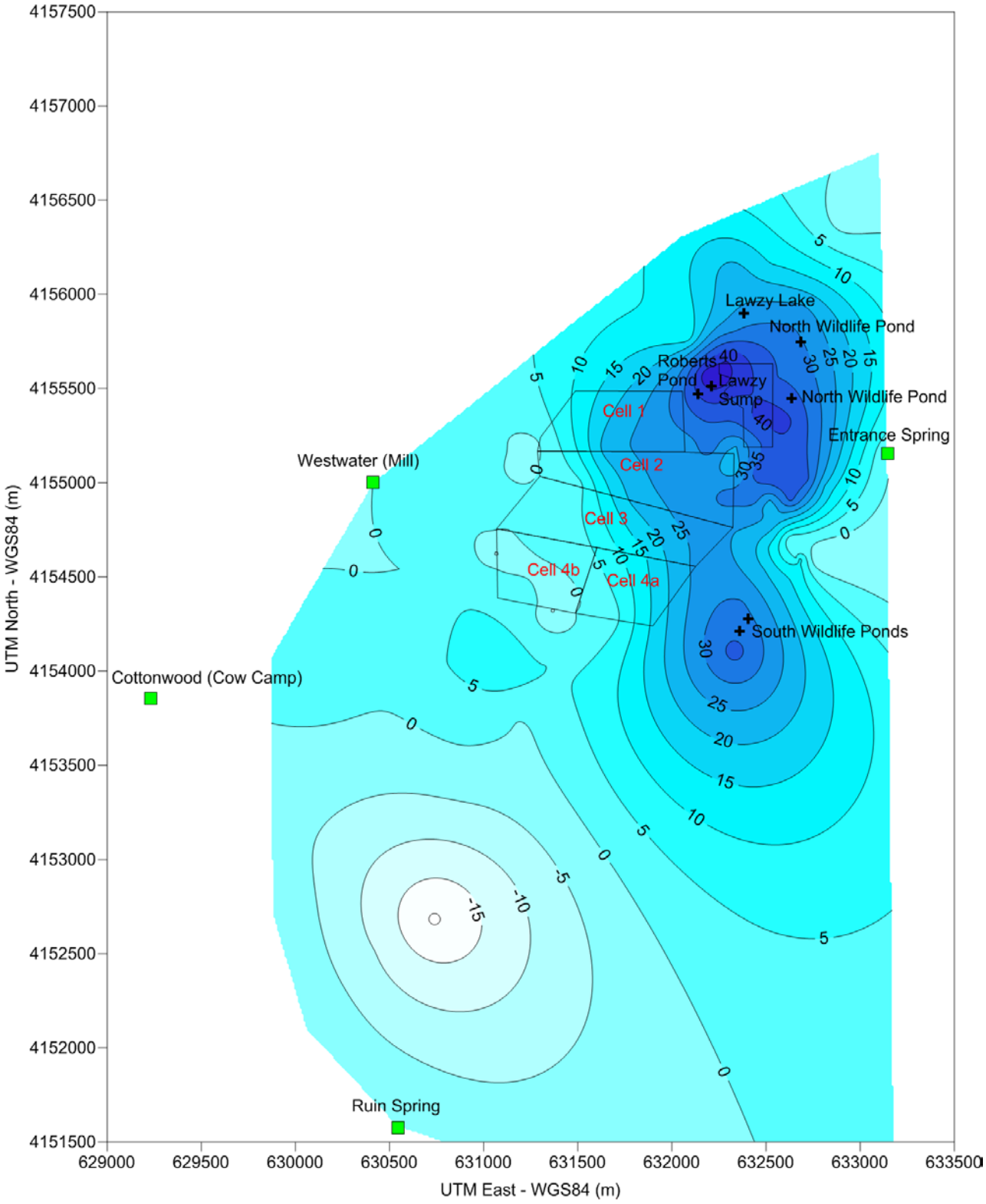

FIGURE 9 - CHANGE IN PHREATIC SURFACE (AUGUST 1994 TO MARCH 2014)

As further evidence of this, it is noted that several other stock watering ponds currently exist at the site. These ponds are normally observed to be dry in aerial photos as well as in past environmental studies due to limited precipitation and runoff at the site (Dames and Moore, 1978). Furthermore, the ponds have not been identified as sources of nitrate or chloride and there is no evidence of mounding associated with any of these ponds based on water level monitoring since 1979.

The volume of water that has infiltrated from the wildlife ponds was estimated using the data from Figure 9 by considering the increase in the groundwater volume in storage within the aquifer since August 1994, while recognizing that additional seepage sources may be contributing to the total seepage during this time period. These calculations are shown in Table 4. Water has been removed from the system since 2010 from pumping of remedial wells. Based on the nitrate groundwater monitoring report for the fourth quarter of 2013 (Energy Fuels Resources, 2014c), the combined pumping from these wells from the third quarter of 2010 through the fourth quarter of 2013 (total of 1280 days) has totaled 8.62 million gallons (1.15 million ft^3) with generally similar total amounts reported for every quarter. This is equivalent to an average pumping rate of 4.7 gpm. We note that the indicated average pumping rate from all wells from Table 3 of the same report is much higher (about 118.6 gpm), presumably due to the fact that the wells do not pump continuously. Over the period used for the comparison of groundwater elevations (August 24, 1994 to March 27, 2014 or 1367 days) it is estimated that the total water removed by pumping from the nitrate wells was 1.23 million ft^3. Thus the total recharge from the wildlife ponds and the additional source is estimated at about 150 gpm over a period of 17.6 years. The total aquifer storage change accounts for about 32% of the total water in the aquifer within the contoured area of Figure 9, suggesting this water has had a significant influence on the current aquifer water chemistry. The seepage rate of 150 gpm, corresponds with total facility usage of 650 gpm less 380 gpm of water consumption in the tailings per Section 2.

TABLE 4 - CALCULATION OF AVERAGE WILDLIFE POND SEEPAGE

COMPONENT	INSIDE 0 FT CONTOUR	INSIDE 5 FT CONTOUR
Aquifer volume change (ft^3)	1,106,216,280	1,029,576,600
Porosity	17.3%	17.3%
Aquifer storage change (ft^3)	191,375,416	178,116,752
Pumping well removal (ft^3)	1,230,269	1,230,269
Start Date	18-Aug-94	18-Aug-94
End Date	31-Mar-12	31-Mar-12
Elapsed time (days)	6435	6435
Total surface discharge (gpm)	155.5	144.8

3.1.6 Hydraulic Properties

The hydraulic properties of the perched aquifer are important to determining the rates of groundwater flow, solute transport, and groundwater storage. Anisotropy in the subsurface may also impact preferred routes or directions of solute migration.

The horizontal hydraulic conductivity of the Burro Canyon and Dakota Sandstone (HGC, 2014) measured from testing of site wells and piezometers are very similar. The measured hydraulic conductivity values are log normally distributed and range from a low of 2.4×10^{-4} ft/d to a maximum of 320 ft/d, with a geometric mean value of 0.15 ft/d, and an arithmetic average value of 4.3 ft/d. Figure 10 shows the horizontal distribution of log hydraulic conductivity values for the perched aquifer zone based on the best fit variogram model of the data.

Figure 10 indicates a higher conductivity zone or channel passing in a north-south direction along the eastern side of the site and below the eastern edge of Tailings Cells 2, 3, and 4A. Higher conductivity channels provide preferential pathways for contaminant migration and their presence is consistent with the lithology of the perched aquifer sandstones as noted previously in section 3.1.3 of this report. The data suggest that a similar higher conductivity channel may exist to the west-southwest of Cell 4B. The eastern channel may also extend to the south or east of MW-17 towards MW-22, as suggested by the previously presented hydrographs. It is important to note that two-thirds of the hydraulic conductivity tests performed, including all of the down gradient tests were slug tests. Slug tests provide only very localized (point) measurements of hydraulic conductivity and are less reliable in predicting conductivity distribution where data are sparse. The well tests also only provide an arithmetic average hydraulic conductivity over the entire saturated aquifer thickness, so horizons with a higher hydraulic conductivity are probably present.

The seepage rates for each pond were calculated based on the average wetted area of each wildlife pond over the period of seepage as shown in Table 5. Seepage rates for each pond likely vary according to subsurface conditions. For example, the upper north pond was originally a stock water pond and later used for storage of reclaim water, and as a result likely contains more fine grained sediments along the pond bottom. Since seepage from the ponds is under a unit hydraulic gradient (i.e. gravity is the only driving force), this indicates an average saturated vertical hydraulic conductivity of 0.193 ft/day for the soils underlying the ponds but overlying the perched sandstone aquifer. Vertical conductivity of the sandstone aquifer is likely less, this being accommodated by lateral spreading of the infiltration over the underlying bedrock surface. Nonetheless, as seen in Figure 9, the center of groundwater mounding associated with the south wildlife ponds and the lower north wildlife pond are close to the center of those ponds.

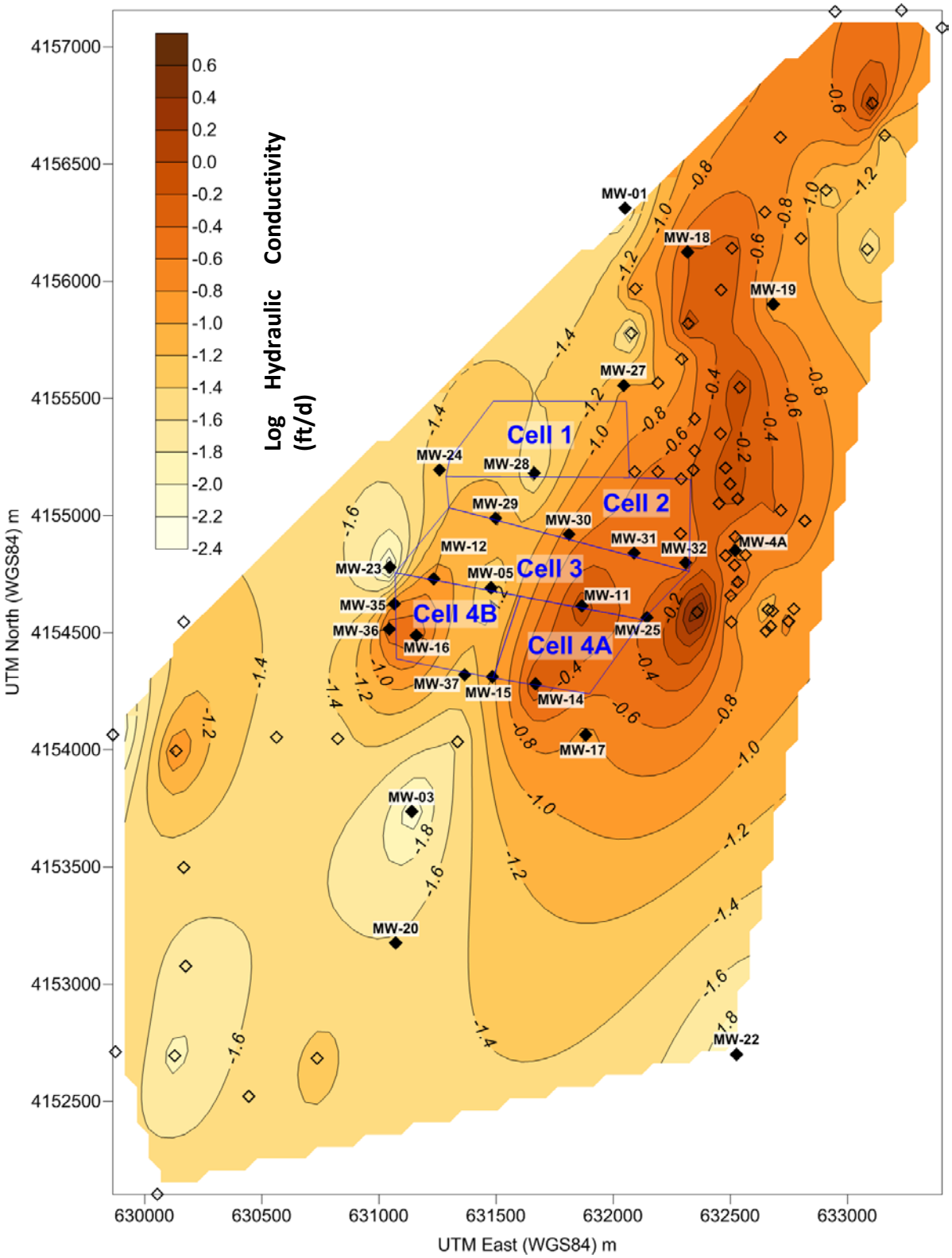

FIGURE 10 - DISTRIBUTION OF LOG HYDRAULIC CONDUCTIVITY

TABLE 5 - CALCULATION OF SEEPAGE RATES FOR WILDLIFE PONDS

WILDLIFE POND	TOTAL POND AREA	FLOODED AREA	WETTED AREA	EQUIVALENT POND RADIUS	SEEPAGE RATE (K=0.193 FT/D)
	(ft^2)	(% total)	(ft^2)	(ft)	(gpm)
Lower South	66,900	44%	29,354	97	29.4
Upper South	42,232	29%	12,374	63	12.4
Lower North	118,116	47%	55,945	133	56.0
Upper North	77,169	68%	52,214	129	52.3
Total	304,417		149,887		150.1

Table 6 shows the calculated travel time for discharge from each pond to initially reach the water table based on a soil hydraulic conductivity of 0.19 ft per day and various estimated vertical bedrock hydraulic conductivity values (equal to the indicated seepage rate of 0.19 ft/d from Table 4, equal to the harmonic mean of all individual well tests of 0.0078 ft/d, and 0.0026 ft/d which approximately matches the expected travel time if the northern wildlife ponds were operational in the early 1980s). Additional review of older aerial photos could reduce the uncertainty in these estimates by establishing the actual time of initial pond flooding. This travel time would be reduced as groundwater mounding raises the water table.

TABLE 6 - CALCULATION OF VERTICAL HYDRAULIC CONDUCTIVITY AND TRAVEL TIMES

WILDLIFE POND	LAYER THICKNESS (ft)		TIME TO REACH WATER TABLE (yrs) WITH BEDROCK HYDRAULIC CONDUCTIVITY (ft/d) OF		
	SOIL	BEDROCK	0.193	0.0078	0.0022
Lower South	13	70	0.17	3.5	12.3
Upper South	15	70	0.17	3.4	11.9
Lower North	15	65	0.16	3.1	10.8
Upper North	5	65	0.16	3.7	12.9

The observed groundwater mounding provides data that can be used to examine hydraulic conductivity over a much larger area than the individual well tests. Therefore, the measured water level response in monitoring wells to seepage from the wild ponds was examined to compare with the well test measurements. These analyses are summarized in Table 7. Graphs of the data matches are presented in Appendix A. Analysis of responses in upgradient wells MW-1, MW-18, and MW-19 to the groundwater mounding from the north wildlife ponds and mill site mounding area indicated a very similar response to the pond infiltration and were therefore analyzed as a single test. As expected analysis from the large scale (site wide) response to the groundwater mounding indicated much more uniform values of hydraulic conductivity and storativity than observed for the well tests since the observed response

involves a much larger area of the perched aquifer. The average hydraulic conductivity from the groundwater mounding analysis (4.0 ft/d) is significantly higher than that measured for all of the individual well tests (0.15 ft/d) as well as the well tests listed in Table 7 (0.63 ft/d). The average storage coefficient from the mounding analysis is also higher (4.7%) compared to 0.81% for all of the individual well pump test analyses and 1.8% for the well tests listed in Table 7. Higher hydraulic conductivity values correspond to faster rates of contaminant migration and may explain the discrepancy between predicted and observed rates of migration as discussed later in section 3.17.

TABLE 7 - ANALYSES OF LARGE SCALE HYDRAULIC CONDUCTIVITY AND STORATIVITY FROM GROUNDWATER MOUNDING

WELL	VALUES FROM GROUNDWATER MOUNDING ANALYSIS				VALUES FROM INDIVIDUAL WELL TESTS		
	TRANS-MISSIVITY	SATURATED THICKNESS	HYDRAULIC CONDUCTIVITY	STORATIVITY	TEST TYPE	HYDRAULIC CONDUCTIVITY	STORATIVITY
	(ft^2/d)	(ft)	(ft/d)	(ft/ft)		(ft/d)	(ft/ft)
MW-1	96	66	1.5	0.16	Pump/Recovery	0.0042	0.0082
MW-18					Slug/Injection	0.23	0.0067
MW-19					Slug/Injection	0.024	0.015
MW-4	187	52	3.6	0.0054	Pump	0.23	0.011
MW-11	102	45	2.3	0.054	Pump/Recovery	3.9	N.A.
MW-17	44	46	0.97	0.0026	Slug/Injection	0.024	0.0065
MW-22	627	54	12	0.013	Slug	0.0074	0.058
Average	211	53	4.0	0.047	Average	0.63	0.018
Geomean			2.8	0.024	Geomean	0.083	0.013

Notes: N.A. = not available, Geomean = geometric mean

Porosity measurements have been made on core samples obtained from the site (Titan, 1994) from monitoring wells MW-16 (center of Tailings Cell 4B) and MW-17 (directly down gradient of Tailings Cell 4A). In general, the porosity values were relatively consistent averaging 19.9% (range of 13 to 26%) for the Dakota Sandstone and 19.1% (range of 12 to 27%) for the Burro Canyon. For sandstone samples above a depth of about 80 ft bgs, the average total porosity was 19.8% and the residual volumetric moisture content was 2.5%, indicating a drainable or effective porosity of 17.3%. Subsequent testing of vadose zone samples (MWH, 2010) indicated an average porosity of 18.4% and a residual volumetric moisture content of 0.3%, indicating a drainable or effective porosity of 18.1%. In comparison, measured storage coefficient from all well tests averaged about 15%, although some of the reported test values exceeded the maximum physically possible (i.e. storage coefficient greater than 0.3). Excluding these values, the average of all tests was about 2.7%. It is noted that single well tests do not provide a reliable estimate of the aquifer storage coefficient due to the very small radius of observation and disturbance of natural conditions near the well. The average storage coefficient obtained from observation wells (excluding TW4-19) during pumping tests was significantly less ranging

from about 0.4 to 1.5% and averaging 0.8%. These values are generally indicative of a semi-confined aquifer (rather than an unconfined aquifer) and indicate that hydraulic connections between wells are via more permeable horizons or channels within the aquifer. One exception for the pumping test data was TW4-19 (located near the northeast corner of Tailings Cell 2) which had a storage coefficient of 0.12, indicating unconfined aquifer conditions.

3.1.7 Groundwater Travel Times

Previous estimates of groundwater travel times have been presented (Titan, 1994; HGC, 2009; HGC, 2014). Previous estimates of travel times below the tailings cells through the unsaturated (vadose) zone are summarized in Table 8.

TABLE 8 - PREVIOUSLY PREDICTED CONTAMINANT TRAVEL TIMES THROUGH THE VADOSE ZONE

SOURCE	LOCATION	VELOCITY (ft/yr)	DISTANCE (ft)	TRAVEL TIME (yrs)
Titan, 1994	Overall site	0.7 to 2.2	109.5	50 to 150
HGC, 2009	Overall site	0.24	67	276
HGC, 2014	Tailings Cells 2, 3, 4A, 4B	0.24	48 to 69	200 to 288

These travel times are dependent upon the assumed leakage rate (rate of seepage). For example the HGC estimates are based on uniform leakage across the entire footprint of the tailings cells. In reality, leakage through liners are concentrated at locations of leaks, and not uniformly distributed across the entire liner footprint. Based on the previous analysis of seepage from the wildlife ponds (Table 5) we know that under saturated conditions at ground surface, water will move downward through the unsaturated zone between 0.045 and 0.013 ft/d (4.6 to 16 ft/yr). Thus if the seepage rate becomes high enough due to a significant breach of the liner, it could potentially travel the 48 to 69 feet below the cells in 3 to 13 years. We also note that saturated conditions can be expected at fairly low rates of seepage (i.e. a seepage rate of less than 0.19 ft/d or only 0.001 gpm/ft^2). However, since seepage from the mill facilities could take up to 13 years to reach the groundwater surface, the detection of seepage in the monitoring wells may be delayed by several years after a release has occurred.

Table 9 summarizes previous estimates of groundwater travel times within the saturated zone. The predicted migration rates are seen to be approximately 100 times slower than the observed rates of migration at the site for the nitrate and chloroform plumes. It is important to note that the observed rates of migration do not account separately for travel time through the vadose zone, so that actual rates of migration within the subsurface would be greater than indicated. The calculations for the nitrate plume migration are based on the assumption that an old stock watering pond (removed during the mill construction) is the source of this release.

However, as discussed previously in section 3.14 of this report there is no supporting evidence for recharge from this pond (or other stock watering ponds in the area). If the travel time is reduced to that of the life of the facility (35 years), the calculated downstream travel velocities equal those calculated for the chloroform plume (which overlaps much of the same plume area).

TABLE 9 - PREVIOUSLY PREDICTED AND OBSERVED RATES OF CONTAMINANT MIGRATION

SOURCE	SITE LOCATION	TRAVEL VELOCITY (ft/yr)	TRAVEL DISTANCE (ft)	HYDRAULIC GRADIENT (ft/ft)	TRAVEL TIME (yrs)
BASED ON CALCULATIONS OF POTENTIAL MIGRATION					
Titan, 1994	Overall site	0.89	8000	0.015	8,900
HGC, 2009	Overall site	1.59	10000	0.012	6,303
HGC, 2014	Downgradient Path 3	0.68	2200	0.012	3,470
	Downgradient Path 4	0.26	4125	0.0046	15,850
	Downgradient Path 5	0.60	11800	0.031	19,900
	Downgradient Path 5	0.91	9685	0.012	19,900
BASED ON OBSERVED RATES OF ACTUAL MIGRATION					
HGC, 2014	Nitrate Path 1	21	1250	0.028	60
	Nitrate Path 1	35	2200	0.048	63
	Chloroform Path 2A	76	1200	0.028	16
	Chloroform Path 2B	38	1450	0.026	38
	Chloroform Path 2B	84	1750	0.038	21

The higher observed rates of migration has been attributed to the fact that channels or zones of higher hydraulic conductivity exist in the areas of the releases, although these conduits were only identified after the releases were detected and considerable additional investigations were performed to track the releases. As discussed in the previous sections, there is certainly significant potential that such zones are also present downgradient of the site, particularly to the southeast where the perched aquifer has a much greater saturated thickness. Such potential conduits of flow have been previously identified as part of the aquifer lithology and there is no indication or expectation that this lithology would change significantly downgradient of the site. Furthermore, if a release occurs, saturated thickness of the perched aquifer would be expected to increase and could potentially saturate higher conductivity zones that are currently dry. Unfortunately, all recent investigations have focused on potential downstream migration to the southwest. Furthermore, the results of the groundwater mounding analysis indicate a higher hydraulic conductivity at site scales than obtained from individual well tests.

The focus of the recent downgradient investigations is based on assuming that the direction of groundwater flow (and contaminant migration) is perpendicular to the groundwater contours.

This is only true for homogeneous, isotropic conditions. In actuality we see movement of the nitrate plume towards the south with some lateral dispersion along the plume length to the southwest. If the nitrate plume was released near well TWN-2, as suggested by previous studies (Intera, 2009; HGC, 2014), the groundwater contours (both historic and current) would have indicated migration from this point to the southwest (towards wells MW-23 and MW-12). The reason for this is that groundwater flow will preferentially follow the more conductive (higher hydraulic conductivity) channels. Groundwater mounding in the vicinity of the south wildlife ponds appears to be trying to divert groundwater flow to the southwest. However, this mounding is slowly dissipating and will not influence plume migration in the same manner in the future.

3.2 Groundwater Chemistry

Groundwater monitoring has been conducted at the site since the start of operations. According to available information (DRC, 2004), groundwater monitoring was conducted between 1979 and 1997 in thirteen monitoring wells. This monitoring included up to 20 parameters and was generally conducted on a quarterly basis. In 1997 this was reduced to six point of compliance or POC wells (MW-5, 11, 12 on the south edge of Cell 3, and MW-14, 15, 17 on the south edge of Cell 4a) and for only 4 parameters (chloride, nickel, potassium, and uranium). In May of 1999, a split sampling round of all wells was conducted by NRC and DRC for a much wider range of parameters including heavy metals, nutrients, general water chemistry parameters, radiological indicators, and volatile organic compounds (VOCs). This sampling round led to the discovery of a chloroform plume and many additional monitoring wells were installed. Subsequent sampling has also detected a larger nitrate and chloride plume leading to the installation of additional upstream monitoring wells.

According to our review of available information a total of 34 permanent monitoring wells (identified as MW series) have been installed at the site between 1979 and 2011, with only 5 of these installed just before or coincident with the start of operations. However, three of these wells (MW-6, 13, and 16) and were destroyed during construction of Tailings Cells 3, 4A and 4B, respectively. Three wells (MW-16, 21, and 33) were dry and never sampled. Two wells (MW-4 and MW-4a) are used for extraction of impacted groundwater and are not currently sampled (although MW-4 was sampled prior to 2010). Well MW-34 is no longer sampled. This leaves a total of 27 monitoring wells in current use. These wells are currently sampled for general water quality parameters, major ions, trace metals, and organic compounds. Figure 11 shows the available period of record of sampling results each of these permanent monitoring wells.

An additional 35 temporary monitoring wells (identified as TW4 series) were installed in the area of the chloroform plume between 2002 and 2014. These wells were sampled for four organic compounds (carbon tetrachloride, chloroform, chloromethane, and methylene chloride), chloride, and nitrate. An additional 19 temporary monitoring wells were installed upstream of the site in 2010 to define the source of a nitrate and chloride plume at the site and

have been sampled for chloride and nitrate. Figure 12 shows the available period of record of water chemistry sampling results for each of these temporary monitoring wells.

Figures 13 and 14 show the location of each of the above monitoring wells. Apart from the location of a few of the initial monitoring wells (Titan, 1994), most of the coordinates of the monitoring wells have not been published and thus are based on interpolation from well locations presented in monitoring report figures (data for wells MW-6, MW-13, and TW4-15 are not available).

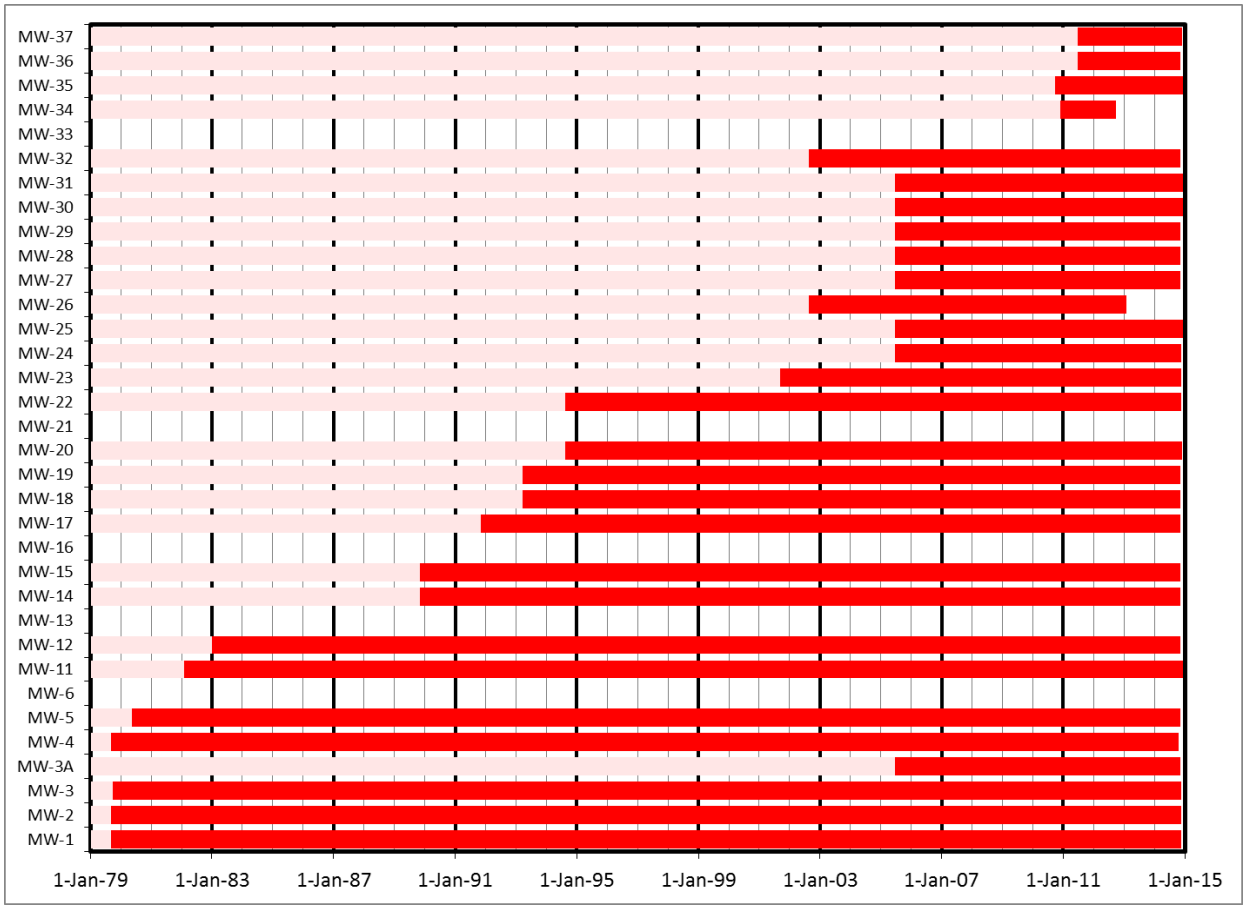

FIGURE 11 - AVAILABLE PERIOD OF RECORD FOR PERMANENT MONITORING WELLS

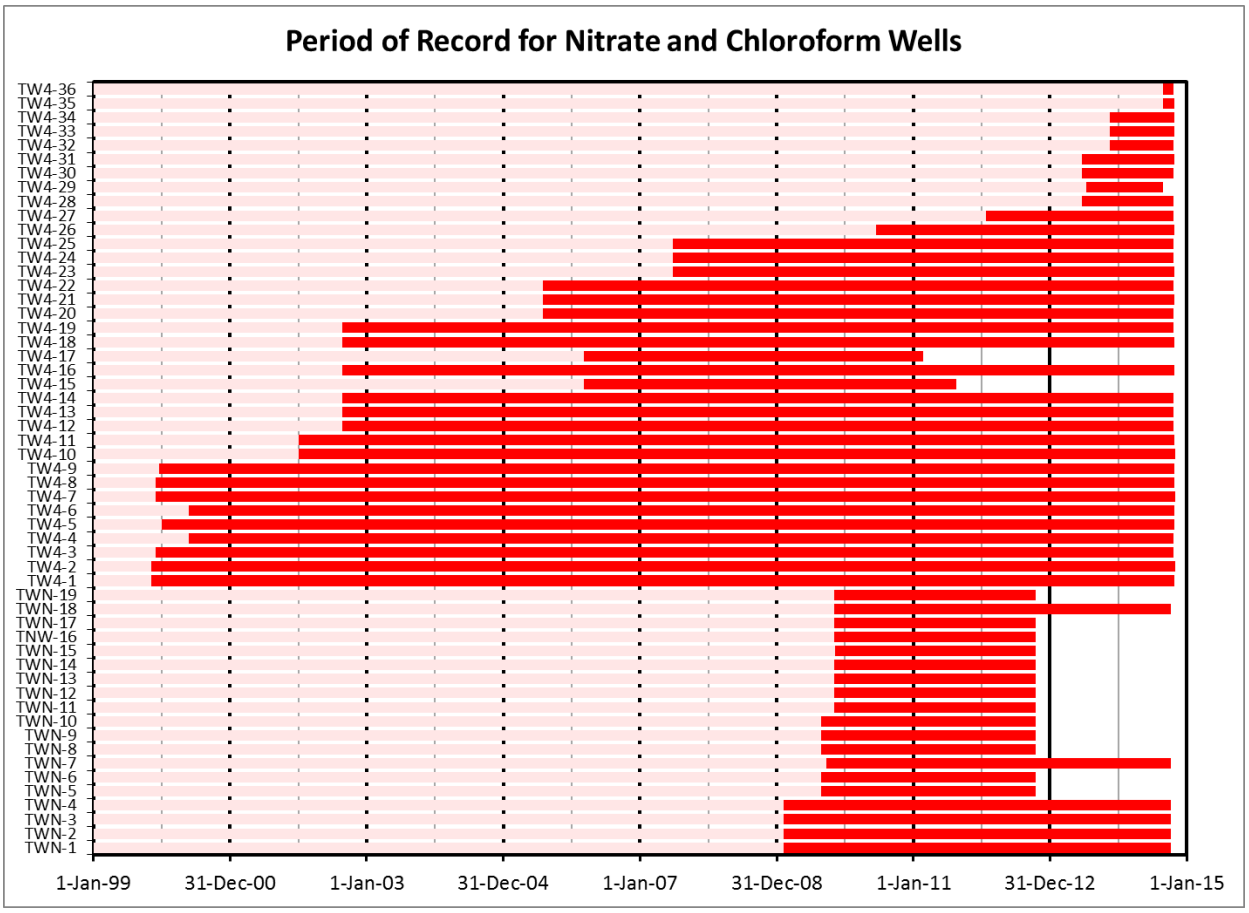

FIGURE 12 - AVAILABLE PERIOD OF RECORD FOR TEMPORARY MONITORING WELLS

FIGURE 13 - LOCATION OF MONITOR WELLS

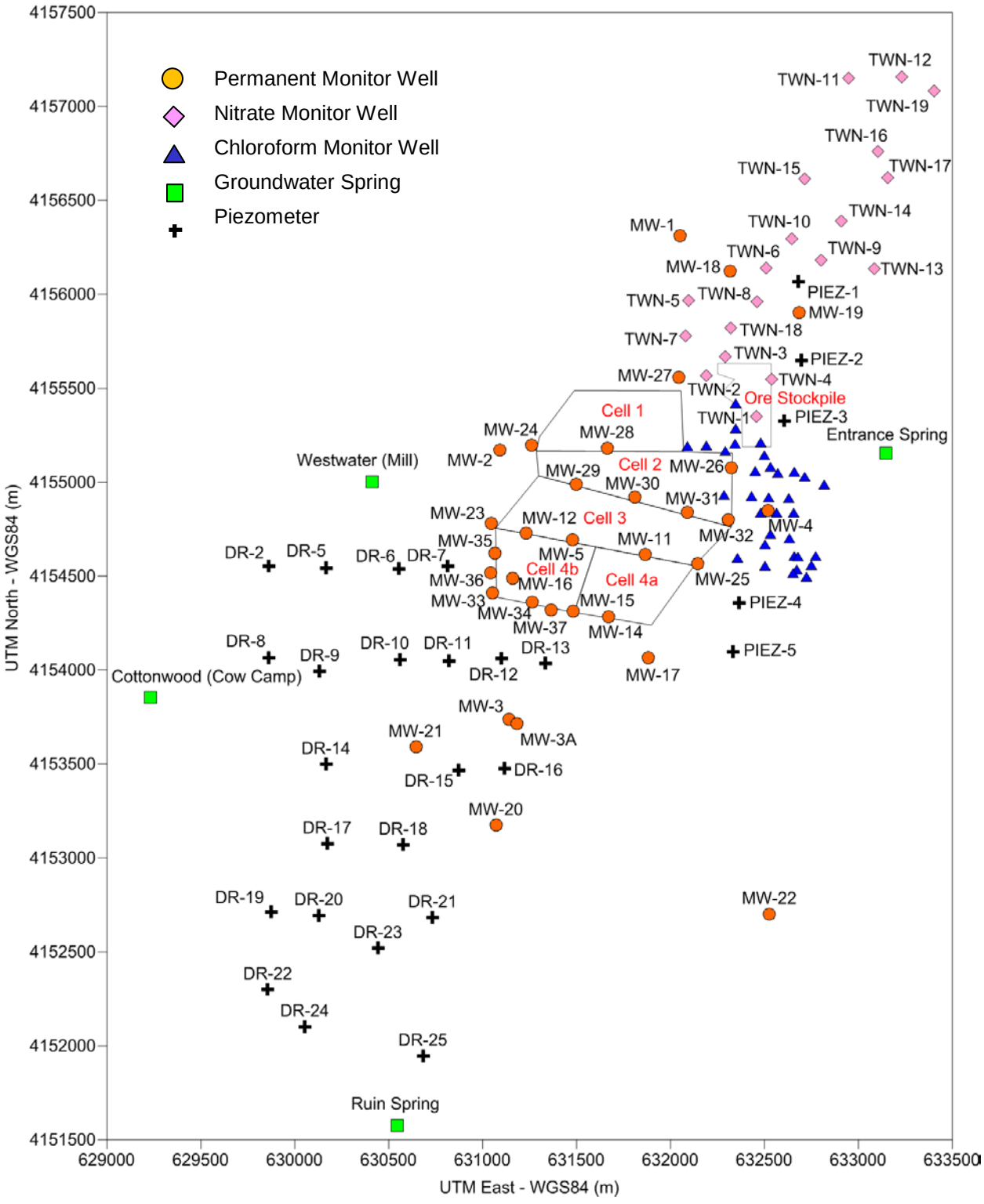

FIGURE 14 - LOCATION OF CHLOROFORM MONITORING WELLS

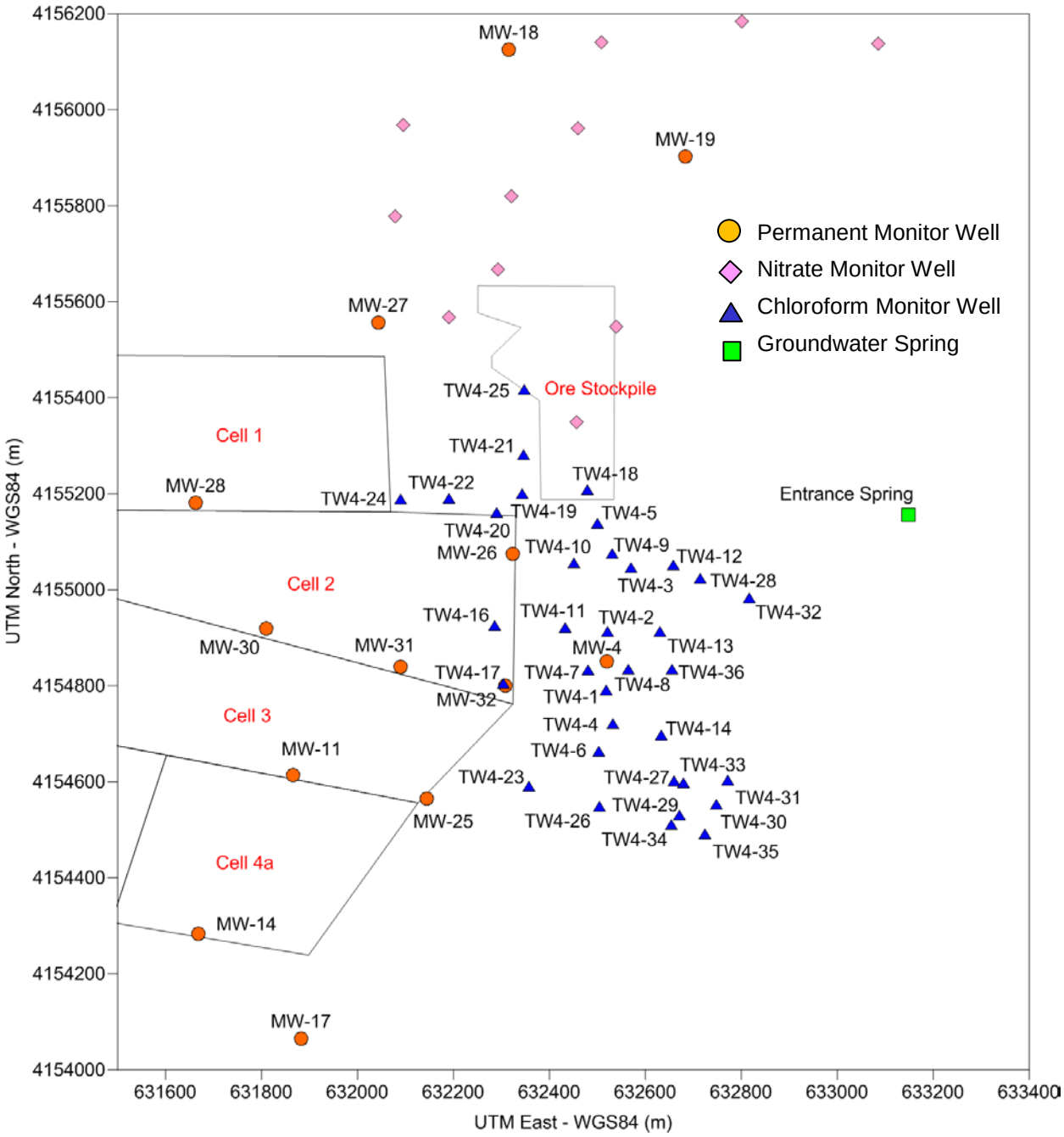

For this study, available groundwater sampling information submitted in electronic format to DRC was obtained and placed into a database. In general this covers the period 2005 to 2014 for most chemical parameters. Data on groundwater elevations and pH in electronic format are limited to those data presented by Intera, 2012. More recent data for late 2012, 2013, and 2014 was added from field sampling notes contained in the published quarterly groundwater monitoring reports. Well ground surface elevations and top of casing (reference elevation for groundwater depths) was determined from well logs although not all well logs are available or contain this information. This information is also not contained in the groundwater monitoring reports, only measured depth to groundwater. Groundwater ground surface and top of casing information was obtained from well logs, where available, or estimated from measured groundwater elevations (from electronic data files) and reported groundwater depths as measured on December 21, 2010. It is noted that small discrepancies exist between TOC elevations determined from reported groundwater elevations and the TOC elevations from well logs.

Data on tailings solution chemistry was obtained from annual reporting (Energy Fuels Resources, 2014d) which includes annual reporting since 2007 as well as 1987 and 2003 data for Tailings Cells 1 and 3. Data for Tailings Cell 4A is available from 2009 and from cell 4B from 2011. Data for cell 2 is from the slimes drain.

Table 10 presents a summary of the average concentrations of the chemical parameters monitored in the permanent monitoring wells for the period 2005 to 2014. The detection frequency for all sample parameters for the period 2005 to 2014 is shown in Table 11. The wells are ordered from left to right to correspond with their position from up gradient to down gradient groundwater flow across the site. Average concentrations for the tailings cell solutions are presented on the left for comparison.

For the general water parameters and the major cations and anions, the table cells are color coded in Table 10 according to the range of values for that parameter with red indicating the highest concentrations (lowest for pH values to indicate higher hydrogen ion concentrations) and blue indicating the lowest concentrations. For the heavy metals and organic compounds highlighting is used in Table 10 to indicate the frequency that the compound was detected. Red shaded cells indicate the parameter was detected in 50% or more of the collected samples, orange shading indicates it was detected in less than 50% of the samples, and yellow shading indicates the parameter was not detected in any of the samples. Where a parameter was not detected, the concentration was assumed to be zero in calculating the average concentrations. This was necessary since the detection limit varies between monitoring rounds and samples, thereby providing background noise when making comparisons. It is also a conservative assumption for the purposes of this analysis since the actual concentration can vary between the detection limit and zero.

We note that while earlier sample data on some heavy metals is available (Titan, 1994) in reviewing the sample results we found results that suggested that there was potential sample

contamination in the field or laboratory. That is when heavy metals were detected (where it had not been detected in previous sampling rounds) it was often detected in all samples collected during that round.

The analysis of the data presented in Table 10 is presented in the following sections of this report.

TABLE 10 - AVERAGE CHEMICAL PARAMETER CONCENTRATIONS (2005 TO 2014) IN PERMANENT MONITORING WELLS

Parameter	Tailings Cells and Slimes	Upgradient			Cell 1				Cell 2						Cell 3					Cell 4A			Cell 4B				Downgradient			
		MW-1	MW-18	MW-19	MW-27	MW-2	MW-24	MW-28	MW-4	MW-26	MW-29	MW-30	MW-31	MW-32	MW-5	MW-11	MW-12	MW-23	MW-25	MW-14	MW-15	MW-17	MW-34	MW-35	MW-36	MW-37	MW-3	MW-3A	MW-20	MW-22
General Parameters																														
Gross Alpha (-Rn&U)		0.92	1.1	1.3	1.5	1.1	1.1	1.4	0.58	3.1	1.3	0.85	1.0	3.7	0.81	0.82	0.79	1.8	1.0	1.1	0.74	1.1	0.93	4.7	1.6	1.6	0.73	1.0	0.96	6.2
pH	2.0	7.4	6.7	7.1	7.3	7.2	6.6	6.4	7.1	6.8	6.8	7.1	7.3	6.5	7.6	7.7	7.0	6.9	6.8	6.8	7.0	7.0	7.3	6.7	6.9	6.9	6.8	6.9	7.8	6.0
Ammonia as N	5,434	0.19	0.08	0.07	0.04	0.08	2.7	0.10	0.05	0.34	0.80	0.06	0.04	0.76	0.51	0.63	0.10	0.12	0.49	0.10	0.06	0.07	0.05	0.10	0.05	0.07	0.10	0.12	0.17	0.48
Nitrate+Nitrite as N	76	0.12	0.06	2.8	5.9	0.08	0.25	0.21	5.3	1.1	0.08	16	22	0.06	0.14	0.08	0.11	0.28	0.07	0.08	0.18	0.81	0.30	0.09	0.19	2.1	0.35	1.1	8.6	2.9
TDS	132,480	1290	3078	1167	1060	2941	3994	3545	3173	3041	4257	1574	1320	3614	2165	1909	3855	3449	2727	3459	3711	3752	3513	3644	4293	3866	5010	5508	5527	7385
TDS @ 180 C		1344	3136	1215	1079	3143	4096	3660	1637	3141	4342	1629	1287	3755	2062	1886	3819	3411	2791	3579	3797	4001	3733	3581	4410	3953	5157	5602	5511	7488
GW Elevation		5575	5580	5594	5576	5503	5507	5543	5543	5558	5512	5538	5547	5546	5502	5514	5500	5497	5538	5493	5493	5492	5492	5487	5493	5490	5471		5458	5449
Major Cations (mg/L)	**Total:**	**399**	**879**	**352**	**318**	**891**	**1152**	**994**	**723**	**863**	**1196**	**462**	**362**	**982**	**653**	**642**	**1037**	**963**	**787**	**993**	**1091**	**1102**	**1068**	**1039**	**1292**	**1137**	**1433**	**1572**	**1749**	**1704**
Calcium	531	162	558	154	167	327	484	510	289	494	489	274	177	517	139	61	508	438	361	498	434	333	503	495	440	466	448	474	353	440
Magnesium	6,338	61	128	54	74	96	175	173	135	165	225	71	85	226	41	19	214	148	124	151	163	178	147	151	140	132	246	305	70	981
Potassium	1,787	6.8	9.3	4.7	4.3	10	15	12	7.9	11	17	12	6.1	14	8.0	6.7	13	11	9.7	12	10	12	14	11	10	15	24	28	41	23
Sodium	12,736	169	184	140	73	458	478	299	291	193	464	104	94	226	465	556	301	366	292	333	484	579	404	382	701	524	716	765	1285	260
Major Anions (mg/L)	**Total:**	**977**	**2175**	**1287**	**910**	**2136**	**2959**	**2550**	**2289**	**2358**	**3076**	**1107**	**918**	**2733**	**1632**	**1416**	**2851**	**2474**	**2073**	**2562**	**2724**	**2836**	**2590**	**2526**	**2998**	**2727**	**3431**	**3929**	**3838**	**5882**
Chloride	10,671	15	47	46	41	9.4	45	102	44	61	37	128	160	33	54	33	62	7.6	31	20	40	32	71	62	59	46	65	59	62	58
Fluoride	735	0.3	0.23	1.0	0.71	0.31	0.22	0.63	0.37	0.29	0.80	0.37	0.84	0.20	0.88	0.53	0.27	0.28	0.33	0.18	0.23	0.29	0.54	0.36	0.30	0.31	0.64	1.2	0.33	5.3
Sulfate	119,257	679	1698	997	437	1768	2615	2293	1893	1898	2711	794	557	2276	1208	1019	2384	2179	1652	2091	2263	2376	2183	2104	2623	2444	3064	3527	3575	5454
Bicarbonate (as HCO3)	0	283	430	244	431	358	299	154	351	399	327	185	200	424	369	363	404	287	390	451	421	429	335	360	316	236	301	342	201	364
Heavy Metals (ug/L)	**Total:**	**632**	**319**	**46**	**51**	**29**	**4959**	**1761**	**55**	**2120**	**7165**	**175**	**77**	**12868**	**308**	**217**	**229**	**463**	**1652**	**2117**	**201**	**155**	**423**	**457**	**289**	**66**	**703**	**998**	**82**	**36813**
Arsenic	134,511	0	0	0	0	0	2.1	15	0	0.05	1.3	0.74	0.19	0.08	0	0	0	0	0	0	0	0	0	0	0.97	0	0	0	0	0
Beryllium	541	0	0	0	0	0	0.04	0	0	0	0.07	0.31	0	0	0	0	0	0	0	0	0	0	0	0	0	0	0	0.95	0	6.0
Cadmium	5,674	0	0	0	0	0.23	1.6	3.8	0	0.12	0.08	0.67	0	1.84	0	0	0.10	0.25	1.4	1.2	0	0.09	0	0	0	0.04	0.95	2.0	0.06	110
Chromium	7,974	0	0	0	0	0	0	0	0	0	0	7.9	0	0	0	0	0	0	0	0	0	0	0	0	0	0	0	0	0	0
Cobalt	38,240	0	0	0	0	0	2.6	30	0	0.42	0.70	0.68	0	45	0	0	0	0.83	2.3	0	0	0	0	1.1	0	0	0	3.6	0	339
Copper	384,312	0	0	0	0	0	0	0.77	0	0.12	0	1.9	0.06	1.1	0	0.34	0	0.59	0	0	0.57	0	0	0	0.80	0	0.51	1.1	0	27
Iron	3,453,133	496	173	10	9.4	0	1522	48	0	897	1423	78	0	7598	64	90	40	18	0	0	3.9	8.6	105	154	0	5.7	7.9	28	12	37
Lead	8,211	0	0	0	0	0	0.68	0.27	0	0	0	0.71	0	0.08	0	0.03	0	0.43	0.04	0	0	0	0	0	0	0	0	0	0	2.2
Manganese	334,742	134	101	13	0	0	3369	1577	0	1171	5709	36	0	5038	240	123	149	363	1628	2041	48.05	105	153	263	0	15	584	769	19	34,889
Mercury	8	0	0	0	0	0	0.06	0	0	0	0	0	0	0	0	0	0	0	0	0	0	0	0	0	0	0	0	0	0	0.03
Molybdenum	59,490	0	0	0	0	0	1.4	0	0	0	1.2	0	0	6.8	0	0	0	0	8.6	0.30	0	0	0	1.4	0	0	0	0	6.5	427
Nickel	77,239	0	0	0	0	0	9.6	26	0	4.1	0.81	2.9	0.34	60	2	1	3	6.7	0	2.08	4	0	0	1.6	0	2.6	5.5	17	0	178
Selenium	4,012	0	0	13	11	11	1.2	2.9	46	3.9	0.61	36	68	0	0	0	20	1.1	0	0	98	8.9	136	13	259	6.5	35	84	0.27	13
Silver	393	0	0	0	0	0	0	0	0	0	0	0	0	0	0	0	0	0	0	0	0	0	0	0	0	0	0	0	0	0
Thallium	1,333	0	2.5	0.27	0	0	0.60	0.89	0	0	0.14	0.03	0	0.03	0	0	0.03	0.60	0.95	0	0	0.29	0.24	0.29	0.78	0.40	1.1	0.76	0.12	1.2
Tin	359	0	0	0	0	0	0	0	0	0	0	0	0	0	0	0	0	9.0	0	0	0	0	0	0	0	0	0	0	0	0
Uranium	235,463	1.5	35	9.0	30	9.7	16	6.2	8.2	40	13	7.3	7.5	2.6	2.5	0.74	16	20	6.2	61	44	30	25	22	23	13	23	20	10	41
Vanadium	751,636	0	0	0	0	0	2.6	5.2	0	0	0	0.61	0	0	0	0	0	4.4	1.4	0	0	0	0	0	0	0	0	1.6	0.79	0
Zinc	393,299	0	6.7	0.90	0.68	8.4	29	46	0	2.9	15	1.6	0.94	114	0	1.1	1.6	39	2.3	11	2.2	2.0	3.7	0.88	4.5	23	45	70	33	742
Organics (ug/L)	**Total:**	**21**	**0**	**0**	**1**	**0**	**45**	**1**	**2023**	**1593**	**1**	**0**	**0**	**0**	**5**	**1**	**5**	**1**	**0**	**0**	**0**	**0**	**1**	**0**	**0**	**0**	**6**	**4**	**0**	**36813**
Acetone	166	6	0	0	0	0	43	0	0	0	0	0	0	0	0	0	0	0	0	0	0	0	0	0	0	0	0	0	0	0
Benzene	0	0	0	0	0	0	0	0	0	0	0	0	0	0	0	0	0	0	0	0	0	0	0	0	0	0	0	0	0	0.47
Carbon tetrachloride	0	0	0	0	0	0	0	0	1.6	0	0	0	0	0	0	0	0	0	0	0	0	0	0	0	0	0	0	0	0	0	0
Chloroform	9	0	0	0	0.20	0	0	0	2021	1572	0	0	0	0	0	0	0	0	0	0	0	0	0	0	0	0	0	0.29	0	0
Chloromethane	3.0	0.42	0.15	0.22	0.51	0.33	0.96	0.52	0.21	0.39	0.79	0.24	0.42	0.27	0.50	0.50	0.40	0.84	0.35	0.23	0.24	0.40	0	0	0	0	0.50	0.93	0	0
Methyl ethyl ketone	23	0	0	0	0	0	0.73	0	0	1.1	0	0	0	0	0	0	0	0	0	0	0	0	0	0	0	0	0	0	0	0
Methylene chloride	0.8	0	0	0	0	0	0	0	0	19	0	0	0	0	0	0	0	0	0	0	0	0	0	0	0	0	0	0	0	0
Naphthalene	2.8	0	0	0	0	0	0	0	0	0	0	0	0	0	0	0	0	0	0	0	0	0	0	0	0	0	0	0	0	0
Tetrahydrofuran	7.2	15	0	0	0	0	0.28	0	0	1.1	0	0	0	0	4.3	0.32	5.1	0.21	0	0	0	0	0	0	0	0	5.7	0.38	0	0
Toluene	0.38	0.08	0	0	0	0	0.08	0	0	0	0	0	0	0	0.07	0	0	0	0	0	0	0	0.37	0	0	0	0	1.96	0.24	0.08
Xylenes	0.29	0	0	0	0	0	0	0	0	0	0	0	0	0	0	0	0	0	0	0	0	0	0.47	0	0	0	0	0	0.18	0.12

TABLE 11 - FREQUENCY OF CHEMICAL PARAMETER DETECTION (2005 TO 2014) IN PERMANENT MONITORING WELLS

Parameter	Tailings Cells and Slimes	Upgradient			Cell 1				Cell 2						Cell 3					Cell 4A			Cell 4B				Downgradient			
		MW-1	MW-18	MW-19	MW-27	MW-2	MW-24	MW-28	MW-4	MW-26	MW-29	MW-30	MW-31	MW-32	MW-5	MW-11	MW-12	MW-23	MW-25	MW-14	MW-15	MW-17	MW-34	MW-35	MW-36	MW-37	MW-3	MW-3A	MW-20	MW-22
General Parameters																														
Gross Alpha (-Rn&U)		100%	100%	100%	100%	100%	100%	100%	100%	100%	100%	100%	100%	100%	100%	100%	100%	100%	100%	100%	100%	100%	100%	100%	100%	100%	95%	96%	100%	100%
pH	100%	100%	100%	100%	100%	100%	100%	100%	100%	100%	100%	100%	100%	100%	100%	100%	100%	100%	100%	100%	100%	100%	100%	100%	100%	100%	100%	100%	100%	100%
Ammonia as N	100%	78%	41%	32%	7%	18%	100%	52%	0%	97%	100%	26%	5%	100%	100%	100%	50%	38%	100%	49%	22%	32%	33%	75%	8%	15%	42%	38%	68%	95%
Nitrate+Nitrite as N	95%	28%	0%	100%	97%	0%	38%	79%	100%	91%	4%	100%	100%	2%	37%	0%	28%	90%	0%	0%	61%	84%	100%	6%	100%	92%	90%	96%	100%	100%
TDS	100%	100%	100%	100%	100%	100%	100%	100%	100%	100%	100%	100%	100%	100%	100%	100%	100%	100%	100%	100%	100%	100%	100%	100%	100%	100%	100%	100%	100%	100%
TDS @ 180 C		100%	100%	100%	100%	100%	100%	100%	100%	100%	100%	100%	100%	100%	100%	100%	100%	100%	100%	100%	100%	100%	100%	100%	100%	100%	100%	100%	100%	100%
GW Elevation		100%	100%	100%	100%	100%	100%	100%	100%	100%	100%	100%	100%	100%	100%	100%	100%	100%	100%	100%	100%	100%	100%	100%	100%	100%	100%		100%	100%
Major Cations																														
Calcium	100%	100%	100%	100%	100%	100%	100%	100%	100%	100%	100%	100%	100%	100%	100%	100%	100%	100%	100%	100%	100%	100%	100%	100%	100%	100%	100%	100%	100%	100%
Magnesium	100%	100%	100%	100%	100%	100%	100%	100%	100%	100%	100%	100%	100%	100%	100%	100%	100%	100%	100%	100%	100%	100%	100%	100%	100%	100%	100%	100%	100%	100%
Potassium	95%	100%	100%	100%	100%	100%	100%	100%	100%	100%	100%	100%	100%	100%	100%	100%	100%	100%	100%	100%	100%	100%	100%	100%	100%	100%	100%	100%	100%	100%
Sodium	100%	100%	100%	100%	100%	100%	100%	100%	100%	100%	100%	100%	100%	100%	100%	100%	100%	100%	100%	100%	100%	100%	100%	100%	100%	100%	100%	100%	100%	100%
Major Anions																														
Chloride	97%	100%	100%	100%	100%	100%	100%	100%	100%	100%	100%	100%	100%	100%	100%	100%	100%	100%	100%	100%	100%	100%	100%	100%	100%	100%	100%	100%	100%	100%
Fluoride	89%	100%	100%	100%	100%	100%	100%	100%	100%	100%	100%	100%	100%	100%	100%	100%	100%	100%	100%	100%	100%	100%	100%	100%	100%	100%	100%	100%	100%	100%
Sulfate	100%	100%	100%	100%	100%	100%	100%	100%	100%	100%	100%	100%	100%	100%	100%	100%	100%	100%	100%	100%	100%	100%	100%	100%	100%	100%	100%	100%	100%	100%
Bicarbonate (as HCO3)	0%	100%	100%	100%	100%	100%	100%	100%	100%	100%	100%	100%	100%	100%	100%	100%	100%	100%	100%	100%	100%	100%	100%	100%	100%	100%	100%	100%	100%	100%
Heavy Metals																														
Arsenic	97%	0%	0%	0%	0%	0%	23%	100%	0%	3%	11%	5%	5%	4%	0%	3%	5%	0%	0%	0%	0%	0%	0%	0%	8%	0%	0%	0%	0%	0%
Beryllium	100%	0%	0%	0%	0%	0%	3%	0%	0%	0%	4%	3%	0%	0%	5%	3%	5%	0%	0%	3%	5%	0%	0%	0%	0%	0%	5%	80%	0%	100%
Cadmium	97%	0%	0%	0%	0%	41%	69%	100%	0%	18%	11%	5%	0%	97%	0%	0%	11%	24%	100%	97%	0%	10%	0%	0%	0%	8%	95%	88%	5%	100%
Chromium	97%	0%	0%	0%	0%	0%	0%	0%	0%	0%	0%	3%	0%	0%	0%	0%	0%	0%	0%	0%	0%	0%	0%	0%	0%	0%	0%	0%	0%	0%
Cobalt	92%	0%	0%	0%	0%	0%	13%	100%	0%	6%	4%	3%	0%	100%	0%	0%	0%	3%	18%	0%	0%	0%	0%	6%	0%	0%	0%	16%	0%	100%
Copper	97%	0%	0%	0%	0%	0%	0%	7%	0%	3%	0%	3%	3%	7%	0%	3%	0%	3%	0%	0%	5%	0%	0%	0%	8%	0%	5%	8%	0%	74%
Iron	100%	89%	100%	10%	4%	0%	100%	59%	0%	100%	100%	77%	0%	100%	84%	70%	47%	17%	0%	0%	8%	10%	67%	100%	0%	8%	14%	4%	16%	53%
Lead	92%	0%	0%	0%	0%	0%	7%	17%	0%	0%	0%	5%	0%	5%	0%	2%	0%	7%	3%	0%	0%	0%	0%	0%	0%	0%	0%	0%	0%	58%
Manganese	97%	97%	100%	45%	0%	0%	100%	100%	0%	100%	100%	100%	0%	100%	100%	100%	100%	100%	100%	100%	10%	100%	100%	100%	0%	38%	100%	100%	53%	100%
Mercury	55%	0%	0%	0%	0%	0%	7%	0%	0%	0%	0%	0%	0%	0%	0%	0%	0%	0%	0%	0%	0%	0%	0%	0%	0%	0%	0%	0%	0%	5%
Molybdenum	100%	0%	0%	0%	0%	0%	7%	0%	0%	0%	7%	0%	0%	55%	0%	0%	0%	0%	74%	3%	0%	0%	0%	5%	0%	0%	0%	0%	32%	100%
Nickel	97%	0%	0%	0%	0%	0%	30%	97%	0%	9%	4%	3%	3%	100%	5%	3%	5%	24%	0%	5%	5%	0%	0%	6%	0%	8%	9%	36%	0%	100%
Selenium	92%	0%	0%	100%	100%	88%	17%	41%	100%	38%	7%	100%	100%	0%	0%	3%	93%	21%	0%	0%	89%	71%	100%	92%	100%	85%	97%	100%	5%	100%
Silver	66%	0%	0%	0%	0%	0%	0%	0%	0%	0%	0%	0%	0%	0%	0%	0%	0%	0%	0%	0%	0%	0%	0%	0%	0%	0%	0%	0%	0%	0%
Thallium	92%	0%	100%	44%	0%	0%	62%	100%	0%	0%	15%	3%	0%	3%	0%	0%	5%	59%	100%	0%	0%	38%	33%	44%	100%	54%	100%	88%	16%	95%
Tin	45%	0%	0%	0%	0%	0%	0%	0%	0%	0%	0%	0%	0%	0%	0%	0%	0%	4%	0%	0%	0%	0%	0%	0%	0%	0%	0%	0%	0%	0%
Uranium	100%	84%	100%	100%	100%	100%	100%	100%	100%	100%	100%	100%	100%	100%	93%	92%	99%	100%	100%	100%	100%	100%	100%	100%	100%	100%	100%	100%	95%	100%
Vanadium	97%	0%	0%	0%	0%	0%	3%	10%	0%	0%	0%	3%	0%	0%	0%	0%	0%	14%	3%	0%	0%	0%	0%	0%	0%	0%	0%	4%	5%	0%
Zinc	92%	0%	17%	5%	4%	41%	73%	97%	0%	19%	78%	8%	6%	100%	0%	3%	11%	100%	13%	76%	11%	10%	33%	6%	15%	77%	100%	100%	74%	100%
Organic Compounds																														
Acetone	82%	4%	0%	0%	0%	0%	10%	0%	0%	0%	0%	0%	0%	0%	0%	0%	0%	0%	0%	0%	0%	0%	0%	0%	0%	0%	0%	0%	0%	0%
Benzene	0%	0%	0%	0%	0%	0%	0%	0%	0%	0%	0%	0%	0%	0%	0%	0%	0%	0%	0%	0%	0%	0%	0%	0%	0%	0%	0%	0%	0%	5%
Carbon tetrachloride	0%	0%	0%	0%	0%	0%	0%	0%	90%	1%	0%	0%	0%	0%	0%	0%	0%	0%	0%	0%	0%	0%	0%	0%	0%	0%	0%	0%	0%	0%
Chloroform	74%	0%	0%	0%	4%	0%	0%	0%	100%	100%	0%	0%	0%	0%	0%	0%	0%	0%	0%	0%	0%	0%	0%	0%	0%	0%	0%	8%	0%	0%
Chloromethane	58%	18%	6%	6%	22%	12%	17%	17%	5%	8%	15%	11%	14%	10%	19%	15%	10%	30%	11%	8%	6%	17%	0%	0%	0%	0%	19%	26%	0%	0%
Methyl ethyl ketone	26%	0%	0%	0%	0%	0%	3%	0%	0%	1%	0%	0%	0%	0%	0%	0%	0%	0%	0%	0%	0%	0%	0%	0%	0%	0%	0%	0%	0%	0%
Methylene chloride	16%	0%	0%	0%	0%	0%	0%	0%	0%	92%	0%	0%	0%	0%	0%	0%	0%	0%	0%	0%	0%	0%	0%	0%	0%	0%	0%	0%	0%	0%
Naphthalene	37%	0%	0%	0%	0%	0%	0%	0%	0%	0%	0%	0%	0%	0%	0%	0%	0%	0%	0%	0%	0%	0%	0%	0%	0%	0%	0%	0%	0%	0%
Tetrahydrofuran	21%	90%	0%	0%	0%	0%	4%	0%	0%	2%	0%	0%	0%	0%	69%	11%	54%	4%	0%	0%	0%	0%	0%	0%	0%	0%	40%	9%	0%	0%
Toluene	16%	5%	0%	0%	0%	0%	3%	0%	0%	0%	0%	0%	0%	0%	5%	0%	0%	0%	0%	0%	0%	0%	33%	0%	0%	0%	0%	4%	5%	5%
Xylenes	11%	0%	0%	0%	0%	0%	0%	0%	0%	0%	0%	0%	0%	0%	0%	0%	0%	0%	0%	0%	0%	0%	33%	0%	0%	0%	0%	0%	5%	5%

3.2.1 Major Ions and General Water Quality Parameters

The principal or major ions in the water samples can provide some insight as to general changes in groundwater chemistry across the site. This is most easily visualized by using a Piper diagram as shown in Figure 15. A Piper diagram shows the relative proportions (in terms of milliequivalents) of the major cations (Ca, Mg, and Na+K) and anions (CO_3+HCO_3, Cl, and SO_4) using separate ternary plots (cations to the lower left and anions to the lower right portion of the diagram). The apexes of the cation plot are calcium, magnesium and sodium plus potassium cations. The apexes of the anion plot are sulfate, chloride and carbonate plus bicarbonate anions. The two ternary plots are then projected onto a diamond (upper portion of diagram). This portion of the diagram is used to show the combined linear trends of the changes in both cations and anions. TDS and pH of the monitor well samples are shown on the same figure in order of upgradient to downgradient from left to right (same as for Table 10). Data for the neighboring springs and Recapture Reservoir (USGS, 2011) are shown for comparison.

Most of the monitoring wells are fairly closely grouped (dashed rectangle in Figure 15) along a mixing line which shows waters with higher percentages of calcium, magnesium and to a lesser extent bicarbonate at one end and waters with higher percentages of sodium and to a lesser extent sulfate at the other end. Specific outliers are identified on Figure 15. MW-1 is similar to the other wells except it contains a slightly higher percentage of bicarbonate. The major ion composition of the water in MW-1 is essentially identical to that for the downgradient Ruin Spring and Mill Spring (a.k.a. Westwater Spring). MW-1 is the furthest upgradient well at the site and the least affected by discharge from the wildlife ponds and the source in the northwest corner of the mill site so it may be the most representative of natural upstream groundwater at the site prior to the influence of this seepage. MW-27 falls in the same cation percentages of the other wells (although at the high calcium end of the range) but contains significantly higher percentages of bicarbonate (about 40%) as well as slightly higher chloride (about 5%) than the other wells. MW-27 appears to represent a mixture of water from that of the other monitor wells and Recapture Reservoir, which suggests that the mounding source near the northwest corner of the mill site is related to water used at the mill. The same is true for water from Entrance Spring which is near the north wildlife ponds although Entrance Spring contains higher chloride (about 15%), possibly leached from the pond sediments. Both MW-27 and Entrance Spring contain measurable tritium (USGS, 2011) which supports this interpretation. Interestingly the water chemistry of upgradient wells MW-18, MW-19 does not appear to be impacted by the wildlife pond recharge, although water levels in these wells have increased significantly due to the north pond recharge. This may be due to the fact that as upgradient wells, the change in water level is more a function of backing up of upstream flow by the recharge than actual mixing of water from the recharge, although MW-19 also contained slightly elevated tritium, albeit lower than observed for MW-27. MW-30 and MW-31 have notably higher chloride than the other wells. These wells are located within the current mapped chloride plume area.

TDS generally increases downgradient, while pH does not. TDS is lowest in the upgradient wells, as well as five wells with distinct water chemistry (MW-27, MW-5, MW-30, MW-31, and MW-

11) associated with the chloride plume source and downgradient movement. The water chemistry of Recapture Reservoir is distinctly different, with a much lower percentage of sulfate and a slightly higher percentage of calcium, although infiltration through the sediments in the bottom of the wildlife ponds (or use in process water) would likely significantly change its water chemistry.

The wells with the lowest pH are found at the downstream edge of Tailings Cell 1 (MW-24 and MW-29), near the southeast corner of cell 2 (MW-32) and at downgradient well MW-22. Wells MW-5, MW-11, and MW-20 have the highest average pH, in part due to some very high pH readings (8.7, 9, and 11, respectively) as well as some very high sodium percentages suggesting some cement invasion into the screen interval during well construction as such high pH values do not occur naturally in groundwater.

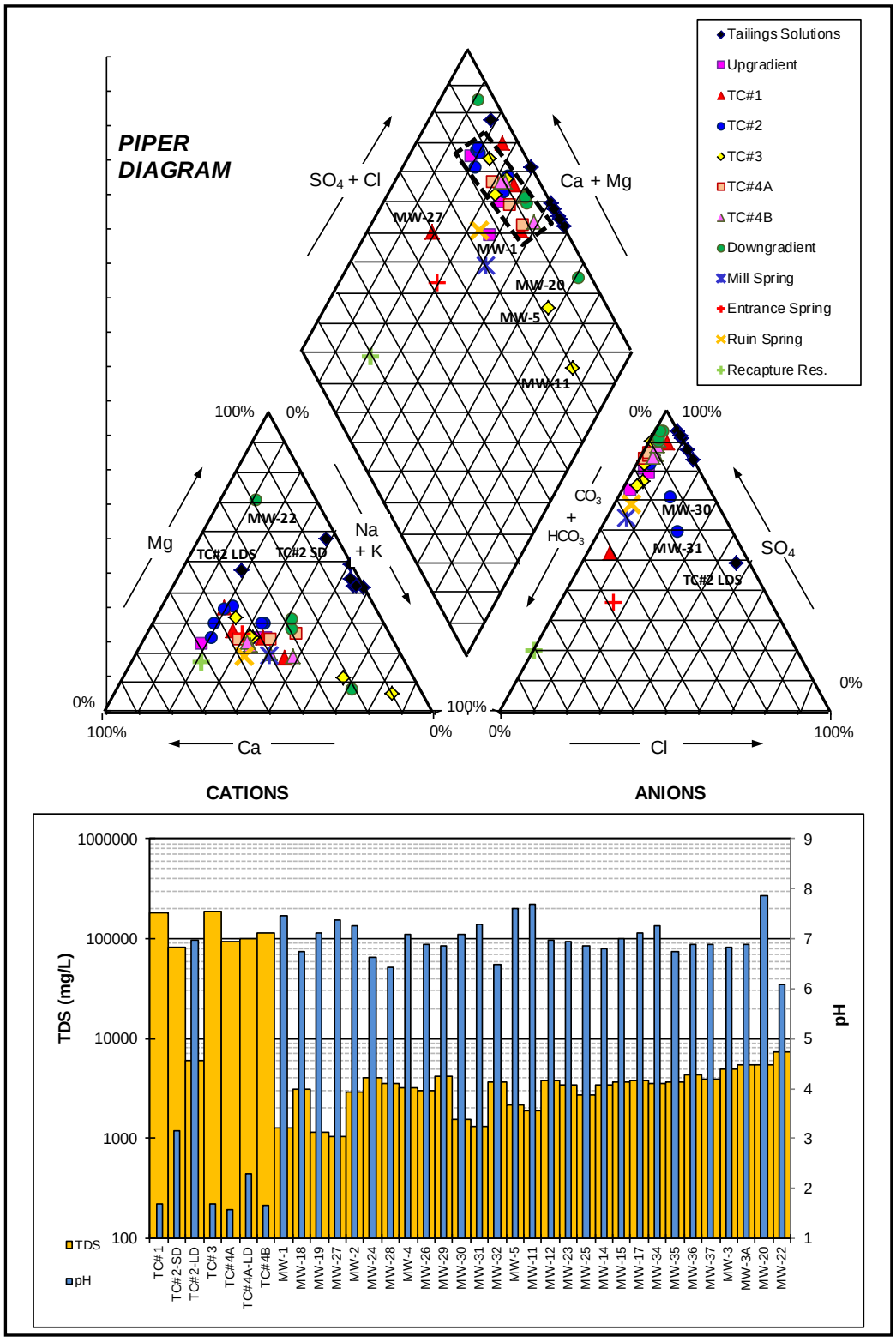

FIGURE 15 - PIPER DIAGRAM OF SITE GROUNDWATER

Average water chemistry for the tailings cells are also presented in Figure 15. The typical water chemistry for the tailings is very high TDS, very low pH, with equal percentages of sodium and magnesium, and a sulfate percentage of almost 100%. The percentage of magnesium is higher in the Tailings Cell 2 slimes drain. Water from the Tailings Cell 2 leak detection system is also distinct. This water has a near neutral pH and contains about 35% higher percentages of calcium and chloride than the other tailings waters suggesting mixing with other waters or geochemical reaction with the material underlying the cells.

Sodium concentrations increase downgradient, with the lowest sodium concentrations observed in the areas of groundwater mounding near the northwest corner of the mill site and along the center of the chloride plume (Figure 16). Calcium does not generally increase downstream but also exhibits lower values along the center of the chloride plume (Figure 16). Magnesium has a similar distribution to calcium. This suggests that the water associated with mounding near the northwest corner of the mill site has unique water chemistry and is not associated with the wildlife pond discharge.

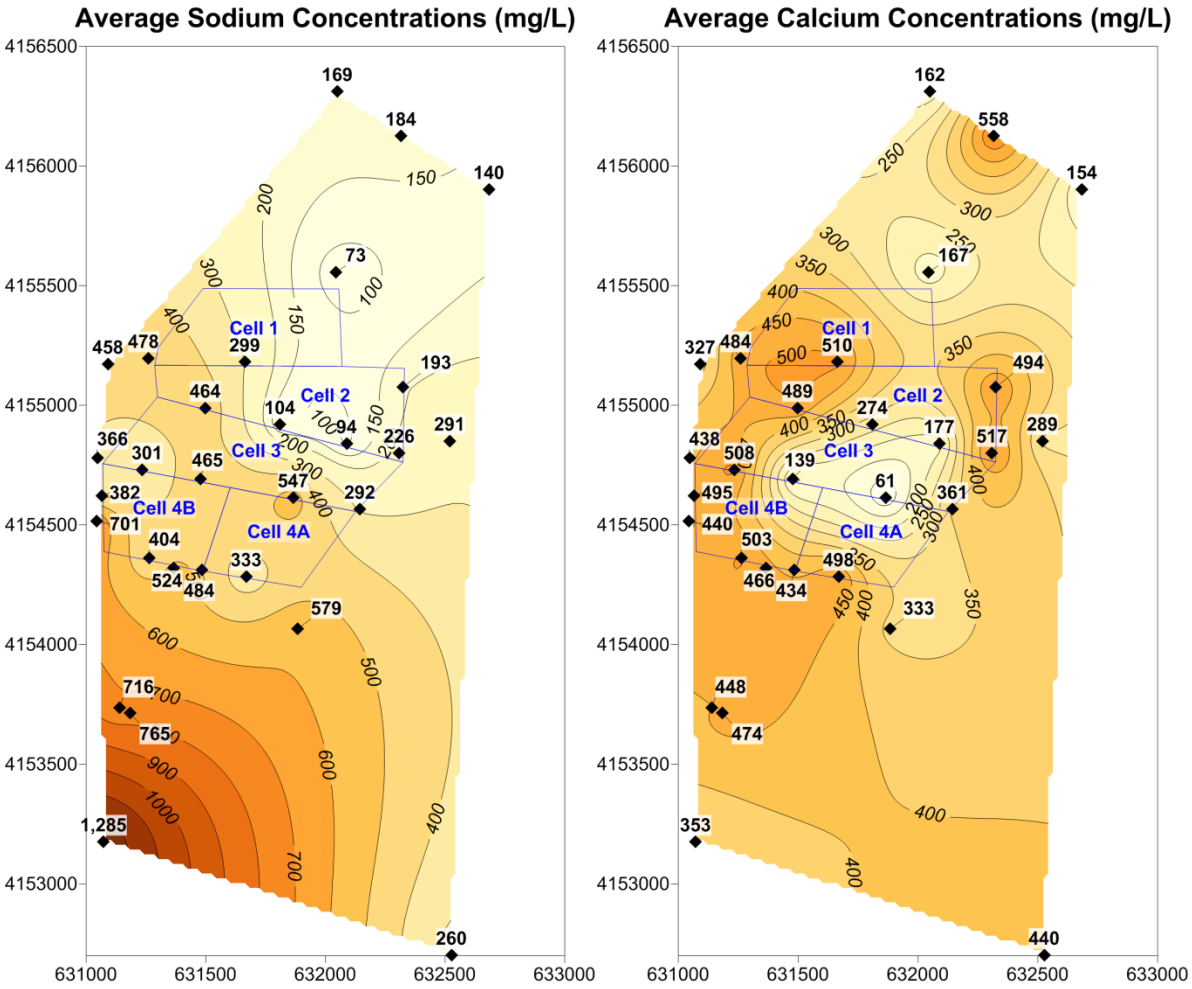

FIGURE 16 - CALCIUM AND SODIUM CONCENTRATIONS IN GROUNDWATER

Sulfate is the dominant anion for almost all of the samples and shows only a slight increase with increasing sodium per the trend of the Piper Diagram. However, sulfate concentrations increase downgradient in the same manner as observed for sodium (Figure 17). Bicarbonate like calcium does not generally increase downstream. However, it is lowest below Tailings Cells 1 and 2 suggesting that some seepage of acid solutions from the tailings cells has occurred in this area. The observed distribution of chloride is essentially the inverse of that observed for bicarbonate (i.e. high chloride is associated with low bicarbonate). This suggests that either the chloride is also an indication of tailings cell seepage, or that the water associated with the chloride plume has lower bicarbonate.

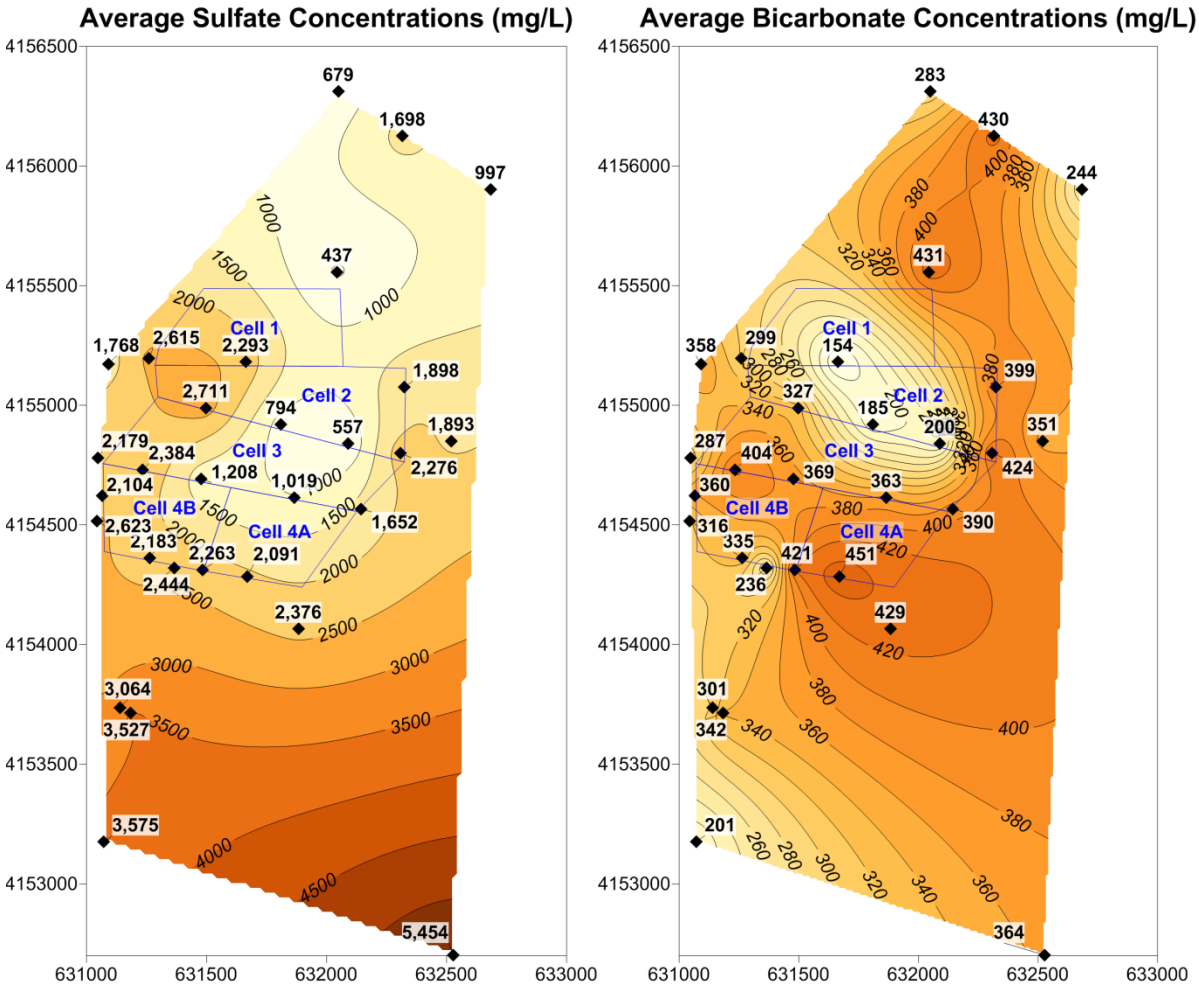

FIGURE 17 - SULFATE AND BICARBONATE CONCENTRATIONS IN GROUNDWATER

The USGS (2011) has identified the following natural mechanisms that impact major ion chemistry at the site:

- Dissolution of calcite and dolomite which results in higher calcium, magnesium, and bicarbonate
- Dissolution of gypsum (and anhydrite) which results in higher calcium and sulfate
- Cation exchange with kaolinite clay which results in lower calcium and higher sodium

Per the previous figures, sodium and sulfate generally increase downstream, while calcium remains relatively constant, although locally variable. From the Piper diagram we see that along the mixing line observed for most monitor wells samples sodium and sulfate increase while calcium, magnesium, and carbonate decrease. The only mechanism of the above three to explain the sodium increase is cation exchange. The only mechanism of the above three to explain the sulfate increase is dissolution of gypsum. The only mechanism of the above three to explain higher calcium, magnesium, and bicarbonate is dissolution of calcite and dolomite. Thus it appears that all three mechanisms impact the groundwater chemistry at the site.

3.3 pH

3.3.1 Site Measurements

A wide spread reduction in pH over time has been observed in monitoring wells at the White Mesa mill site (Intera 2008, Intera, 2012). The observed change is reported to generally correspond with wells where the groundwater elevation is increasing, although it is also noted that the TWN-series wells, which are located up gradient of the site, have not exhibited changes in pH over time.

Figure 18 shows the average pH distribution at the site and the change in the groundwater elevation from 1994 to 2014. This figure shows no correlation between the change in water levels at the site and the current pH of the groundwater. The lowest pH values are found near the source of the nitrate/chloride plume, near the southeast corner of tailing cell 2, and below tailing cell 1. The highest pH values are found in wells MW-5, MW-11, and MW-20, which as previously explained have exhibited occasional elevated pH readings that do not occur naturally in groundwater, possibly related to well construction.

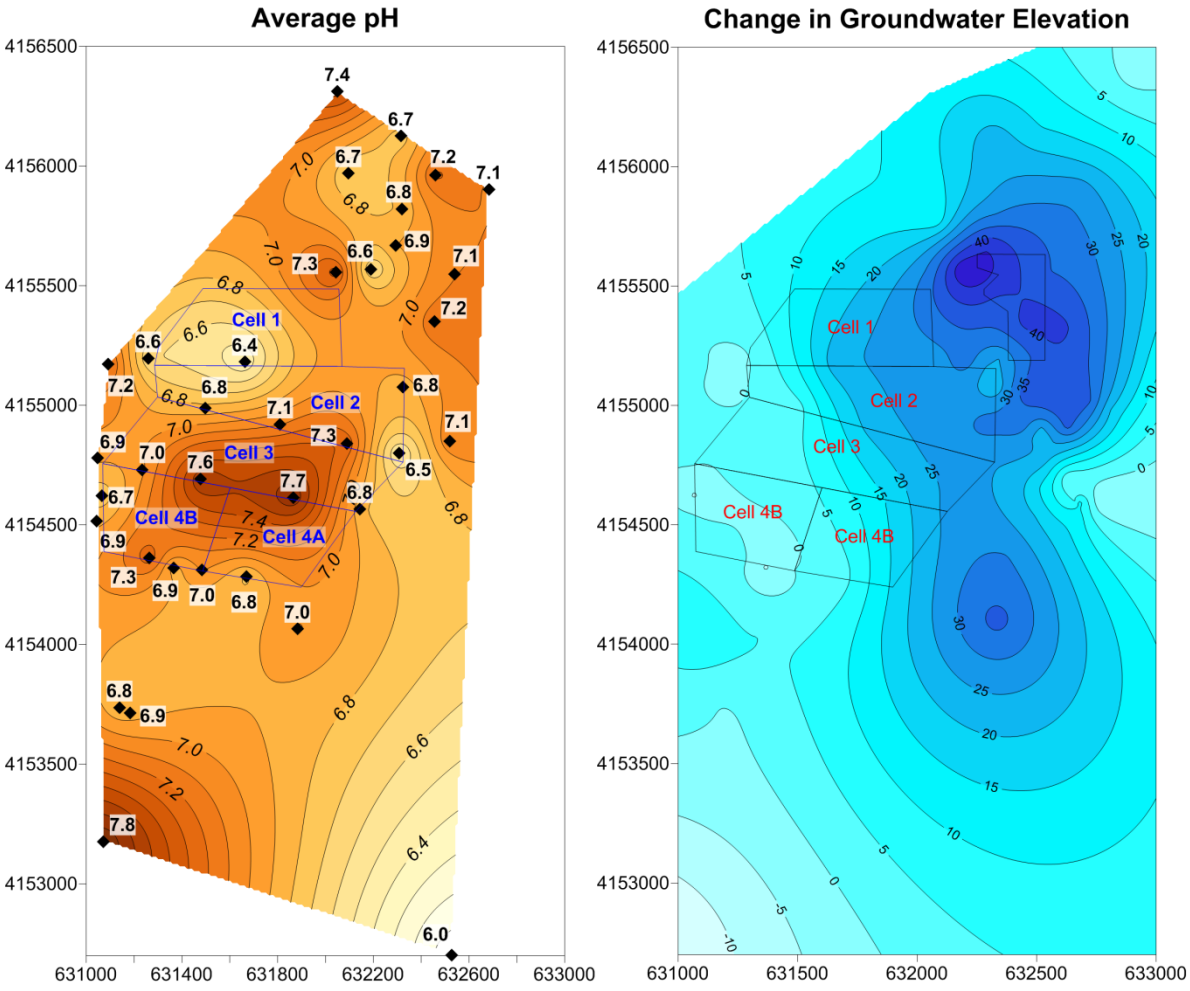

FIGURE 18 - CURRENT PH VS CHANGE IN GROUNDWATER ELEVATION (1994 TO 2014)

Figure 19 shows the annual rate of change of pH at the site compared to the annual rate of groundwater level change for the same period of time (2005 to 2014). This figure clearly shows that there is no correlation between the annual rate of change in pH and the corresponding annual rate of change in groundwater levels over the last 10 years, with the greatest reductions in pH occurring where water levels have changed the least. In the areas most influenced by mounding only small rates of pH change are observed, possibly due to the addition of bicarbonate from the infiltrating water. Although, it is observed that pH is generally declining across the site, the highest rates of change are observed in areas adjacent to or downgradient of the tailings cells. It is noted that the large change in pH at MW-34 is based on only two years of measurements.

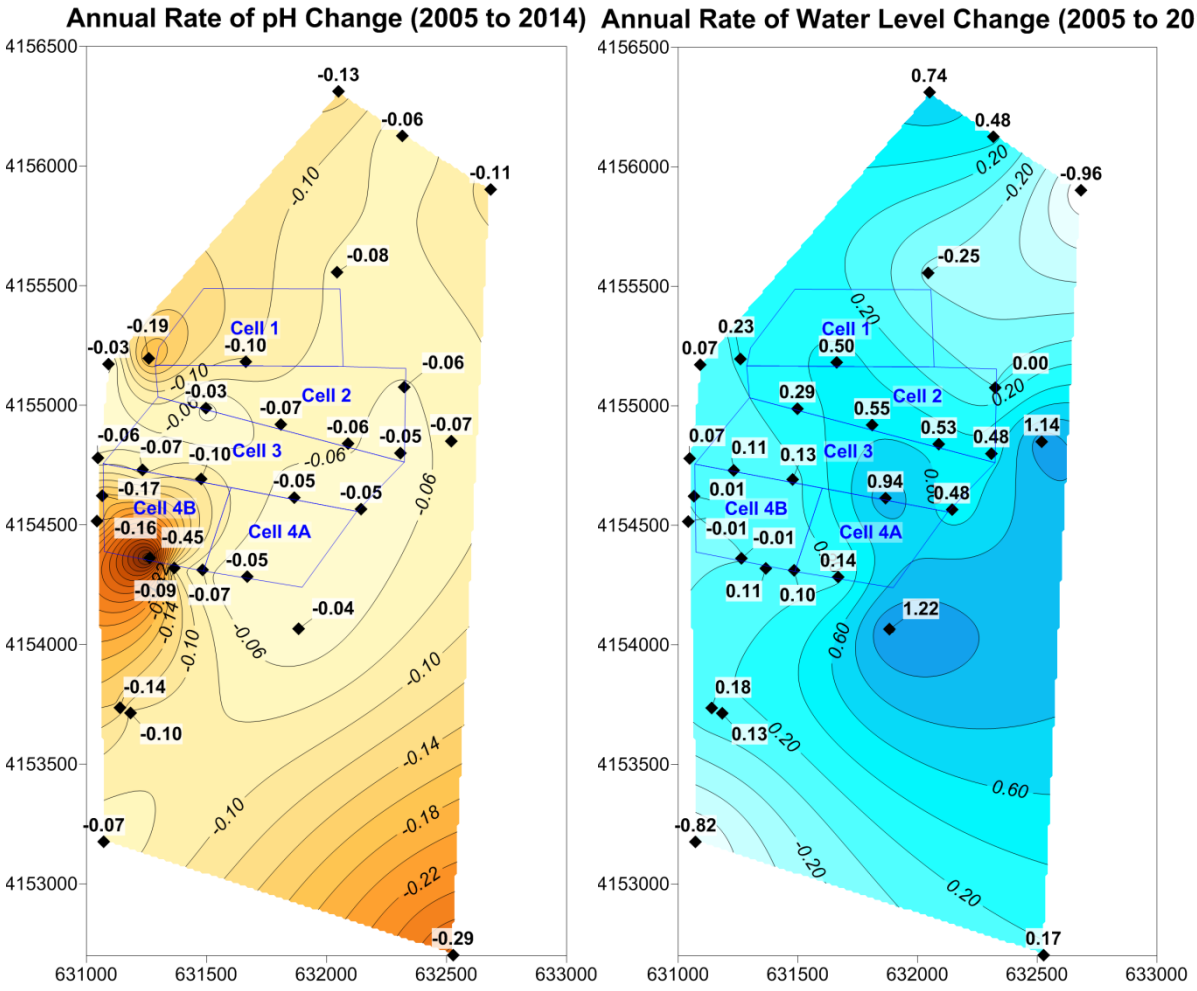

FIGURE 19 - ANNUAL RATE OF CHANGE OF PH VS GROUNDWATER LEVEL (2005 TO 2014)

3.3.2 Pyrite Oxidation

Prior reports have attributed changes of pH to oxidation of pyrite within the Burro Canyon and Dakota sandstones (HGC, 2012, HGC, 2014). The oxidation of pyrite is controlled by several factors as discussed in detail by Nordstrom (1982) who states: "*The oxidation of pyrite in aqueous systems is a complex biogeochemical process involving several redox reactions and microbial catalysis. Although oxygen is the overall oxidant, kinetic data suggests that ferric iron is the direct oxidant in acid systems and that temperature, pH, surface area, and the presence of iron and sulfur-oxidizing bacteria can greatly affect the rate of reaction.*"

The oxidation of pyrite (iron sulfide) requires two essential components: oxygen and water. Because of the extremely low solubility of oxygen in water (maximum of 8 mg/L at site temperatures), oxidation of pyrite does not occur at any significant rate under saturated conditions. Measured dissolved oxygen in two perched aquifer wells located approximately 13,000 ft downgradient of the site ranged from 0 to 5 mg/L (USGS, 2011). For this reason, subaqueous disposal of sulfide containing mine wastes is commonly used to prevent sulfide

oxidation as is flooding of mine workings. Thus if pyrite oxidation is occurring then it must be occurring above the pre-mill static water table (pre-mill vadose zone). However, pyrite in this zone has had a long period of time to oxidize (at least hundreds if not thousands of years) so it is not expected that significant amounts of unoxidized pyrite would remain in this zone due to the abundance of oxygen and water infiltration from precipitation.

Inorganic oxidation of pyrite is not considered a self-sustaining reaction at near neutral pH since the formation of insoluble iron oxides will coat the mineral surface and terminate the reaction. The oxidation of pyrite is primarily caused by microbial regulated reactions. These microbes are hardy and can exist under near neutral pH and without significant nutrients (such as nitrogen, carbon, and phosphate). Under conditions of near neutral pH and normal ambient temperatures, these microbial controlled reaction rates are slow. Again the application of limestone covers or solutions has been used to control sulfide oxidation in mine wastes by maintaining near neutral pH. As the pH becomes more acidic (<4.5), the rate of reaction increases significantly, temperature increases due to the heat of the reaction, and pyrite oxidation occurs primarily due to reaction with ferric (Fe^{+3}) iron which is now soluble and constantly replaced by microbial oxidation of ferrous (Fe^{+2}) iron. Even when pyrite oxidation occurs, the reduction of pH can be controlled by the presence of alkalinity from carbonates. It is important to note that the creation of acidity from sulfide oxidation is due to the oxidation of the sulfur and not the associated metal.

To support modeling of potential seepage from a proposed expansion of the tailings facilities, MWH (2010) analyzed 34 randomly selected samples of the Burro Canyon formation from four borings in the immediate vicinity of the proposed tailings facilities for acid neutralization potential (NP). The results of their sample analyses are summarized in Table 12 by well location, lithology, and depth. The results indicate variable amounts of neutralization potential with an average of 13.8 kg $CaCO_3$ per metric ton. It is noted that all but the three deepest samples from TW4-22 were collected from the vadose zone.

MWH also analyzed seven samples (including one duplicate) for measurement of the paste pH. The paste pH ranged from 7.7 to 8.1, averaging 8.0, indicating slightly alkaline conditions (i.e. the presence of soluble carbonates). The presence of carbonates in the perched aquifer is supported by the slightly alkaline pH (average of 7.7) reported in the earliest sampling at the site between 1979 and 1982 as well as the current sampling measurements which indicate an average bicarbonate content of 330 mg/L across the site between 2005 and 2012.

TABLE 12 - SUMMARY OF NEUTRALIZATION POTENTIAL TESTS (MWH, 2010)

NEUTRALIZATION POTENTIAL (kg $CaCO_3$/1000 kg)				
SAMPLE LOCATION	**COUNT**	**MINIMUM**	**MAXIMUM**	**ARITHMETIC MEAN**
MW-23	10	0.5	182	22.6
MW-24	9	2.0	27	7.0
MW-30	7	0.5	69	13.1
TW4-22	8	2.0	36	11.1
Upper Sandstone	18	1.0	69	10.1
Conglomerate	4	2.0	182	48.5
Siltstone	3	6.0	9	7.7
Lower Sandstone	9	1.0	27	7.7
29-54 ft. depth	16	0.5	69	10.3
54-79 ft. depth	12	0.5	182	21.3
79-104 ft. depth	6	4.0	27	7.8
All Samples	**34**	**0.5**	**182**	**13.8**

The presence of pyrite within the Burro Canyon formation has also been indicated. HGC (2012) in referencing previous studies (Shawe, 1976) noted: "*pyrite is more common below the water table and iron oxides (likely formed by oxidation of pyrite) are more common in the vadose zone" with limonite identified as the observed weathering product from pyrite oxidation"*. This is consistent with the previous statement that pyrite does not readily oxidize below the water table, and would have been expected to already have oxidized in the vadose zone where it forms iron oxides.

HGC (2012) collected stored core and cuttings samples from various borings where pyrite was recorded in the drill logs for further testing. Unfortunately, the sample collection was not random but favored intervals that were believed to likely contain the highest pyrite concentrations. As stated in the HGC report, *"…core or cuttings material from the above borings was screened to identify intervals likely to have pyrite. Sample screening consisted of using the portable XRF to measure the iron contents of samples having a greenish or grayish to white color consistent with reduced conditions. The samples having the highest iron were then selected for analysis."* Therefore, the sample analyses from the HGC study cannot be considered to represent the average conditions within the Burro Canyon formation, but rather conditions most favorable to pyrite occurrence.

Selected samples were submitted either for optical microscopy (total of 18 samples) or x-ray diffraction (XRD) and total sulfur analysis (total of 12 samples), but not both. Optical microscopy photos identified pyrite as occurring mainly as part of the cement matrix holding the particle grains together. Optical microscopy is not a quantitative method but did provide

indications of the presence of pyrite in 17 of the 18 of the samples selected for testing, marcasite in 8 of the samples, and chalcopyrite in 2 of the samples. Indicated marcasite content was generally much lower than pyrite, and chalcopyrite content was extremely low. There was no analysis presented of the indicated degree of pyrite oxidation.

XRD provides a quantitative analysis of the principal minerals present in the 12 samples selected for testing. The results of the XRD and total sulfur analyses are summarized in Table 13 with an indicated precision and detection limit of 0.1% for each of the mineral species analyzed by XRD and 0.01% for total sulfur. The total "equivalent pyrite" presented in Table 13 is calculated from the measured total sulfur under the assumption that all sulfur is associated with pyrite (i.e. unoxidized). However, it is current practice to use sulfur present as sulfides (i.e. sulfide sulfur) instead of total sulfur, since sulfur present as sulfates (i.e. sulfate sulfur) is already oxidized and not acid generating. Also presented for comparison are the sample depths with reported depths to groundwater, which indicates if the sample was from the vadose (above water table) or saturated (below water table) zones. Of the 11 samples tested, 7 were from the saturated zone and only 4 were from the vadose zone.

The XRD analysis also provides a quantitative analysis of pyrite, gypsum, and anhydrite, all of which contain sulfur. The weight percentage of sulfide sulfur (i.e. from pyrite) was calculated from the laboratory reported weight percentage of pyrite. The weight percentage of sulfate sulfur (i.e. from gypsum and anhydrite) was calculated from the reported weight percentage of gypsum and anhydrite. For comparison, the amount of sulfur as sulfate was also calculated from the laboratory reported concentration of total sulfur minus the calculated concentration of sulfur as sulfate. In general, this comparison shows reasonable agreement was obtained with the maximum difference within 0.1% (precision of the measurements) and the average difference being only 0.02%. Therefore, the total sulfur is not indicative of the pyrite concentration.

Pyrite was not detected by the XRD analysis in any of the samples collected from above the water table (vadose zone) suggesting that most of the pyrite in the vadose zone is already oxidized. Pyrite was detected in all but one of the samples (MW-31 cuttings) collected from below the water table (saturated zone). Total iron was consistent for samples above and below the water table, with pyrite accounting for about 50% of the total iron in the samples from below the water table. Again this is consistent with the presence of significant pyrite only below the water table.

The standard geochemical procedure for determining the potential for acid generation is acid-base accounting. Table 13 presents calculated acid generating potential (AP) and neutralizing potential (NP) based on this procedure. AP and NP are both expressed as equivalent amounts of $CaCO_3$ per metric ton (i.e. 1000 kg) of material. It is important to note that this procedure does not take into account the rate of reactions. Kinetic (humidity cell) procedures are used to assess reaction rates under the most favorable oxidizing (i.e. unsaturated) sample conditions.

Calculations of AP, based on the calculated sulfide sulfur content and total sulfide content, produce only small differences as the total amount of sulfur present is very low. AP ranges from 0 to 13 kg $CaCO_3$ per metric ton of rock based on sulfide sulfur with AP equal to 0 for all of the samples above the water table (vadose zone) and an average AP of 5 kg $CaCO_3$ per metric ton of rock for samples below the water table. This calculation follows the standard procedure per EPA guidelines (EPA, 1994) that one mole of pyrite is neutralized by two moles of calcium carbonate per the following stoichiometric equation (Skousen et al, 2002) which assumes that carbon dioxide is off gassed (as would be expected in the vadose zone):

Equation 1: $FeS_2 + 2CaCO_3 + 3.75O_2 + 1.5H_2O \rightarrow Fe(OH)_3 + 2SO_4^{-2} + 2Ca^{+2} + 2CO_2\uparrow$

TABLE 13 - SUMMARY OF THE XRD ANALYSES (data from HGC, 2012)

Mineral	Formula	MW-3A core	MW-23 core	MW-24 core	MW-25 cuttings	MW-26 cuttings	MW-27 cuttings	MW-28 core	MW-29 cuttings	MW-30 cuttings	MW-31 cuttings	MW-32 cuttings	SS-26 play sand	Average of all samples	Average of all samples above water table	Average of all samples below water table
		Sample Depth (ft)														
		89.5	108	118.5	65-67.5	90-92.5	80-82.5	88.5	102	65-67.5	95-97.5	105-107.5	N.A.			
	Date	Water Table Depth (ft)														
	on 2/21/2010	85.3	115	114.6	74.73	81.31	50.93	77.3	102	76.8	68.95	76.27	N.A.			
	on 3/27/2014	84.6	117	113.7	73.44	68.8	52.59	75.6	101	74.73	67.45	74.27	N.A.			
	Below water table?	Yes	No	Yes	No	Yes	Yes	Yes	No	No	Yes	Yes	N.A.			
		Concentration (% by weight)														
Quartz	SiO_2	79.7	96.2	88.4	90	86.9	95.4	90.1	95.8	87	91.7	94.1	39.2	86.2	92.25	89.47
K-feldspar	$KAlSi_3O_8$	ND	0.2	0.6	2.4	2.4	0.7	1.5	0.5	1.4	2	0.8	21.6	2.84	1.13	1.14
Plagioclase	$(Na,Ca)(Si,Al)_4O_8$	ND	ND	ND	1.4	1.6	1.5	1.8	1.5	1.5	0.5	0.2	29	3.25	1.10	0.80
Mica	$KAl_2(Si_3Al)O_{10}(OH)_2$	0.3	1.2	4.5	2.2	2	0.2	3	0.2	5.9	3.1	1.2	5.2	2.42	2.38	2.04
Kaolinite	$Al_2Si_2O_5(OH)_4$	1.1	1	4.3	3.2	2.5	1.4	2.9	1.7	3.6	2.4	1.6	0.8	2.21	2.38	2.31
Calcite	$CaCO_3$	14	ND	ND	ND	3.9	ND	ND	ND	ND	ND	1.2	0.6	1.64	ND	2.73
Dolomite	$CaMg(CO_3)_2$	4.1	ND	ND	ND	ND	ND	ND	ND	ND	ND	ND	ND	0.34	ND	0.59
Anhydrite	$CaSO_4$	0.4	0.8	0.4	0.4	ND	ND	ND	ND	ND	ND	ND	ND	0.17	0.30	0.11
Gypsum	$CaSO_4 \cdot 2H_2O$	ND	0.2	0.8	ND	ND	ND	0.3	ND	0.3	ND	ND	ND	0.13	0.13	0.16
Iron	Fe	0.3	0.4	0.2	0.4	0.4	0.4	0.2	0.3	0.3	0.3	0.4	0.2	0.32	0.35	0.31
Pyrite	FeS_2	0.1	ND	0.8	ND	0.3	0.4	0.2	ND	ND	ND	0.5	ND	0.19	ND	0.33
Hematite	Fe_2O_3	ND	ND	ND	ND	ND	ND	ND	ND	ND	ND	ND	1.4	0.12	ND	ND
Magnetite	Fe_3O_4	ND	ND	ND	ND	ND	ND	ND	ND	ND	ND	ND	2	0.17	ND	ND
Total Sulfur	S	0.14	0.14	0.63	0.05	0.13	0.15	0.04	0.03	0.02	0.02	0.26	0.02	0.14	0.06	0.20
Sulfide S	S	0.05	0.00	0.43	0.00	0.16	0.21	0.11	0.00	0.00	0.00	0.27	0.00	0.10	0.00	0.18
"Equivalent Pyrite"	From Total S	0.26	0.26	1.18	0.09	0.24	0.28	0.07	0.06	0.04	0.04	0.49	0.04	0.25	0.11	0.37
Sulfate S (method 1)	Total S - Sulfide S	0.09	0.14	0.20	0.05	-0.03	-0.06	-0.07	0.03	0.02	0.02	-0.01	0.02	0.03	0.06	0.02
Sulfate S (method 2)	Gypsum & Anhydrite	0.09	0.23	0.13	0.09	0.00	0.00	0.04	0.00	0.04	0.00	0.00	0.00	0.08	0.09	0.04
Sulfate S difference	Difference 1 minus 2	0.01	0.09	-0.07	0.04	0.03	0.06	0.10	-0.03	0.02	-0.02	0.01	-0.02	0.04	0.03	0.02
AP (sulfide S)	kg CaC03/1000 kg	2	0	13	0	5	7	3	0	0	0	8	0	3	0	5
AP (total S)	kg CaC03/1000 kg	4	4	20	2	4	5	1	1	1	1	8	1	4	2	6
NP	kg CaC03/1000 kg	144	0	0	0	39	0	0	0	0	0	12	6	17	0	28
Net neutralization potential	NNP (sulfide S)	143	0	-13	0	34	-7	-3	0	0	0	4	6	14	0	22
	NNP (total S)	140	-4	-20	-2	35	-5	-1	-1	-1	-1	4	5	13	-2	22

The standard procedure for assessing NP is via titration of a sample in the laboratory with sulfuric acid to a pH of 6.0 or 3.5 (depending upon the procedure) to dissolve calcium and magnesium carbonates, although other procedures have been used to measure neutralization contributions from other minerals as well. In the absence of such test results, NP was calculated from the XRD measured calcium and dolomite weight percentages. NP ranges from 0 to 144 kg $CaCO_3$ per metric ton of rock with no NP indicated for the samples above the water table (vadose zone) and an average NP of 28 kg $CaCO_3$ per metric ton of rock for samples below the water table. Based on the previous testing by MWH (Table 12) there is potentially higher NP in the vadose zone than indicated in Table 13. For example the samples collected in the vadose zone for borings MW-23, 24 and 30 averaged 16 kg $CaCO_3$ per metric ton of rock. Still the average NP for all of the XRD samples (17 kg $CaCO_3$ per metric ton of rock) as well as the observed range of values is very close to the average measured NP in the MWH samples via standard laboratory procedures.

The results of the AP and NP analyses are compared in Table 13 to evaluate net neutralization potential (NNP) of the Burro Canyon formation. NNP equals NP minus AP. The accepted criteria is that for NNP values greater than 20 kg $CaCO_3$ per metric ton of rock, the rock is not considered acid generating. Only two samples (MW-3A and MW-26) meet this criterion, both located below the water table. For NNP values between -20 and 20 kg, the sample may or may not be acid generating and further kinetic testing is required to determine if the rock is acid generating. All of the remaining samples fall within this interval (including the play sand blank sample), with the majority very close to the center of this interval due to the presence of little or no AP or NP, particularly those collected within the vadose zone. The NNP result for MW-3A contradicts the predictions made by HGC that oxidation of pyrite would produce a reduction in pH as there is more than sufficient alkalinity in the sample to neutralize the acid generated.

In summary, the results of the HGC testing are generally inconclusive as to the potential to generate sufficient acidity to lower the pH of the groundwater using standard acid rock drainage assessment methods. Most samples exhibit little or no acid generating potential and some exhibit significant excesses of neutralizing carbonates consistent with previous laboratory analyses of NP. HGC has shown the presence of pyrite by visual inspection, although the sample selection was significantly biased toward potential horizons containing pyrite and the visual results are not quantitative. The available quantitative assessments by XRD provided by HGC for similarly selected samples (although not of the same horizons) do no indicate detectable amounts of pyrite above the water table (i.e. weight percentages below 0.1%). Furthermore the total sulfur is not an indicator of additional pyrite (as presumed by HGC) as much of the sulfur is present as sulfate sulfur (i.e. in the form of gypsum and anhydrite) which is already oxidized. While all of the samples contain similar amounts of iron, this iron is indicated to not be present as pyrite and is probably present in other forms (per referenced observations of previous investigators). Limonite is a mixture of various amorphous hydrated ferric oxide-hydroxides that may be individually indistinguishable by XRD.

In lieu of kinetic testing, HGC (2012) conducted screening level and geochemical model (PHREEQC) calculations. The following observations pertain to those calculations:

- The calculations apparently do not account for the rate of pyrite oxidation (no reaction rates are provided or indicated). The pyrite oxidation rate is very slow at near neutral pH, and even more so under saturated conditions.
- The screening level calculations do not account for dissolution of calcium and magnesium carbonates present in the aquifer. It is also unclear why the modeling would show a reduction in pH at MW-3A when the carbonates present are more than sufficient to neutralize the pyrite present.
- Oxygen supply is essentially unlimited as the initial oxygen content in the geochemical model was adjusted to provide as much oxygen as necessary which is a valid assumption for the vadose zone. However, the simulations are all based on samples collected from the saturated zone where oxygen supply would be significantly limited and where pyrite concentrations were much higher (no pyrite was detected above the water table).
- The modeling indicates reductions in pyrite concentrations of 33%, 6%, and 3% for MW-3A, MW-24, and MW-7, respectively, over a period of 5 years. If pyrite actually reduces at this fast a rate in five years, then there would be no pyrite present at the site in the vadose zone after 15 to 170 years under natural (pre mill) conditions.

Based on the results of the previous analyses, the following observations and conclusions are presented:

- Oxidation of pyrite below the water table is not expected to occur due to the very low solubility of oxygen in water and the slow rate of oxygen diffusion through water. In fact, subaqueous disposal of acid generating mine wastes is a proven and practiced method of preventing pyrite oxidation. This means that if oxidation of pyrite is occurring, it has to be occurring above the water table. However, as previously shown, water levels have been increasing over the site.
- Diffusion of oxygen combined with natural barometric pressure fluctuations at the ground surface, as well as along the exposed outcrops of the Burro Canyon formation that border White Mesa can be expected to fully oxygenate the vadose zone at the mill site. Oxygenation of the vadose zone is also indicated by the presence of aerobic conditions within the underlying aquifer. It is also reasonable to assume that climatic conditions have been sufficiently stable for at least hundreds if not thousands of years that there has been little change in groundwater elevations prior to the mill construction. Thus any significant amounts of sulfides within the vadose zone (as defined by groundwater levels prior to the mill construction) would be expected to have completely oxidized over such a long time period. This is supported by the fact that no pyrite was detected in the XRD diffraction analyses in any of the samples from above the water table.
- Infiltration of oxygenated water from surface ponds is not expected to increase oxidation within the vadose zone as the solubility of oxygen in water is much lower than the

capacity for oxygen movement through the saturated zone per the mechanisms described in the previous paragraph. The surface pond infiltration could actually reduce oxygen diffusion by increasing the saturation of certain layers within the Burro Canyon formation (reducing air flow and oxygen diffusion) including the potential creation of local perched zones. The discharge from the ponds has increased water levels over the entire area and could potentially flush residual sulfide oxidation products from the sandstones in pore spaces that are not usually water filled. However, this possibility is not supported by the measurements of paste pH or neutralization potential of vadose zone samples which suggest net alkalinity and rates of pH change are lowest in areas of the largest amount of flooding and highest in areas below the cells with the least amount of flooding. This suggests that seepage from the tailings cells is a more likely cause of the observed changes in pH.

- Purging or pumping of wells can cause temporary lowering of the water table, exposing zones containing pyrite to oxygen. For well purging, this would be expected to be a fairly brief period of time which limits the amount of pyrite oxidation that can occur. For pumping or purging the effect would also be limited to the immediate vicinity of the wells as the hydraulic conductivity of the formation is relatively low. Based on hydrographs of the pumping wells MW-4 and MW-26, the groundwater mounding at the site has raised the water table sufficiently above the pre-mill levels, that subsequent pumping has not lowered the water table below the pre-mill levels.

3.4 Heavy Metals

The average concentrations of heavy metals for each well are summarized in Table 10. The tailings solutions are characterized by a very low pH and very high concentrations of heavy metals so it is expected that any seepage from the tailings cells would result in an increase in heavy metals concentrations and a decrease in pH of the underlying groundwater. The ratio of the concentration of total dissolved solids in the tailings to that in upgradient groundwater is approximately 72:1, whereas the ratio of the concentration of total heavy metals in the tailings to that in upgradient groundwater is approximately 18,000:1. Therefore, any seepage from the tailings is expected to be most apparent in changes in heavy metal concentrations.

Several heavy metals including iron, manganese, selenium, thallium, uranium, and zinc have been detected in one or more of the upgradient wells (MW-1, 18, 19) indicating that these are naturally occurring in the perched aquifer or are present from upgradient sources. However, many more types of heavy metals have been detected in the groundwater below and downgradient of the tailings cells including arsenic, beryllium, cadmium, chromium, cobalt, copper, lead, mercury, molybdenum, nickel, and vanadium, as shown in Table 10 and Figure 20. Although iron, manganese, selenium, and zinc are detected in the upgradient wells, higher concentrations of iron, manganese, selenium, and zinc are often found in the groundwater below and downgradient of the tailings cells in association with the detection of other heavy metals.

The wells below the tailings cells exhibiting the largest number of heavy metals detected and/or the highest concentrations of heavy metals include: MW-24 and MW-28 (downgradient side of tailings cell 1); MW-26, 29, 20, and 32 (Tailings Cell 2); MW-11, 12, 23, and 25 (Tailings Cell 3); and MW-35 (Tailings Cell 4B). Figure 20 suggests the highest amount of seepage is from Tailings Cells 1 and 2 and heavy metals are detected more frequently below these cells. These are the oldest tailings cells, which has permitted more time for seepage to reach the water table. Tailings Cell 1 has also remained filled with solution and has been absent of tailings solids during the entire operating life of the mill, which provides a higher driving head for seepage. High concentrations and numbers of heavy metals are also found in the monitoring wells downgradient of the tailings cells, particularly MW3, 3A, and MW-22. These include all of the heavy metals found in the groundwater below the tailings cells except arsenic and chromium.

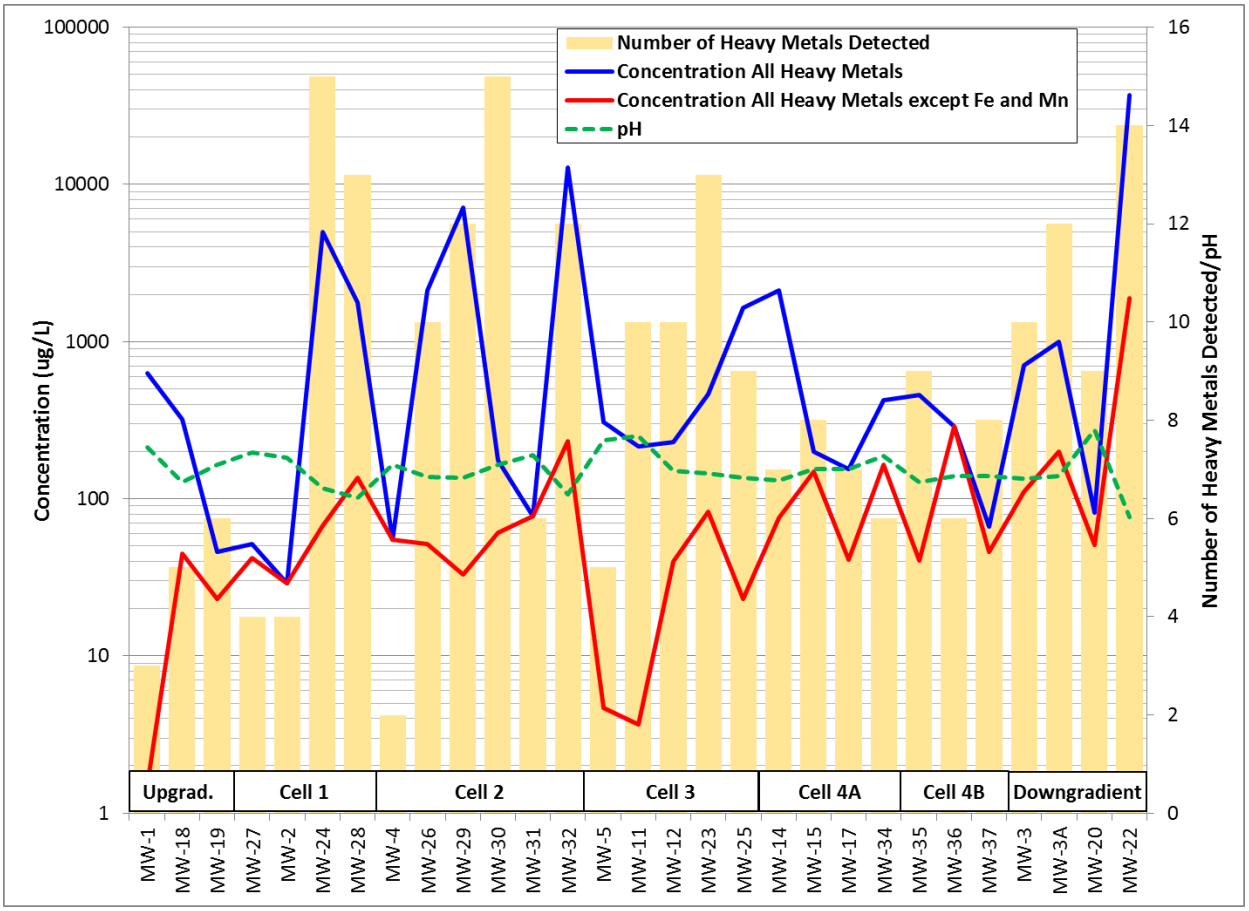

FIGURE 20 - HEAVY METALS IN MONITORING WELLS

Wells with a pH below 7 or equivalently a hydrogen ion concentration greater than 0.1 µg/L (i.e. slightly acidic) typically exhibit higher concentrations of some metals including cadmium, cobalt, manganese, nickel, and zinc (Figure 21). While the solubility of many metals is pH dependent, some including cobalt and nickel are only weakly dependent within the small range of pH variations observed (Figure 22) with an expected water solubility in excess of the

observed concentrations. Figure 22 shows this relationship based on testing of a simulated low pH waste water solution containing 13 heavy metals and neutralized with sodium hydroxide. Although it is noted that solubility varies with the specific solution composition the test solution is reasonably similar to the tailings solution waters. Furthermore, metal solubility as a function of pH is distinctly different for different metals. As shown in Figure 21 the concentrations of cadmium, cobalt, manganese, nickel, and zinc in site groundwater only increase below a pH of 7, which would not be expected for all five of these metals based on solubility constraints. Therefore, the association of low pH and high metals appears to be the result of the source chemistry (seepage of solution from the tailings cells) and not changes in solubility. High concentrations of iron (whose solubility is very pH dependent) are only found in the wells with pH values of 6.8 or less (MW-24, 26, 29, 32), although iron is not found at relatively high concentrations in some wells with low pH (MW-28 and MW-22). Iron is not expected to be as easily transported by groundwater due to its strong dependency of solubility on pH and quick oxidation under aerobic conditions to normally insoluble ferric oxides and oxyhydroxides.

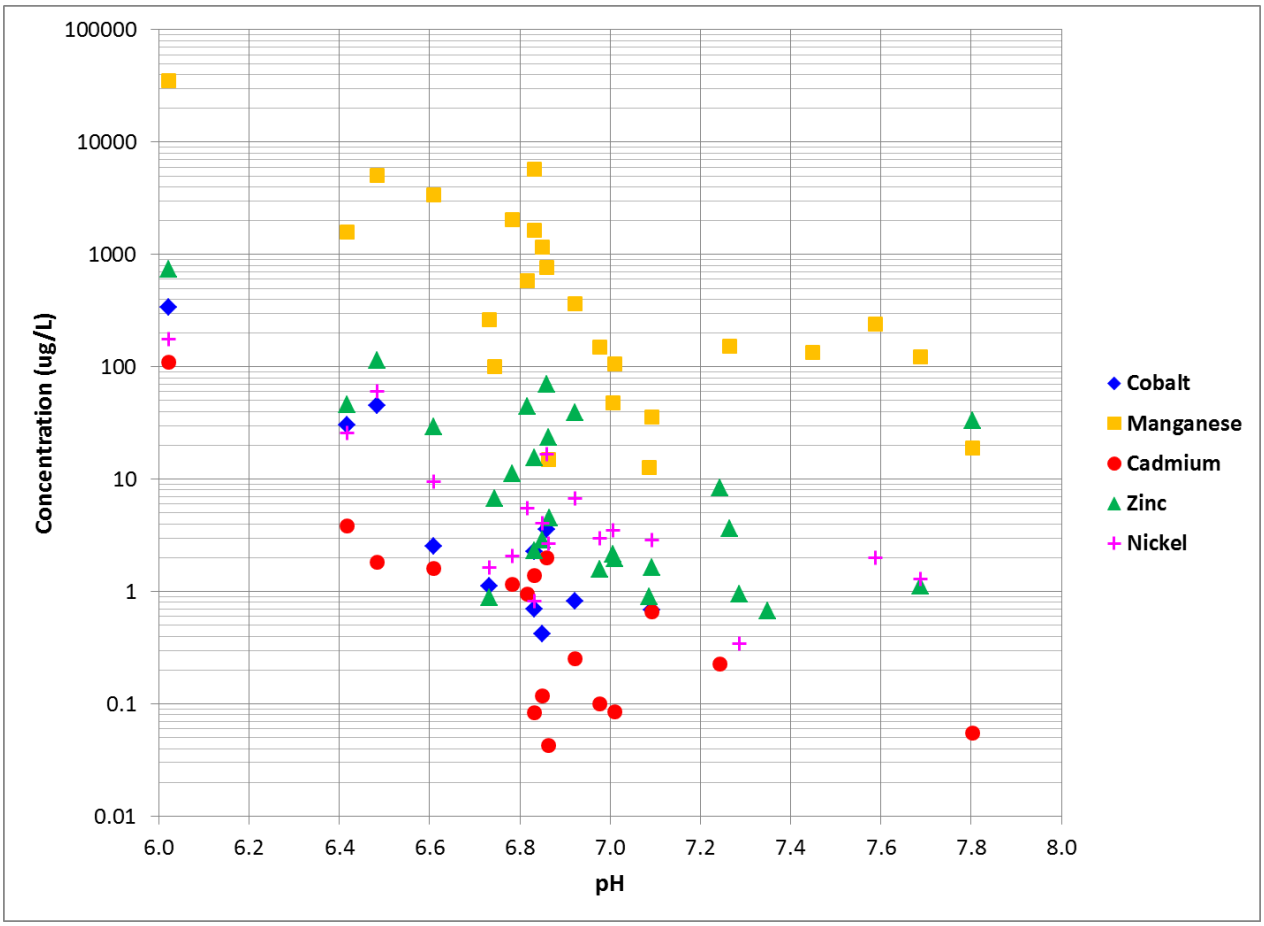

FIGURE 21 - VARIATION OF Cd, Co, Mn, Ni, and Zn CONCENTRATIONS WITH pH

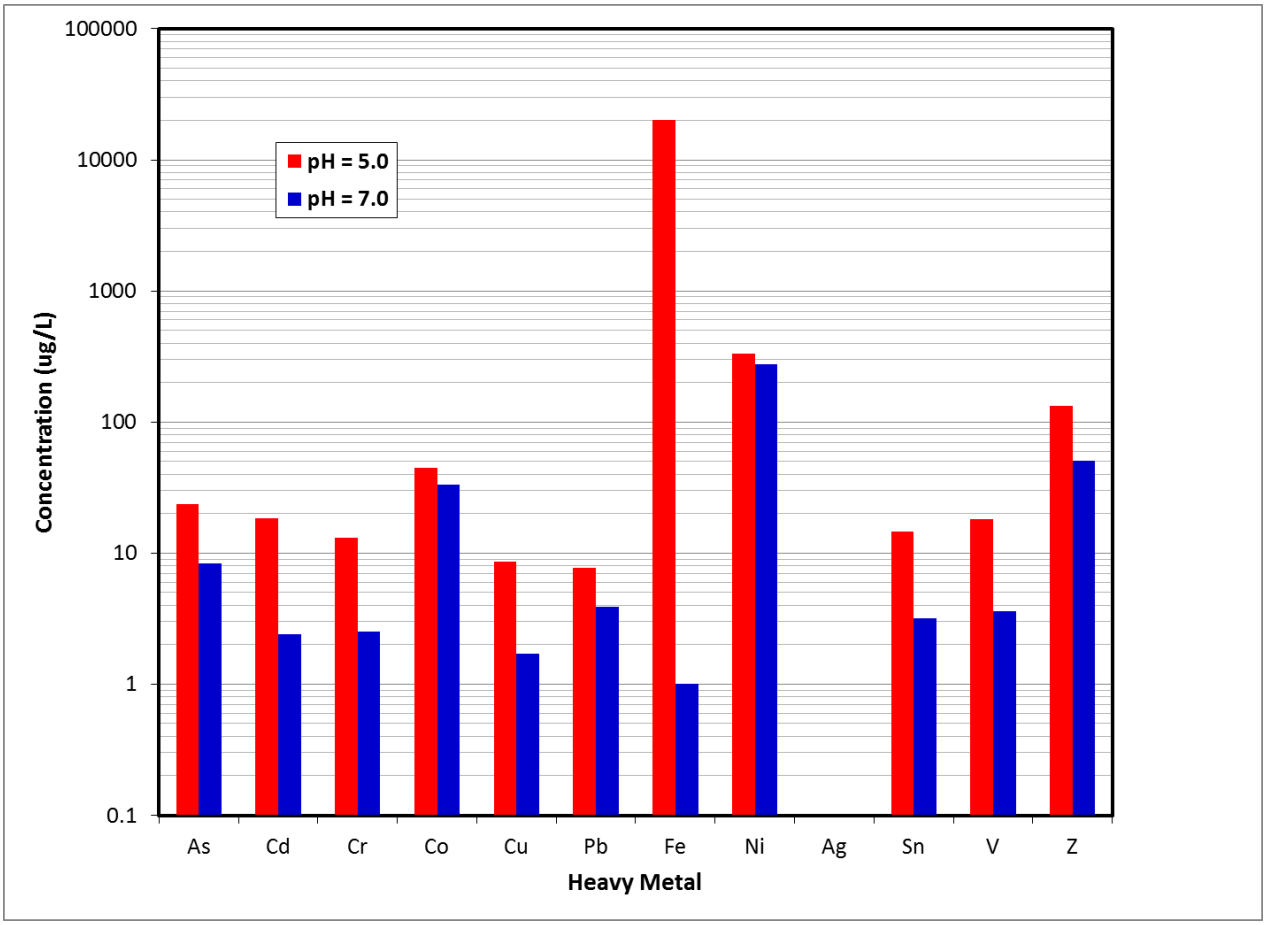

FIGURE - 22 INDICATED SOLUBILITY LIMITS OF HEAVY METAL CONCENTRATIONS FOR pH OF 5 AND 7

A comparison of the heavy metals concentrations in groundwater below the tailings cells with the tailings cell solutions is shown in Figure 23 using a Schoeller diagram. Because concentrations are presented on a logarithmic scale, the exhibited patterns at different dilutions would generally be the same providing a fingerprint of the contaminant source. Note that the tailings solutions are plotted on the right hand scale, while the other data is plotted on the left hand scale. The scales are aligned to show an equivalent 0.1% of the tailings solution concentration in groundwater. Also presented on this figure are the estimated solubility limits for pH values of 5 and 7 taken from Figure 22 or similar published test results for manganese (Mn, Fe, SO4 solution) and selenium (Se, Fe solution). The patterns observed show a general similarity in the relative concentrations of the various heavy metals, particularly for Tailings Cell 1, suggesting that the tailings solution is a likely source for the observed heavy metals concentrations in groundwater below the tailings cells. Concentrations of chromium, copper, silver, vanadium, and zinc in the groundwater are lower than expected due to limits on the solubility of these metals in the range of groundwater pH values (silver was not detected in the solubility test at a detection limit of 0.1 µg/L). Iron is the only compound whose groundwater concentrations exceed the indicated solubility limit for pH 7, although it is only detected in

association with lower pH values. Tin is found at lower than expected concentrations because the detection limit was normally 100 µg/L and non-detected values were assumed to be zero as previously discussed. Iron, manganese, selenium, and thallium are somewhat higher because of natural background concentrations.

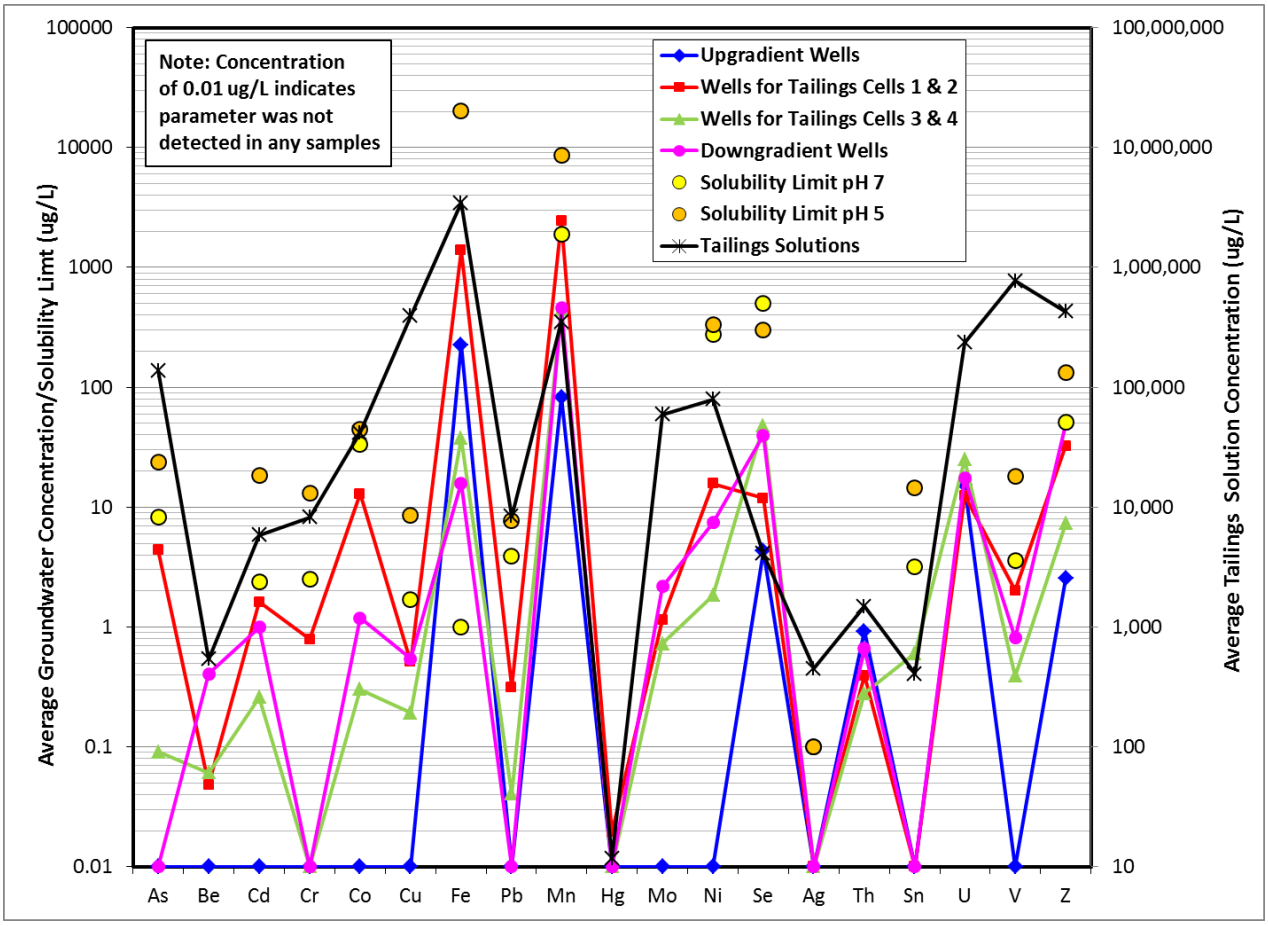

FIGURE 23 - COMPARISONS OF HEAVY METALS CONCENTRATIONS IN TAILINGS SOLUTION WITH GROUNDWATER

Figure 24 shows the distribution of heavy metals concentrations at the site. The highest concentrations of heavy metals are found in the vicinity of Tailings Cells 1 and 2. Total heavy metals other than iron and manganese decrease significantly in wells MW-5 and MW-11. As discussed previously, these wells have exhibited pH values that are higher than expected for natural groundwater.

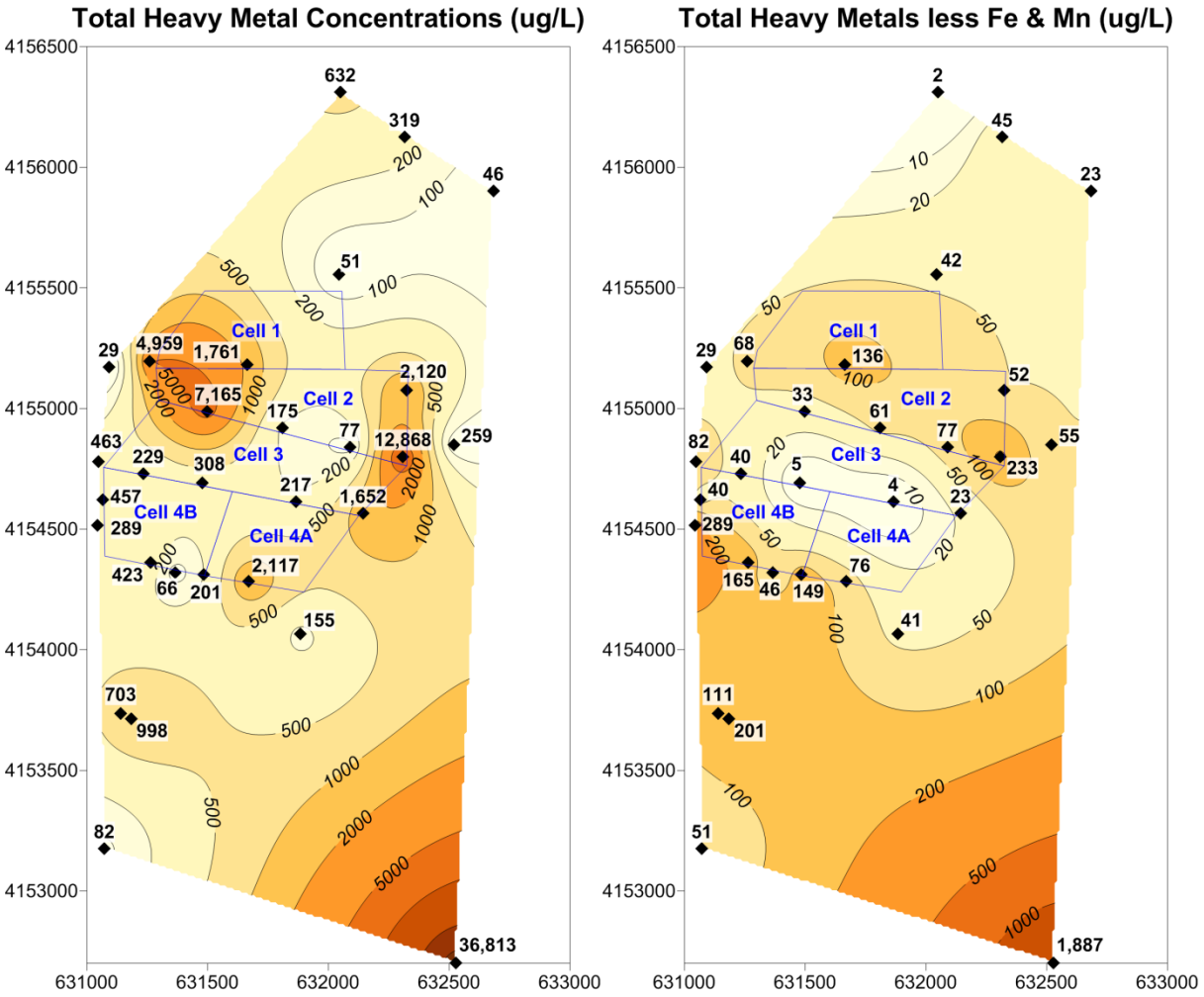

FIGURE 24 - HEAVY METALS CONCENTRATIONS IN GROUNDWATER

3.5 Organic Constituents

Organic constituents are not naturally occurring in groundwater and are clear indications of recent seepage sources. Most organic compounds were not in use prior to the 1940s when they were first developed for commercial use. An analysis of the data was performed to determine the current distribution of organic constituents and the effectiveness of current remedial efforts.

Table 10 summarizes the average concentrations of organic constituents found in the MW series wells at the site from 2005 to 2014. Acetone, benzene, carbon tetrachloride, chloroform, chloromethane, methyl ethyl ketone (MEK), methylene chloride, tetrahydrofuran, toluene, and xylenes have all been detected at least once at the site. Chloromethane, tetrahydrofuran, and toluene have all been detected in upgradient wells, although generally infrequently except for tetrahydrofuran in MW-1. In the tailings cell solutions detected organic constituents include acetone, chloroform, chloromethane, MEK, methylene chloride, naphthalene, tetrahydrofuran,

toluene, and xylenes. However, only chloroform is always detected in these solutions, with chloroform and naphthalene being detected about 70% of the time, and the measured concentrations of organic compounds in the tailings solution are low, suggesting that the tailings solution are not a significant source of organic compounds in the subsurface.

Within groundwater below or near the tailings, acetone, carbon tetrachloride, chloroform, chloromethane, MEK, methylene chloride, tetrahydrofuran, toluene, and xylenes have been detected, although generally infrequently and at low concentrations. The highest concentrations of organics are found in the area of the chloroform plume which extends from the mill site (somewhere east of Tailings Cell 1) to south southeast for approximately 3,000 ft (Intera, 2009), and includes monitor wells MW-4 and MW-26. The chloroform plume has been further defined by additional temporary monitoring wells (TW4 series) dedicated to this purpose. Figure 25 shows the current extent of the chloroform plume as well as the observed change in average concentration between 2014 and 2013.

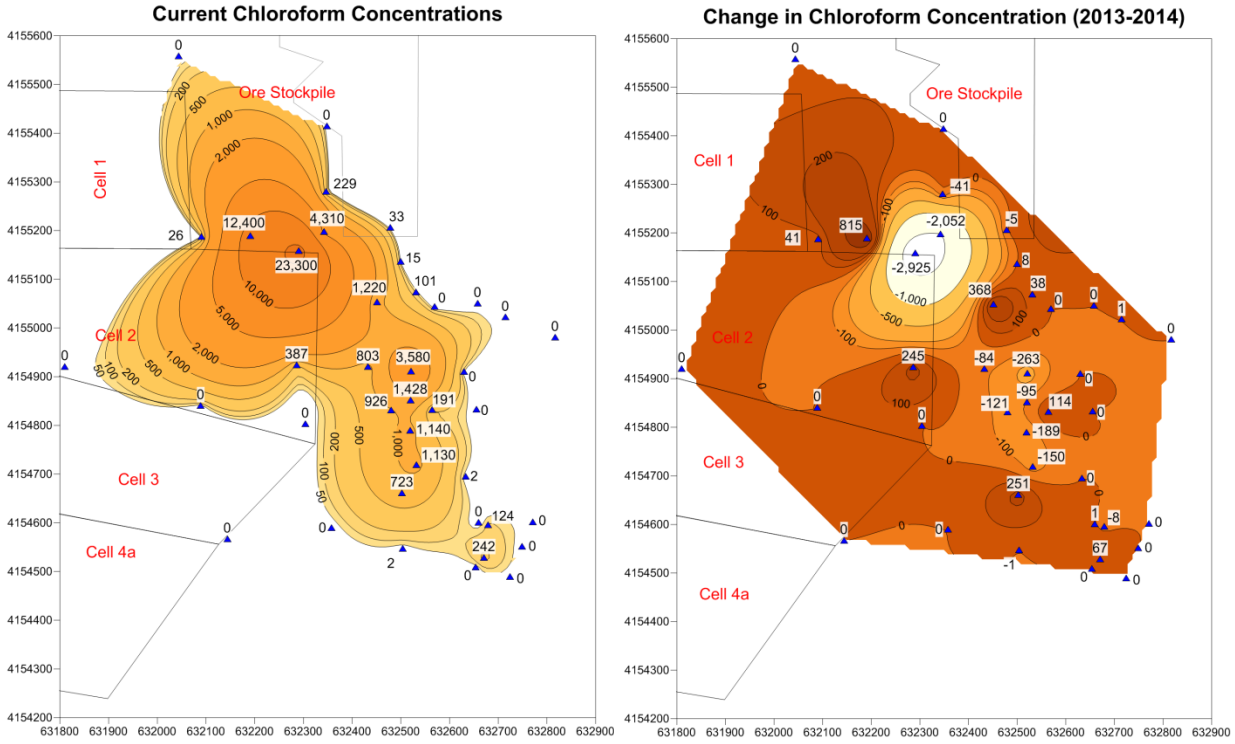

FIGURE 25 - CHLOROFORM CONCENTRATIONS

The highest chloroform concentrations are found near the northeast corner of Tailings Cell 2, although the exact upgradient extent of the plume is not well defined. Concentrations have decreased significantly since 2013 in the areas of highest concentrations, but are increasing slightly in areas surrounding the highest concentrations indicating some lateral dispersion of the chloroform plume is occurring around the areas of highest concentration. The largest increases are at TW4-22 (815 µg/L or 7%), TW4-10 (368 µg/L or 43%), TW4-16 (245 µg/L or 172%), TW4-6 (251 µg/L or 53%), and TW4-8 (114 µg/L or 148%). However, the lateral extent of

the plume boundaries was stable over this period, and the current lateral extent corresponds with the earliest mapped extent of the plume suggesting that plume migration is being largely controlled by the groundwater pumping program. Based on the plume configuration of Figure 25 and an estimated average saturated thickness of 50 ft, it is estimated that approximately 350 lbs of chloroform are presently in the perched aquifer. Average removal rate by pumping is approximately 60 lbs/yr (Energy Fuels Resources, 2014e) since the second quarter of 2007, suggesting that removal of the plume should be completed in about 10 years (accounting for decline of concentrations and associated removal rates with time).

Tetrahydrofuran has been detected with some frequency at MW-5 and MW-12 (southwest side of Tailings Cell 3) as well as at downgradient well MW-3, although not at average concentrations exceeding those found in upgradient well MW-1.

3.6 Isotope, CFC, and Noble Gas Studies

Additional groundwater chemistry studies include isotope, chlorofluorocarbon, and noble gas measurements (Hurst and Solomon, 2008; USGS, 2011). These studies were reviewed to provide additional insight into the sources and ages of groundwater at the site.

3.6.1 Isotope Studies

Tritium, which arises from atmospheric sources due to nuclear testing in the 1950s to 1970s, is an indication of fairly recent groundwater recharge. Atmospheric tritium concentrations over Utah peaked in 1963 at about 180 TU and are currently about 5 or 6 TU. Measured tritium levels in the wildlife ponds and tailings solutions are similar with values ranging from 5.54 to 6.63 TU although a considerably lower tritium level of 0.99 TU was measured in the Tailings Cell 2 slimes drain. Figure 26 shows the distribution of tritium in the wells, wildlife ponds, and springs. As expected, the recharge from the wildlife ponds is seen to impact tritium levels in the areas surrounding the ponds. Upgradient well (MW-19) which is closest to the north wildlife ponds had tritium levels of 3.54 TU, compared to up to 0.02 and 0.05 TU for upgradient wells MW-1 and MW-18. The highest level of tritium (8.67 TU) was found in MW-27 near the northwest corner of the mill, which suggests a separate recharge source in this area as discussed previously. Elevated levels of tritium were also detected in Entrance Spring (4.20 TU) which is expected given its close proximity to the north wildlife ponds, but also in Cottonwood Spring (not shown in Figure 26) at 5.45 TU which is not expected given that the source of this spring is in the Brushy Basin formation (not the perched aquifer). This suggests mixing of this spring discharge with surface waters. Other monitoring wells with measured tritium (in at least one sample) included MW-2 (0.24 TU), MW-11 (up to 0.05 TU), MW-14 (up to 0.36 TU), MW-22 (up to 0.87), and MW-29 (up to 0.07). Wells where tritium was not detected included wells MW-3, 3A, 5, 30, and 31. These low concentrations of detected tritium could be the influence of lesser sources of surface recharge or seepage. The presence of any measurable amount of tritium indicates the groundwater contains at least some recharge water younger than 1954.

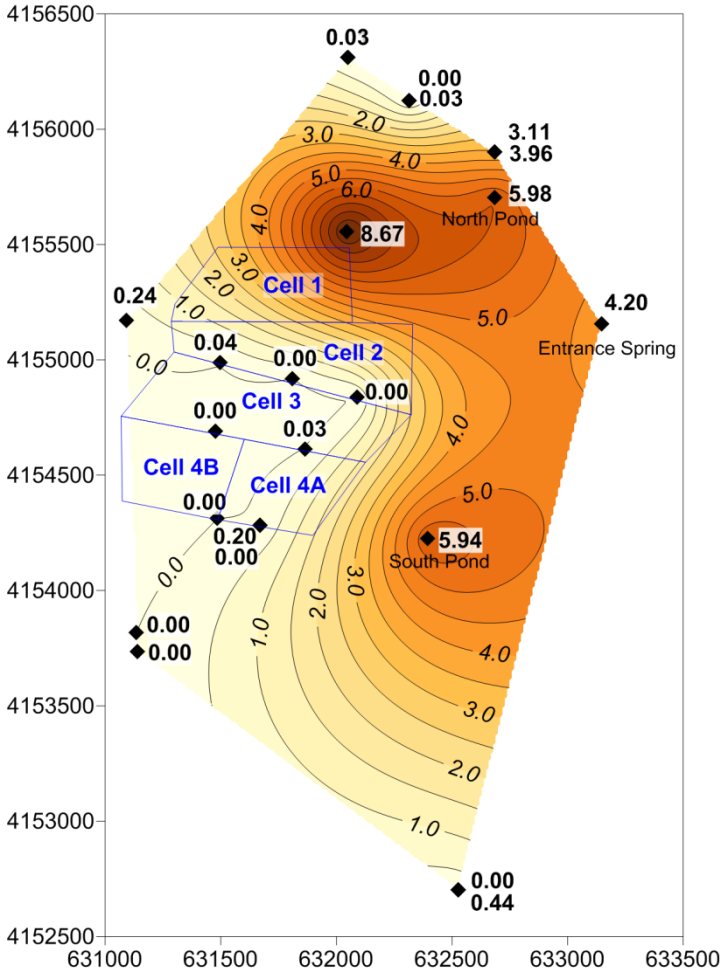

FIGURE 26 - TRITIUM CONCENTRATIONS

Deuterium and oxygen-18 isotope ratios were measured in samples collected from selected monitoring wells, the wildlife ponds, and the Tailings Cell 3 solution (Hurst and Solomon, 2008). These measurements were later supplemented with different sampling points around the site including Entrance, Westwater (Mill) , Ruin, and Cottonwood (Cow Camp) groundwater springs, one upgradient agricultural well (Lyman Well), a stock watering pond (South Mill Pond), Recapture Reservoir, and two downgradient deep wells completed in the Navajo Sandstone (USGS, 2011).

The relationship between deuterium and oxygen-18 isotope ratios is compared to the global and arid zone meteoric lines in Figure 27. Groundwater at the site as well as water from the South Mill Pond lie along a line between water from the Navajo Sandstone and Recapture Reservoir (both of which have been used as a water supply at the mill site). Wells MW-19, MW-27, and Entrance Spring all have nearly identical isotopic signatures to that of Recapture Reservoir. In comparison, the site monitoring wells, springs and stock watering pond are depleted in deuterium and oxygen-18, while the upstream agricultural well, the wildlife ponds,

and the tailings water are enriched in these heavier isotopes due to evaporation losses (causing them to fall above the meteoric lines).

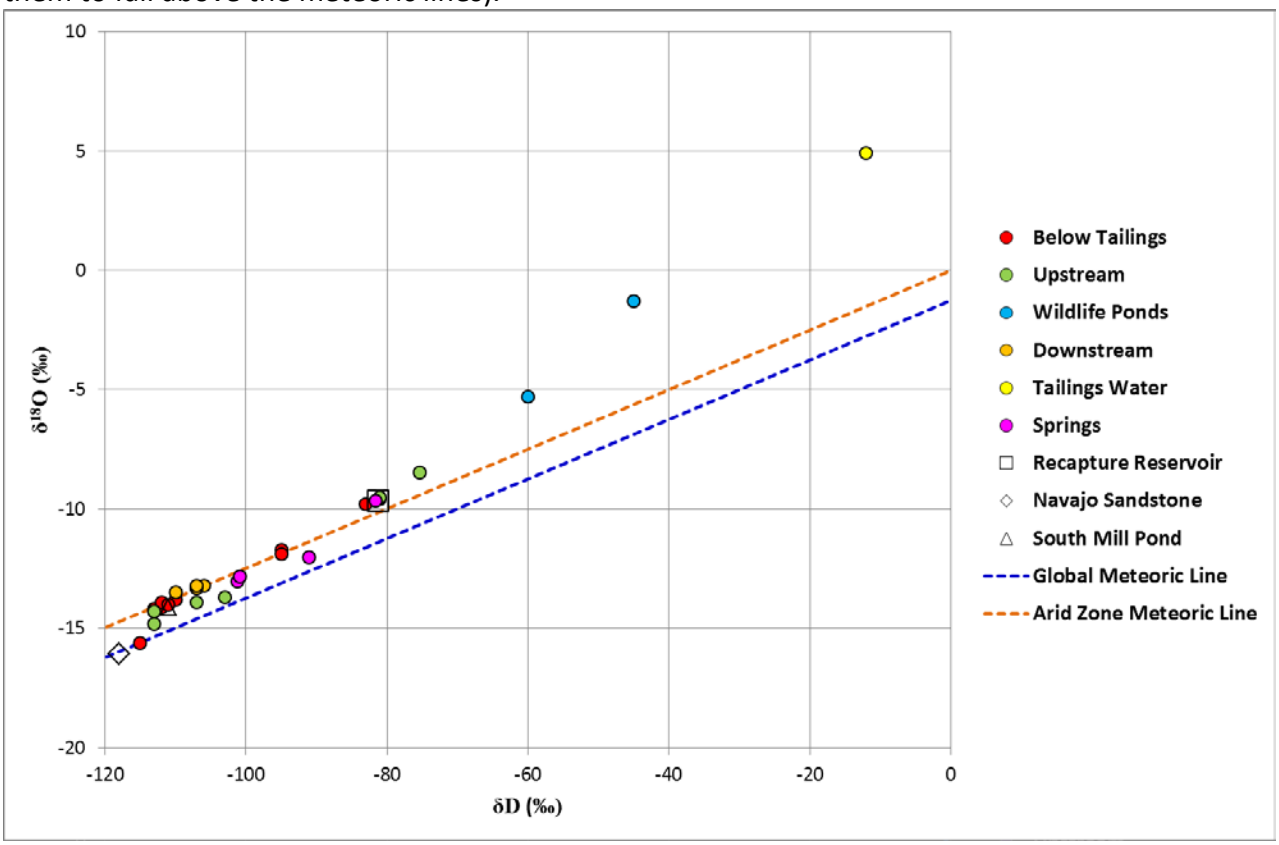

FIGURE 27 - OXYGEN-18 VS DEUTERIUM ISOTOPE RATIOS

Figure 28 shows the distribution of the deuterium and oxygen-18 isotope ratios which clearly indicates the influence of the wildlife ponds in a similar manner to that seen for tritium. Wells MW-27, MW-19, and Entrance Spring have slightly enriched deuterium and oxygen-18 relative to most groundwater at the site, although for MW-27 a separate seepage source is suspected as previously discussed. Below and just upstream of the tailings cells, both deuterium and oxygen 18 are more depleted, possibly from the prior use of water from the Navajo Sandstone during the early years of operation.

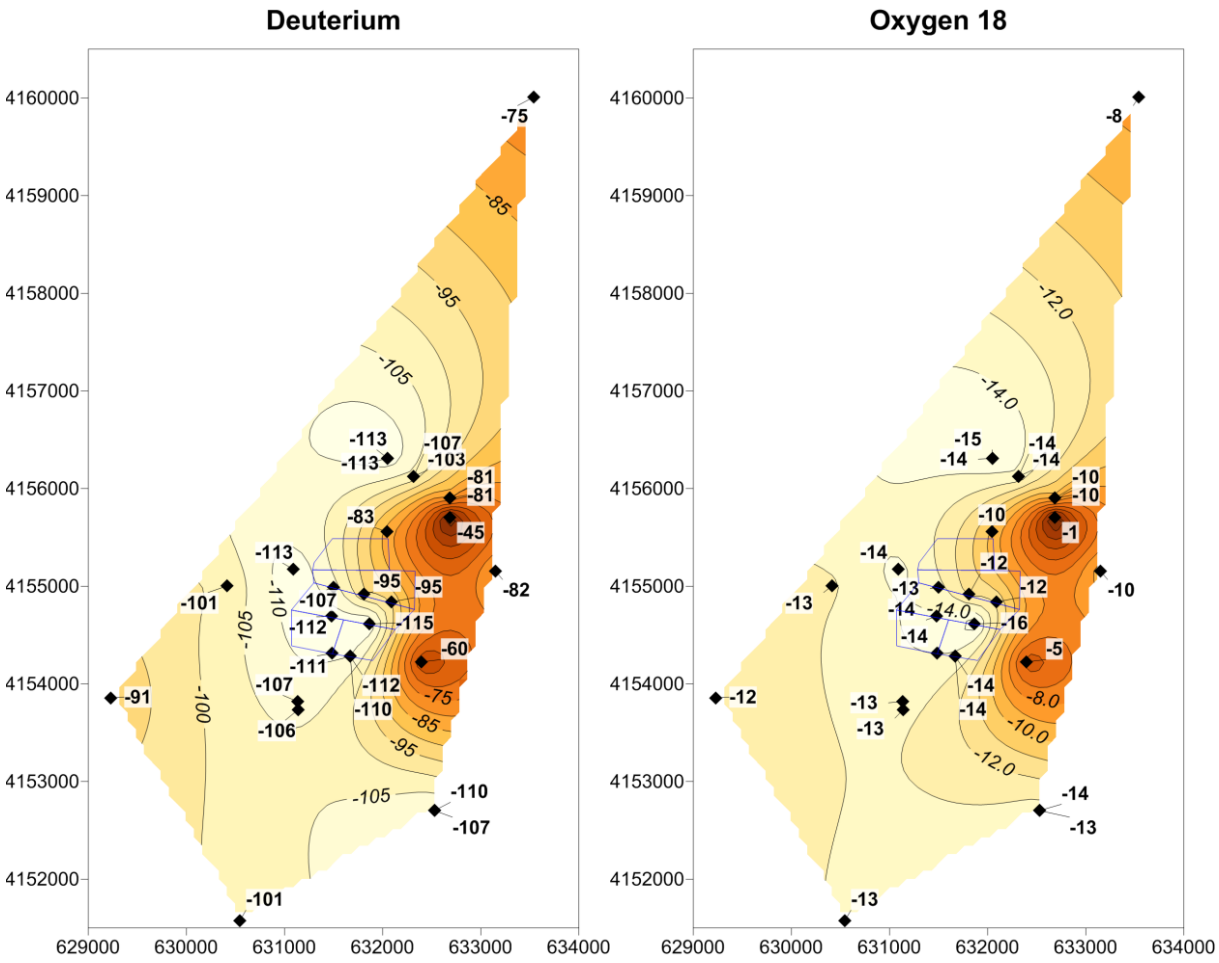

FIGURE 28 - DISTRIBUTIONS OF DEUTERIUM AND OXYGEN-18 ISOTOPE RATIOS

Figure 29 shows the relationship between sulfate oxygen-18 and sulfate sulfur-34 isotope ratios at the mill site as reported by Hurst and Solomon (2008) for the site monitoring wells, wildlife ponds, and tailings and the USGS (2011) for the Entrance, Westwater (Mill) , Ruin, and Cottonwood (Cow Camp) groundwater springs. The isotopic ratios of sulfur-34 and oxygen-18 are similar for the wildlife ponds, the tailings, and well MW-27, showing oxygen-18 enrichment and sulfur-24 depletion. Although the similarity of the sulfate isotope ratios of MW-27 has been related to the wildlife ponds, MW-19 which is much closer to the ponds and has similar deuterium and oxygen-18 ratio is not similar to MW-27 or the wildlife ponds with regard to the sulfate isotopes. This supports the previous indication of a separate recharge source near the northwest corner of the mill and that this source appears to be related to process solutions at the mill. Figure 29 shows a general tendency for oxygen-18 enrichment with sulfate-34 depletion. Although it has been suggested that this is due to evaporation, this would lead to both sulfur-34 and oxygen-18 enrichment. A more likely explanation is that dissolution of gypsum and anhydrite is occurring from the infiltration of the pond waters and the isotopic composition of the sulfate in these minerals is influencing the isotopic ratio observed in the monitoring wells. This is supported by the observation that oxygen-18 is depleted and sulfur-34

enriched as sulfate concentrations in groundwater increase at the site. Gypsum and anhydrite have been shown to contain higher sulfur-34 ratios ($\delta^{34}S$ of 14 to 18‰) in a recent study in western Colorado (Nordstrom et. al., 2007). Water from MW-22 exhibits a unique sulfur-34 to oxygen-18 ratio, although the cause of this cannot be ascertained.

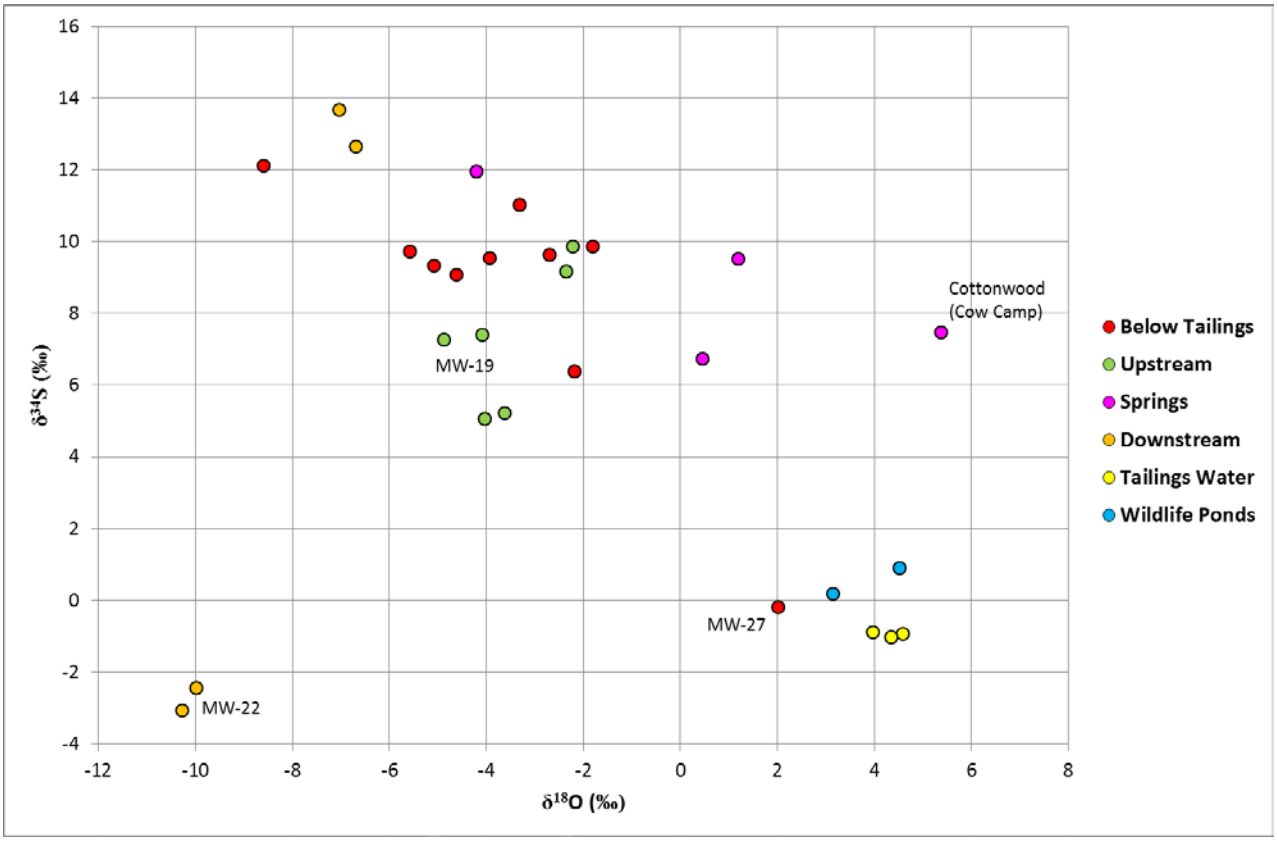

FIGURE 29 - SULFUR 34 VS OXYGEN 18 RATIOS

3.6.2 CFC Studies

Chlorofluorocarbons (CFCs) in groundwater are a result of atmospheric sources due to releases of these compounds from the 1940s through the 1990s. The Hurst and Solomon (2008) measured concentrations of these organic compounds in groundwater and calculated corresponding apparent ages (recharge dates) for the groundwater by assuming that the concentration of CFCs is fixed at the time that the precipitation falls on the land surface and infiltrates to recharge the aquifer. Generally speaking higher concentrations of CFCs correspond to more recent apparent ages. Table 14 summarizes the calculated recharge dates from their report. It is noted that there are discrepancies between the text and the table of values presented in the report as valid results. There is also considerable discrepancy in indicated ages calculated for different CFCs, indicating significant uncertainty in the calculated ages (average standard deviation of 6.4 years between different CFCs). Six samples had no detectable CFC-113 (which has the lowest atmospheric concentration), although other CFCs were detected in the same sample. Two samples had very high concentrations of CFC-12 relative to the other CFCs. To further complicate things, different recharge temperatures were assumed although it is not clear that recharge temperature selection relates to actual site conditions for most cases. To compare the samples an average data was calculated from all three samples. Where one sample was in significant disagreement with the other samples (values highlighted in yellow in Table 14), this value was ignored and the average date was calculated from the remaining values (corrected average in Table 14).

The corrected results generally show apparent groundwater recharge dates ranging from 1959 to 1985. This is equivalent to groundwater ages of 23 to 49 years (relative to the date of sample collection or 2007), and are indicative of relatively recent groundwater recharge. This would suggest that the perched groundwater at the site is locally recharged, given previous estimates of groundwater velocities. However, water in the wildlife ponds had apparent ages of 34 to 41 years, which would appear inconsistent with the fact that the water in the ponds is from Recapture Reservoir which presumably is composed mainly of surface runoff (i.e. younger waters). The youngest waters (apparent ages of 22 to 33 years) are generally found in areas that are not impacted by the wildlife ponds (for example MW-1, 23, and 3A), while the oldest waters (apparent ages of 40 to 48 years) are found below the tailings facilities (for example wells MW-5, 11, 14, 15, 29, and 31). This distribution of ages suggests that the apparent ages are not actual ages, but simply reflect different concentrations of CFCs due to different water temperatures and atmospheric exposure. The low CFCs below the tailings could be due to the presence of the lined tailings facilities above these areas combined with seepage from the facilities that would reduce atmospheric interaction with the groundwater, or it could indicate that CFCs are reduced during evaporation from the ponds resulting in older apparent ages due to seepage below the ponds (no CFC samples of the tailings solution were analyzed). The intermediate ages of the wildlife pond recharge water could be due to higher temperatures of this water combined with pond evaporation, which would reduce dissolved organic compounds. The youngest waters are associated with areas where the most stable groundwater conditions occur. The report also states: "*Samples collected near the water table are always higher in concentration than deeper samplers*". In fact just the opposite is true with

corresponding older ages observed for the shallower samples. Given all of the observed discrepancies, no truly meaningful interpretation of the CFC sample results appears to be possible.

TABLE 14 - APPARENT GROUNDWATER RECHARGE DATES FROM CFC MEASUREMENTS

SAMPLE ID	CALCULATED RECHARGE DATE			AVERAGE	CORRECTED AVERAGE
	MEAN CFC-11	MEAN CFC-12	MEAN CFC-113		
MW-1	1984.0	2001.5	1980.0	1988.5	1982.0
MW-1B	1985.0	1991.0	1980.0	1985.3	1985.3
MW-2	1979.5	1983.0	1984.0	1982.2	1982.2
MW-3	1971.0	1972.5	1980.0	1974.5	1974.5
MW-3A	1981.5	1989.5	1985.5	1985.5	1985.5
MW-5	1969.5	1966.5	1943.0	1959.7	1968.0
MW-11	1961.5	1958.0	1943.0	1954.2	1959.8
MW-14 S	1962.0	1957.0	1943.0	1954.0	1959.5
MW-14 D	1961.5	1958.0	1943.0	1954.2	1959.8
MW-15	1967.0	1971.0	1963.5	1967.2	1967.2
MW-18 S	1967.5			1967.5	1967.5
MW-18 D	1974.5	1961.5	1971.0	1969.0	1969.0
MW-19 S	1975.0	1978.5	1971.5	1975.0	1975.0
MW-19 D	1975.5	1981.5	1979.5	1978.8	1978.8
MW-27	1967.5	2001.5	1963.5	1977.5	1965.5
MW-29	1967.0	1965.0	1943.0	1958.3	1966.0
MW-31	1970.5	1978.5	1943.0	1964.0	1974.5
North WLP		1973.5	1962.0	1967.8	1967.8
South WLP	1973.5	1975.0	1974.5	1974.3	1974.3

3.6.3 Noble Gas Studies

The Hurst and Solomon (2008) also measured concentrations of dissolved noble gases (^{3}He, ^{4}He, ^{20}Ne, ^{40}Ar, ^{84}Kr, and ^{129}Xe) in selected monitoring wells, tailings solution (Tailing Cells 1, 3, and the slimes drain of Tailings Cell 2), and the wildlife ponds. Figure 30 shows the distribution of the concentration of noble gases expressed as a ratio of their average concentration (i.e. 1.20 equals 20 percent higher than average concentration). This figure clearly shows higher concentrations of noble gases associated with the wildlife ponds and associated seepage, as well as a smaller increase below the western side of Tailings Cell #2 near an area of expected seepage. Noble gas concentrations within the tailings solutions were variable with ratios of 0.62 and 0.92 for solutions from Tailings Cell 3 and Tailings Cell 1, but a high ratio of 6.88 for the Tailings Cell 2 slimes drain.

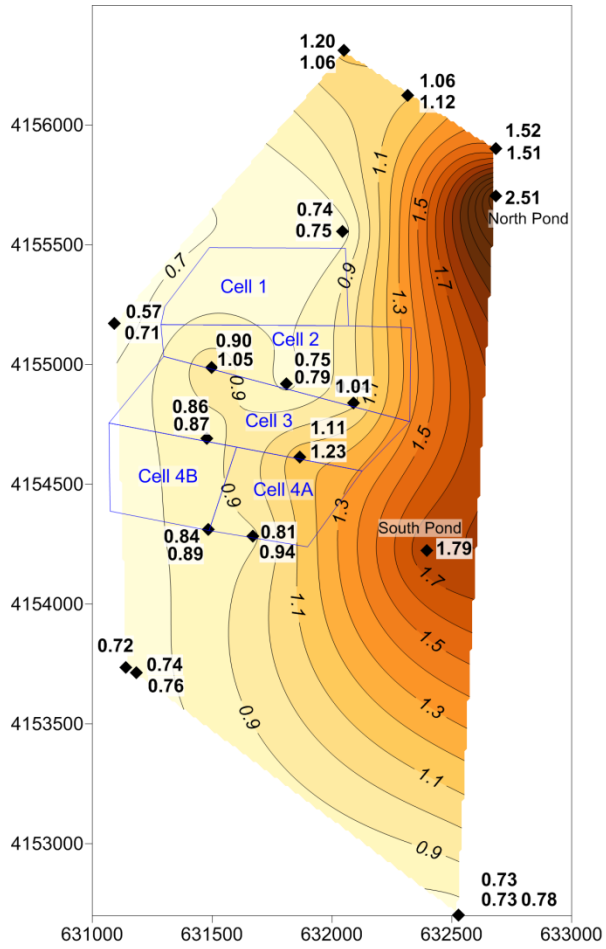

FIGURE 30 - NOBLE GASES IN WILDLIFE PONDS AND GROUNDWATER AS RATIO OF AVERAGE CONCENTRATION

4.0 SUMMARY AND CONCLUSIONS

Based on a review and analysis of the available data and reports of groundwater monitoring at the White Mesa Uranium Mill site, the following observations and conclusions are noted.

The site groundwater at the facility has been impacted by various releases over its operational history. These releases include the previously documented releases of 1) a nitrate/chloride source from somewhere in the vicinity of the northwest corner of the mill and 2) organic compounds (chiefly chloroform) from somewhere in the vicinity of the southwest corner of the mill (although the upstream extent of the later is not well defined). Other indicated releases have included seepage from lined facilities due to documented damage to the liners and/or collected seepage from leak detection systems. These include Roberts Pond (located near the northwest corner of the mill site) and the older tailings cells. Given the age (34 years) and construction (single 30 mil PVC liner) of Tailings Cell 1 and the continuous storage of tailings solutions within this facility, seepage from the facility is to be expected. Another older source of seepage is the former unlined fly ash pond located near the southwest corner of the mill.

The groundwater levels at the site have raised significantly due to seepage from the wildlife ponds with a maximum rise of up to 40 feet since 1994, although another significant seepage source is also indicated near the northwest corner of the mill as evidenced by continued localized mounding in this area. Seepage from this source is also indicated by increases in downstream water levels that predate the arrival of the wildlife pond seepage to the groundwater table in about 1993, but not the start of facility operations, indicating that seepage from an old (pre-mill) stock watering pond in this area is not the source. Fresh water as well as some sewage reclaim water (from mid-1980s to 1991) was discharged to the wildlife ponds. The seepage from the wildlife ponds does not appear to be significantly impacting water quality at present, although it has impacted groundwater flow directions and is expected to continue to do so for another 11 to 14 years due to the slow rate of seepage from the ponds to the water table surface. Estimates of travel times for vertical seepage from ground surface to the water table ranges from 4.6 to 16 feet per year. This means that releases may be occurring that are not yet being seen in the monitoring wells and that closure monitoring will be required for many years after final facility closure.

Past predictions of the rate of contaminant migration downstream of the facility (Titan, 1994; HGC, 2009) have been one to two orders of magnitude slower than actual observed rates from the documented releases. It has recently been argued (HGC, 2014) that downgradient migration will be much slower than observed upstream migration. However, past migration patterns have been significantly influenced by conductive channels and zones within the perched aquifer that were only identified during subsequent investigation of the releases, and it is considered highly probable that similar channels and zones also exist downgradient of the facility. Observed water level changes in downgradient wells, including MW-22, support the existence of such channels. Downgradient investigations have focused only on the southwestern portion of the aquifer, which is either unsaturated or only very slightly saturated, whereas much higher saturated thickness is observed to the southeast. Downstream migration has also been assumed to follow perpendicular to indicated contours of piezometric head, when actual directions of groundwater flow are likely to deviate from this direction due to the presence of more conductive zones. Indeed this is evidenced by the observed movement of the chloride/nitrate plume downstream of its source area. Additional investigation and monitoring of the southeastern portion of the site is required to better identify potential migration routes and groundwater impacts.

Groundwater at the site is generally characterized by high sulfate content, very low chloride content, with variable calcium and magnesium vs sodium content. Natural groundwater quality appears to be influenced primarily by three mechanisms:

- Dissolution of calcite and dolomite which results in higher calcium, magnesium, and bicarbonate
- Dissolution of gypsum (and anhydrite) which results in higher calcium and sulfate
- Cation exchange with kaolinite clay which results in lower calcium and higher sodium

Recharge from the wildlife pond seepage appears to contribute waters with higher calcium and bicarbonate and lower sodium and sulfate, although the source of these pond waters has changed over time and the chemistry of these waters is likely influenced significantly during seepage through the subsurface (former vadose zone) below the ponds.

The pH of the site waters is generally near neutral, although there is an indicated trend of decreasing pH with time. Previous studies (Intera, 2012; HGC, 2012) have suggested that this change is associated with rising water levels at the site, although there is no correlation between the magnitude of water level rises and current average pH values. Furthermore, the rate at which pH is declining is slower in areas with higher rates of water level increases than in the areas with lesser rates of water level increases. Other studies (HGC, 2012) have attributed the change to oxidation of pyrite within the aquifer. However, detectable quantities of pyrite (greater than 0.1%) were not found in the vadose zone (above the water table) despite that fact that sampling was biased towards samples expected to contain higher concentrations of pyrite (i.e. exhibiting high iron content and visual evidence of reduced conditions). Pyrite does not readily oxidize below the water table surface due to lack of oxygen (measured dissolved oxygen ranges from 0 to 5 mg/L in downgradient wells as cannot exceed 8 mg/L based on groundwater temperatures), and water tables have been rising site wide due to seepage from site facilities, not declining since the start of mill operations. This indicates that any pyrite oxidation must be occurring above the water table. However, pyrite above the water table would have been expected to already have oxidized over the last hundreds to thousands of years of expected stable groundwater conditions prior to mill operation. Furthermore, the measured paste pH of vadose zone samples is alkaline which indicates that accumulation of pyrite oxidation products has not occurred.

Seepage from the tailings cells (particularly the older cells) is indicated by increased concentrations of heavy metals, reduced pH (increased acidity), and lower bicarbonate concentrations. The indicated rate of seepage is currently low, although it is likely masked to some degree by the much higher seepage from the wildlife ponds and other sources. Because the total heavy metal concentrations in the tailings solution is approximately 18,000 times higher than that in the upgradient groundwater (compared to 40 times higher for TDS), the impact on the groundwater chemistry is more significant.

The chloroform plume resulting from the release of organic constituents appears to have been stabilized and groundwater pumping is currently being used to remove the plume. Although lateral dispersion from the zones of highest concentration is occurring within the center of the plume, the boundaries of the plume do not appear to be currently expanding. The plume is estimated to currently contain approximately 350 lbs of chloroform and remedial pumping is reported to have removed an average of about 60 lbs/yr since the first quarter of 2007, suggesting that removal of the plume will be completed in about 10 years (accounting for decline in concentrations and associated removal rates over time). The northern and western extents of the chloroform plume are not well defined. Apart from the chloroform plume area,

organic constituents are infrequently detected and average concentrations have not exceeded those found in upgradient wells.

Additional site investigations include measurement of isotopes (deuterium, tritium, oxygen-18, and sulfur-34), noble gases, and chlorofluorocarbons. The isotope and noble gas study results are dominated by the substantial recharge from the wildlife ponds with higher levels of tritium, higher isotope ratios of deuterium and oxygen-18, and dissolved concentrations of noble gases. However, these data suggest that a second recharge source is located near the northwest corner of the mill site as indicated by higher tritium levels and a sulfur-34 to sulfate oxygen-18 ratio similar to the process solutions and wildlife ponds in MW-27 that is not found in other wells at the site.

5.0 REFERENCES

Dames and Moore (1978) as cited by International Uranium (2000).

Denison Mines USA (2007) White Mesa Uranium Mill, License Application, February 28.

Energy Fuels Resources USA (2014a) Renewal Application State of Utah Groundwater Discharge Permit No. UGW370004, June.

Energy Fuels Resources USA (2014b) Public Participation Summary, Dawn Mining Alternative Feed Request. July 10.

Energy Fuels Resources USA (2014c) White Mesa Uranium Mill Nitrate Monitoring Report, 4th Quarter (October through December) 2013. February 21.

Energy Fuels Resources USA (2014d) White Mesa Mill 2014 Annual Tailings Wastewater Report, Tab D: Chemical and Radiological Summary Tables.

Energy Fuels Resources USA (2014e) White Mesa Uranium Mill Chloroform Monitoring Report, 1st Quarter (January through March) 2014. May 19.

Energy Fuels Resources USA (2015) Roberts Pond Excavation Report. April 6.

Roberts, Harold (2004) Supporting Information for GWDP. E-mail to Loren Morton, February 19.

Hurst T.G. and Solomon D.K. (2008) Summary of work completed, data results, interpretations and recommendations for the July 2007 Sampling Event at the Denison Mines, USA, White Mesa Uranium Mill near Blanding, Utah, University of Utah.

Hydro Geo Chem (2007) Preliminary Contamination Investigation Report, White Mesa Uranium Mill near Blanding, Utah. November 20.

Hydro Geo Chem (2009) Site Hydrogeology and Estimation of Groundwater Travel Times in the Perched Zone, White Mesa Uranium Mill Site near Blanding, Utah. August 27.

Hydro Geo Chem (2012) Investigation of Pyrite in the Perched Zone, White Mesa Uranium Mill Site, Blanding, Utah. December 7.

Hydro Geo Chem (2014) Hydrogeology of the White Mesa Mill, Blanding Utah. June 6.

Intera (2007) Revised Addendum, Evaluation of Available Pre-Operational and Regional Background Data, Background Groundwater Quality Report: Existing Wells For Denison Mines (USA) Corp.'s White Mesa Uranium Mill Site, San Juan County, Utah. November 16.

Intera (2008) Revised Addendum Background Groundwater Quality Report: New Wells for Denison Mines (USA) Corp.'s White Mesa Mill Site, San Juan County, Utah. April 30.

Intera (2009) Nitrate Contamination Investigation Report, White Mesa Uranium Mill Site, Blanding, Utah. December 30.

Intera (2012) pH Report, White Mesa Uranium Mill, Blanding, Utah. November 9.

International Uranium USA (2000) Reclamation Plan White Mesa Mill. July.

MWH (2010) Revised Infiltration and Contaminant Transport Modeling Report, White Mesa Mill Site, Blanding, Utah. March.

Nordstrom, D.K. (1982) Aqueous pyrite oxidation and the consequent formation of secondary iron minerals, InKittrick, J. A., Fanning, D. S., and Hossner, L. R., eds., Acid Sulfate Weathering, Soil Sci. Soc. Am. Publ., 37‑56.

Roberts, H (2004) Supporting Information for GWDP. Memo to Loren Morton of DRC, February 19.

Titan Environmental (1994) Hydrogeologic Evaluation of White Mesa Uranium Mill. July.

UMETCO Minerals Corp and Peel Environmental Services (1993) Groundwater Study, White Mesa Facility, Blanding, Utah, January.

Nordstrom, D.K., Wright, W.G., M. Mast, M.A., Bove, D.J. and R.O. Rye (2007) Aqueous-Sulfate Stable Isotopes—A Study of Mining-Affected and Undisturbed Acidic Drainage. Chapter E8 of Integrated Investigations of Environmental Effects of Historical Mining in the Animas River Watershed, San Juan County, Colorado. Edited by S. E. Church, P. von Guerard, and S. E. Finger, Professional Paper 1651, U.S. Geological Survey.

USGS (2011) Assessment of Potential Migration of Radionuclides and Trace Elements from the White Mesa Uranium Mill to the Ute Mountain Ute Reservation and Surrounding Areas, Southeastern Utah. Scientific Investigations Report 2011–5231, U.S. Geological Survey.

Utah Division of Radiation Control (2004) Ground Water Quality Discharge Permit Statement of Basis for a Uranium Milling Facility at White Mesa, South of Blanding, Utah. December 1.

Utah Division of Radiation Control (2011) Ground Water Quality Discharge Permit UGW370004, Statement of Basis for a Uranium Milling Facility, South of Blanding. Document DR-2011-001889, February.

Utah Division of Water Quality (2008) Ground Water Quality Discharge Permit UGW370004. Issued to Dennison Mines, March 17.

White J.L., Wait T.C. and M. L. Morgan (2008), Geologic Hazards Mapping Project for Montrose County, Colorado. Colorado Geological Survey, Denver, Colorado.

Appendix A Matching of Groundwater Mounding Response in Monitor Wells

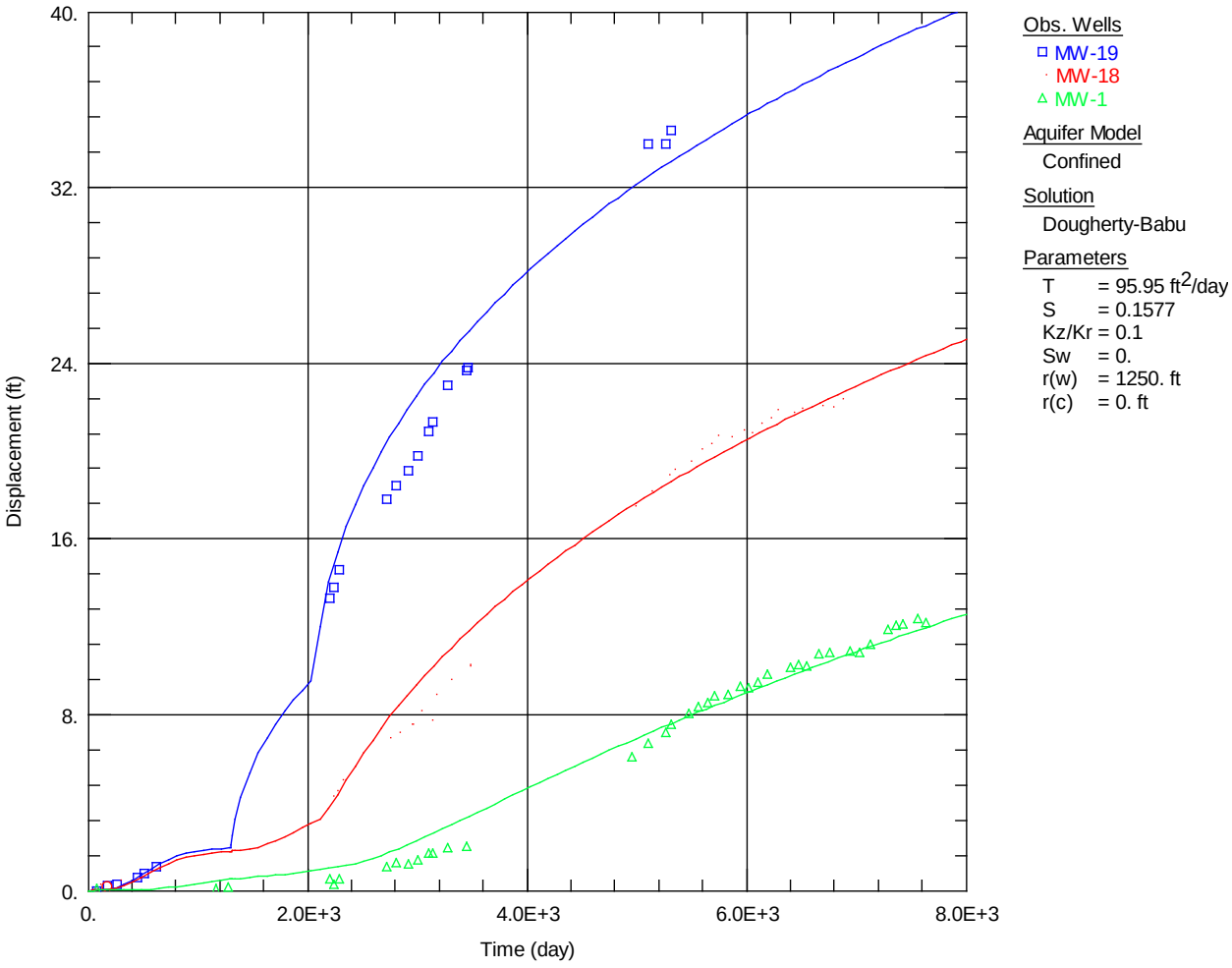

FIGURE A1 - MATCH TO WELLS MW-1, MW-18, AND MW-19

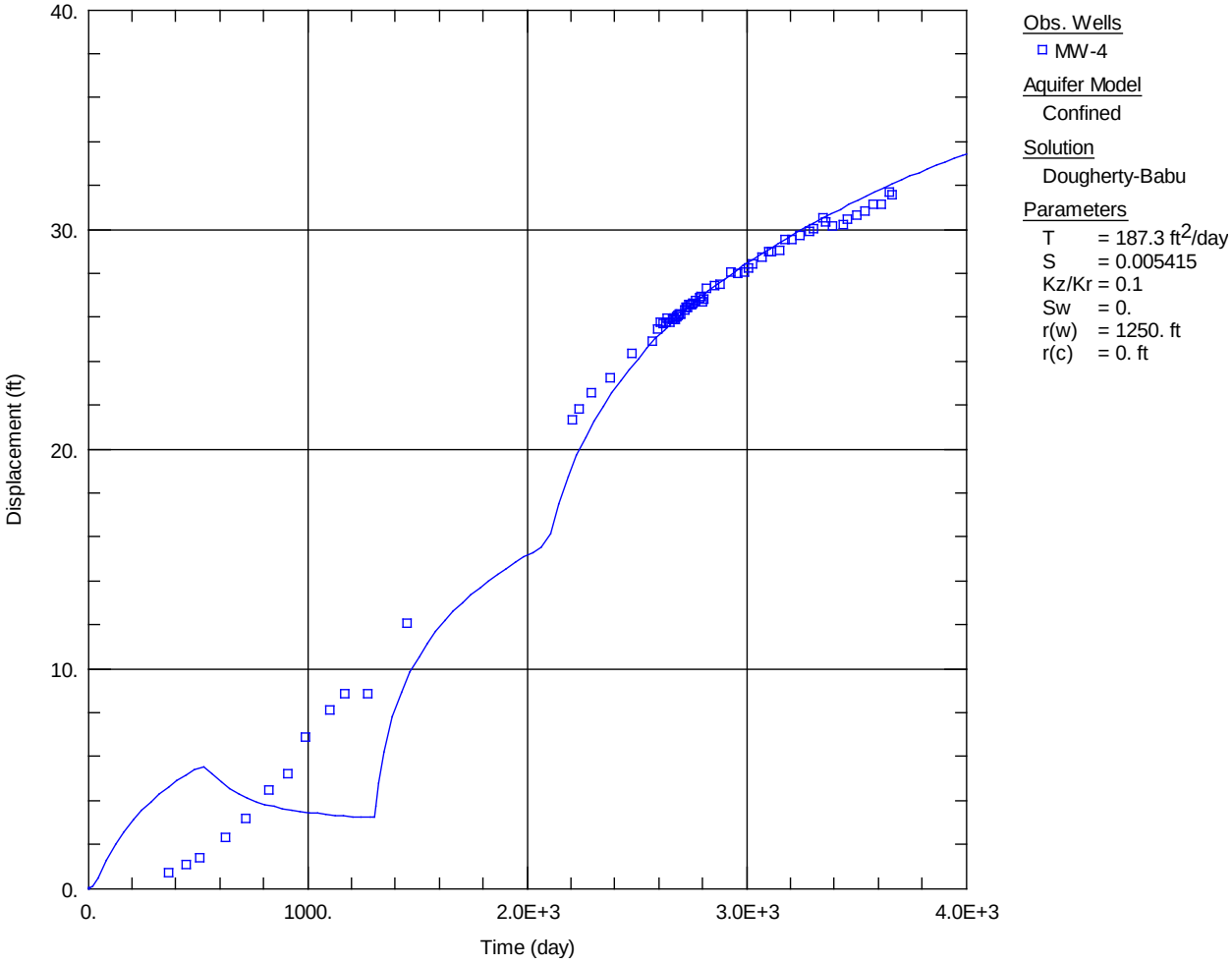

FIGURE A2 - MATCH TO WELL MW-4

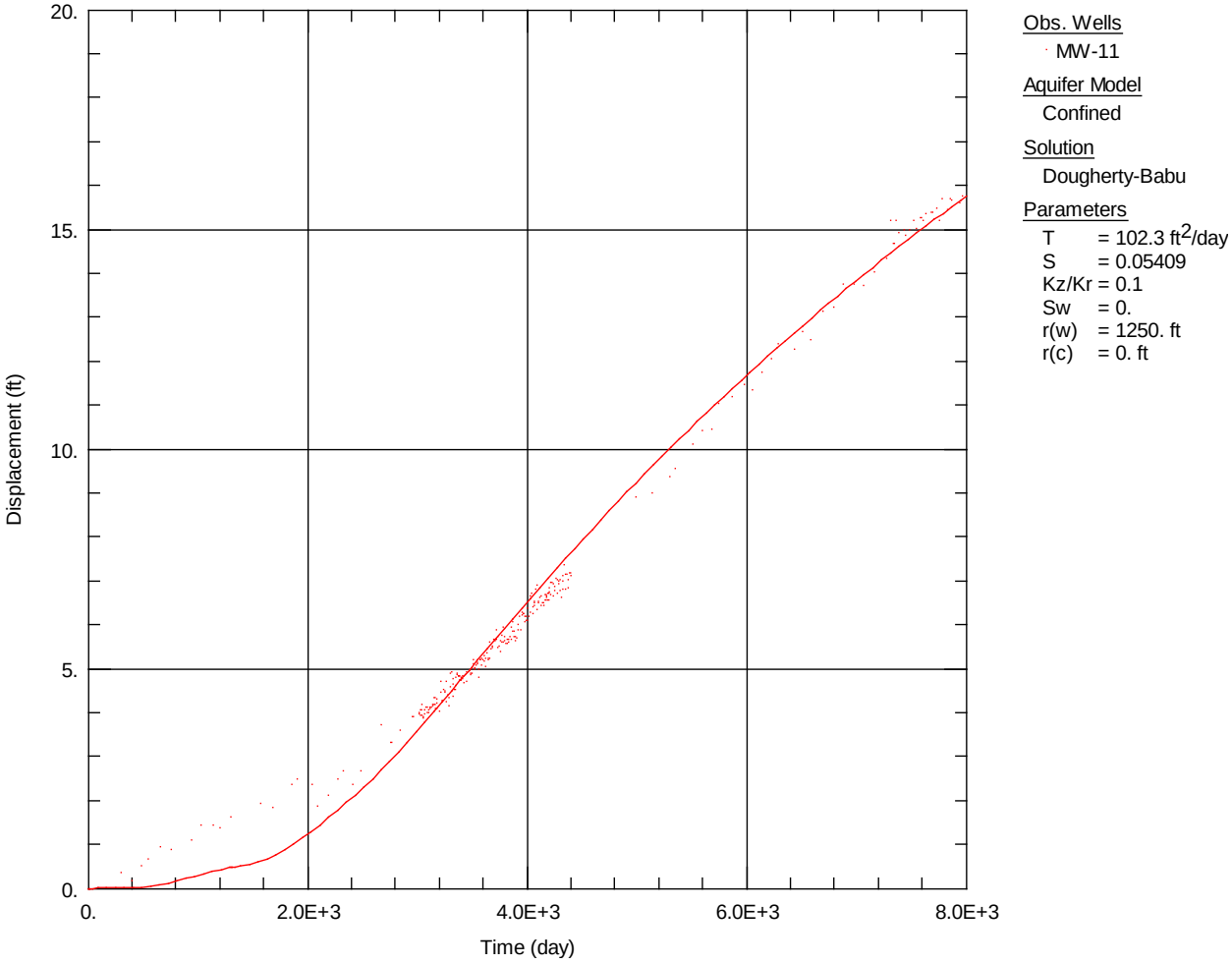

FIGURE A3 MATCH TO WELL MW-11

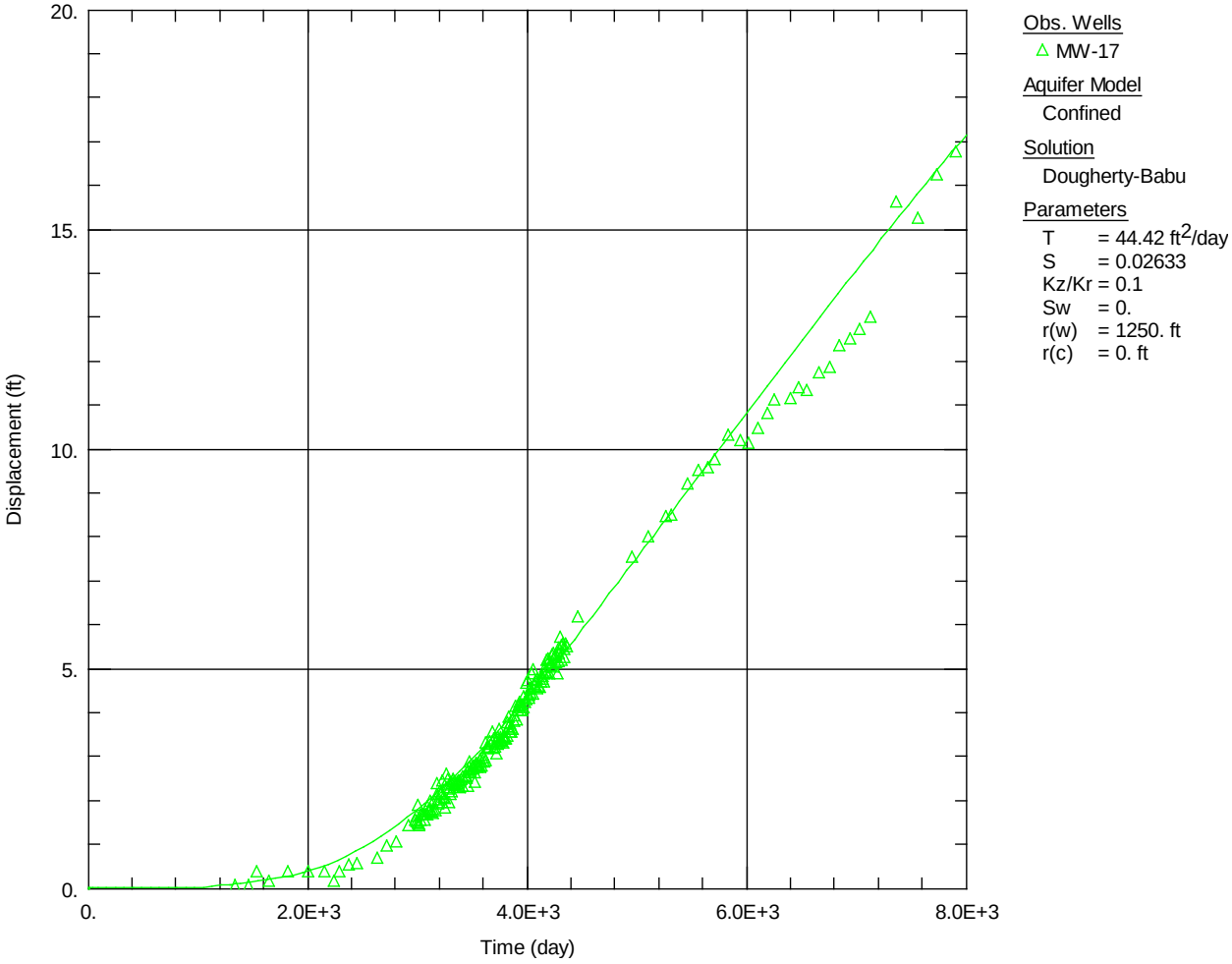

FIGURE A4 - MATCH TO WELL MW-17

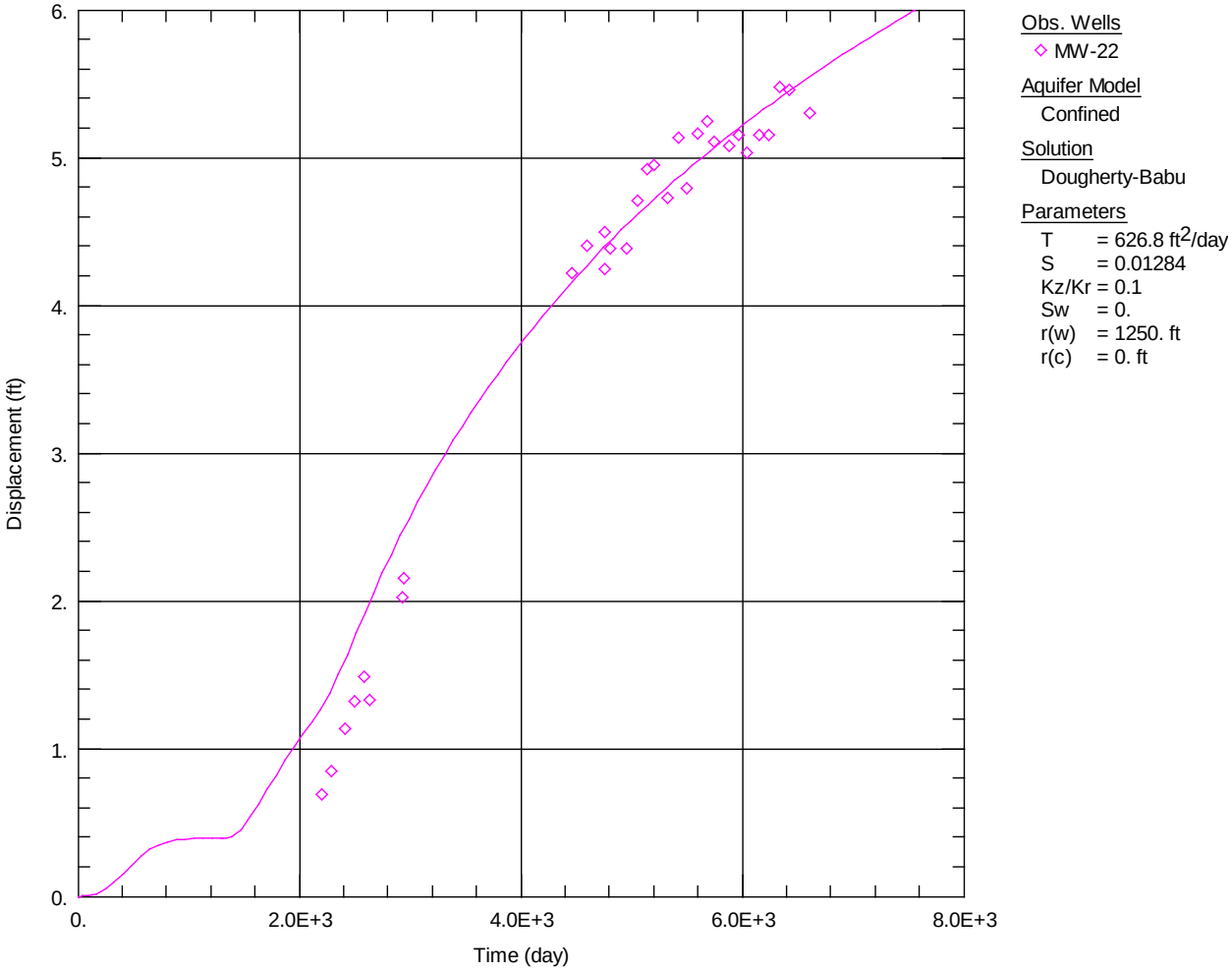

FIGURE A5 - MATCH TO WELL MW-22